6-6-2022

Effectiveness of Air Pollution Mitigation Systems: Transport, Transformation, and Control of Ozone in the Indoor Environment

Pradeep Ramasubramanian
Portland State University

Recommended Citation

Ramasubramanian, Pradeep, "Effectiveness of Air Pollution Mitigation Systems: Transport, Transformation, and Control of Ozone in the Indoor Environment" (2022). *Dissertations and Theses*. Paper 6059.
https://doi.org/10.15760/etd.7929

Effectiveness of Air Pollution Mitigation Systems: Transport, Transformation, and Control of Ozone in the Indoor Environment

by

Pradeep Ramasubramanian

A dissertation submitted in partial fulfillment of
the requirements for the degree of

Doctor of Philosophy
in
Mechanical Engineering

Dissertation Committee:
Elliott Gall, Chair
Olyssa Starry
Raúl Bayoán Cal
Gerry Recktenwald

Portland State University
2022

Abstract

Buildings are critical environments governing our collective exposure to air pollution and energy consumption. While there exist concerns regarding increases in building energy consumption due to indoor air interventions, improvements to the quality of air indoors can improve health, comfort, and productivity. Air cleaning technologies that can improve indoor air quality with minimal energy consumption have become ever more important. These technologies are utilized at various scales; from passive removal of pollutants in the air entering the indoor environment to active cleaning of air within the breathing zone. To better understand the effectiveness of active and passive ozone mitigation technologies at the building scale, a field campaign, chamber experiments, and a multi-zone mass balance model are used. Field measurements of ozone removal, CO_2 exchange, and evapotranspiration (ET) were conducted on a rooftop above a big-box retail store housing a green roof and standard rooftop. Rooftop vegetation and substrate material were collected from the field site and evaluated in chamber experiments to better understand the uptake potential of rooftop surfaces. HVAC filter samples were also collected to understand the ozone removal potential and secondary VOC formation on green and standard filtration mediums. Finally, a multi-zone model is built to evaluate the effectiveness of various mitigation techniques on breathing zone concentrations and ozone exposure fractions.

Ozone removal estimates to rooftop surfaces were found to be modest; if uptake at the rooftop is idealized, removal is transport limited and the overall impact to occupants

indoors is near negligible. On HVAC filters studied, ozone removal ranged between 3.5 % ± 2.8 % to 14 % ± 2.8 %; subsequent modeling suggests that further increases in removal efficiencies to HVAC filters can substantially impact indoor concentrations, but the realized effectiveness is also dependent on HVAC duty cycle and run-time. Ozone removal to HVAC filters may also form secondary compounds; ozonolysis reaction products were measured downstream of loaded filters. Finally, this work shows that ozone removal methods applied at the room-scale must compete with other sinks in the indoor environment, where removal rates necessary to reach a threshold 50 % minimum effectiveness may be unrealistic for room-scale air cleaning technologies. Breathing zone air cleaning shows potential; clean air delivery rates necessary for effective breathing zone air cleaning are two orders of magnitude smaller than the room air cleaners but air cleaning technology applied at this scale still needs development.

Acknowledgments

I would first and foremost express my profound gratitude towards my family and my partner. Without them providing me with unfailing support and encouragement throughout the years, I would not have been able to complete my study.

I would like to thank my graduate advisor and mentor, Dr. Elliott Gall. The door (sometimes a virtual door) to Dr. Gall's office was always open for help and support throughout my research and writing. Without his guidance, encouragement, and mentorship, the research and dissertation would not be at the level and completion it is at.

I would also like to thank Dr. Olyssa Starry, Aurélie Laguerre, and the entire Ecoroof/HBRL team. Without their passionate participation, support, and advice, this research could not have been successfully conducted.

I would like to recognize Dr. Raúl Cal and Dr. Gerry Recktenwald as well, for being part of my dissertation committee and being a reader of this dissertation. I am grateful and indebted for their valuable comments throughout this process.

Table of Contents

List of Tables

List of Figures

1. Introduction

1.1. Problem statement

Globally, 3.8 million people a year die prematurely due to illnesses attributed to household air pollution.[1] In the US, residents spend roughly 87% of their time inside buildings.[2,3] The dominant amount of time spent in indoor environments means the health impact of air pollutants may result from indoor, rather than outdoor exposure.[4–11] The air inside buildings is composed of a mix of compounds; including gases, such as ozone, carbon monoxide, and radon; volatile organic compounds (VOCs) like formaldehyde and benzene, as well as particulate matter, bacteria, bioaerosols, virus-laden aerosols, and degradation products of phthalate esters and brominated flame-retardants.[4,12,13] Sources of these indoor contaminants can be from outdoor origin, through infiltration and natural/mechanical ventilation systems, or of indoor origin, such as indoor combustion sources, building materials, and indoor human activity.

Health effects associated with pollutants in the indoor environment have been well studied and range from acute to chronic effects. A variety of respiratory diseases, such as acute respiratory infection, asthma, tuberculosis, and respiratory tract cancer have been associated with the indoor burning of biomass, a common method for cooking and generating heat in many rural areas.[14,15] In developed nations, there has been a recent trend in weatherization and sealing to reduce building energy load, which can be upwards of 40% of national energy demand, that creates ‘tighter’ buildings.[16] This effectively reduces fresh air movement into and out of the indoor environment leading to the accumulation of

pollutants from indoor emission sources. Also, recent changes to building construction materials and consumer products have introduced or changed the emission profiles for many indoor pollutants that occupants are exposed to.[12] As Americans spend roughly 22 hours a day indoors, susceptible occupants are at greater risk from chronic low-level exposure to indoor pollutants. Chronic exposure to indoor pathogens and pollutants can lead to headache, fatigue, dizziness, nausea, respiratory irritation and infections, asthma and allergy, alveolitis, chronic bronchitis, as well as more toxic outcomes such as severe acute respiratory disease and cancer.[4,13,15,17]

The focus of this work is ozone, a gaseous molecule composed of three oxygen atoms. In the troposphere, ozone is attributable to several sources, including the stratospheric-tropospheric exchange, but it is predominately a secondary pollutant formed through a photochemical reaction process that involves biogenic methane emissions or reactive hydrocarbons, nitrogen dioxide (NO_2), and sunlight.[18–21] Exposure to tropospheric ozone mostly occurs via inhalation although there may be reactions of ozone with human skin lipids that can be sources of detrimental compounds that can be inhaled.[22] Short term inhalation of elevated ozone (anywhere between 5 minutes to 6.6 hours) has been linked with respiratory symptoms such as throat irritation, chest discomfort, increased cough; increased airway reactivity, permeability, and inflammation, and general pulmonary function decrements.[21]

Indoor sources of ozone stem from office equipment such as computers, photocopy machines, and laser printers as well as electrostatic air cleaners that require high voltages

and may produce ozone when air cleaning.[23–26] While there exists the potential for indoor ozone formation, indoor ozone is largely of outdoor origin and indoor ozone concentrations are usually lower than outdoor levels, between 20 – 80% of typical outdoor concentrations.[27–30] But as residents spend roughly 90% of their time indoors, indoor exposure to ozone can account for 45–75% of total daily exposure.[31] As ozone is brought indoors, it readily reacts with unsaturated compounds present on indoor surfaces and indoor air, potentially producing harmful byproducts, such as some VOCs and secondary organic aerosols (SOA).[32–36] Gas-phase reactions must compete with air exchange in the indoor environment, but roughly 10-50% of the ozone consumed by surface reactions produces a measurable gas-phase product in a typical home and reaction products will likely be in the 'tens-of-parts-per-billion' levels during high ozone days.[29,37,38]

A wide body of literature has quantified indoor ozone surface-reaction rates for squalene, a major component of human skin sebum; terpenes, a compound found in numerous cleaning and consumer products, and other compounds sorbed to indoor surfaces including HVAC systems, building materials, furnishings, and appliances.[39–67] Health effects associated with indoor oxidation byproducts have also been extensively studied.[4,27,68,69] Terpene/isoprene-ozone oxidation byproducts have been shown to cause sensory and airway irritation, reduced respiratory function, symptoms of sick building syndrome, and general pulmonary effects.[43,70–72] Formaldehyde, a potential byproduct of ozone-terpene reactions, is known to cause acute poisoning, irritation, and other immunotoxin effects.[73–78] Ultrafine particles (UFPs), which can be formed from surface and gas-phase ozonolysis, can induce coughs, worsen asthma, generate ischemic

cardiovascular disease, hypertension, and have also been linked to diabetes and cancer.[35,36,79–83]

In summary, indoor ozone can have acute and chronic effects on human health, and reductions in ozone levels indoors can reduce the detrimental health effects associated with ozone and its reaction products, therefore, technologies that focus on ozone removal, before entering or within the indoor environment, are imperative to human health, comfort and productivity.[4,21,84–86]

1.2. Research objectives

Buildings are critical environments governing our collective exposure to air pollution and energy consumption.[4,15,16,86–88] While there exist legitimate concerns regarding increases in building energy consumption due to indoor air interventions, improvements to the quality of air indoors can improve health, comfort, and productivity.[4,86,89–93] Air cleaning technologies that can improve indoor air quality with minimal energy consumption have become ever more important. These are utilized at various scales and with differing necessary input; in this work, an important distinction is that of *passive* removal, removal mechanisms that require no added energy outside of normal building operations, and *active* removal, removal mechanisms that require non-trivial energy.[94]

Currently, there remains a gap in our understanding of the effectiveness of different active and passive air cleaning technologies at scale in terms of ozone removal and

byproduct formation. The proposed research aims to fill this gap through four research goals that evaluate air cleaning strategies for reducing breathing zone concentrations of ozone:

Research Aim 1: *Economical methods of pollutant deposition measurements at the rooftop scale and local-scale CO_2 exchange and evapotranspiration between urban green and hard surfaces*

Specific questions:

1) Utilizing CO_2 and H_2O gradient methods, can we determine the feasibility of pollutant deposition measurements to rooftops using the atmospheric gradient method and the modified Bowen ratio method?
2) Can urban greenery be used as a sink for urban CO_2 emissions and impact evapotranspiration (ET) within the urban biosphere?

Research Aim 2: *The potential for rooftops to passively remove ozone prior to entering the indoor environment*

Specific questions:

1) What are green roof surface resistances for ozone and how do they vary based on environmental conditions?
2) How does ozone removal to green roofs compare with other rooftop types and building materials?

Research Aim 3: *Impact of rooftops on air handler filter loadings, filter ozone removal, and secondary emissions*

Specific questions:

1) Do filter loadings from local rooftops impact ozone removal?
2) How does the presence of ozone impact VOC emissions from filters?

Research Aim 4: *Effectiveness of cleaning and ventilation technology to exposure of ozone*

Specific questions:

1) What are the modeled impacts of active and passive air cleaning methods on ozone inhalation intake fraction?
2) What are threshold ozone removal values necessary for various air cleaning methods to be impactful to breathing zone ozone concentrations?

Currently, there is limited empirical data on ozone removal to green roofs, a proposed passive mitigation technique, as compared to standard rooftop surfaces. Also unexplored is the impact of green roofs versus standard rooftops to rooftop ventilation units in terms of filter loading, ozone–filter reaction byproduct formation, and the effectiveness of these passive mitigation techniques relative to active mitigation techniques. This research is focused on providing experimental data on the impacts of passive, outdoor ozone mitigation to the indoor environment, exploring the potential for secondary impacts due to ozone removal, and analyzing the effectiveness of mitigation technologies in improving the quality of inhaled air through values taken from field measurements and literature.

2. Background

2.1. Sources of ground-level ozone and transport to indoor environments

As mentioned in section 1.1, while indoor ozone sources exist, they are relatively uncommon compared to the ubiquity of ozone of outdoor origin which impacts every building. Ozone in the troposphere is formed through a photochemical process that utilizes hydrocarbons, nitrogen dioxide (NO_2), and sunlight.[18–21] Sources of hydrocarbons and NO_x, whose constituents are nitrogen oxide (NO) and NO_2, in the troposphere are largely from industrial and fossil fuel emissions such as motor vehicle emissions.[18,19] Transport to the indoor environment occurs either via infiltration of the building envelope or natural and/or mechanical ventilation.

2.1.1. Infiltration

In most buildings, outdoor ozone is brought into the indoor environment through infiltration in cracks and other unintentional openings in the building envelope. Many buildings are not equipped with mechanical ventilation systems and when doors/windows are closed during heating and cooling seasons, air exchange between the indoor and outdoor environment occurs through uncontrolled cracks and leaks in the building envelope. This exchange is called *infiltration* and is one pathway in which indoor occupants can be exposed to pollutants of outdoor origin, such as ozone.

Infiltration pathways to the indoor environment are narrow and tortuous, and a portion of outdoor ozone can interact with building materials before entering the indoor space, quantified using a metric known as the ozone penetration factor.[95,96] Liu and

Nazaroff (2001) modeled ozone penetration factors based on crack geometries and surface reaction probabilities. They found that the relationship between ozone penetration and reaction probabilities can be divided into three regimes: if the reaction probability is $\gamma > \sim 10^{-3}$, ozone penetration is small and independent of reaction probability and ozone uptake is mass-transport limited; if the reaction probability is $\sim 10^{-5} < \gamma < \sim 10^{-3}$, ozone penetration varies with reaction probabilities and surface uptake, and gas-phase mass transfer contributes to ozone penetration; finally if the reaction probability is $\gamma < \sim 10^{-5}$, ozone penetration is large and surface uptake is dependent on surface kinetics.[95] Stephens et al. (2012) studied ozone penetration factors for 7 single-family homes and one unoccupied test house and discovered the mean penetration factor of the 8 homes to be 0.79 ± 0.13 with higher penetration in exterior painted wood cladding and with longer cracks in the envelopes and lower penetration in newer homes.[97] While infiltration is one method of ozone transport to the indoor environment, mechanical and natural ventilation are more direct pathways for ozone to enter the indoor environment: Lai et al. (2015) studied the impact of infiltration and ventilation on indoor-to-outdoor ozone ratios and found indoor-to-outdoor ozone ratios were lower for infiltration, 0.09, than for mechanical ventilation, 0.19, and natural ventilation, 0.47.[96]

2.1.2. Mechanical and natural ventilation

Mechanical and natural ventilation are common pathways in which outdoor ozone can enter the indoor environment. Mechanical ventilation is the movement of air between the indoor and outdoor environments through four general methods that require non-trivial

energy: exhaust, supply, balanced, and energy recovery. Exhaust ventilation systems work by depressurizing the indoor environment through exhausting air from the indoors and pulling make-up air from the outside through doors, windows, and large openings as well as leaks and cracks in the building enclosure. Supply ventilation uses a fan to pressurize the building and force air outside the building through leaks, cracks, and larger openings. Balanced ventilation systems introduce and exhaust air in approximately equal quantities, neither pressurizing nor depressurizing the indoor environment. Finally, energy recovery ventilation systems are like balanced systems but provide fresh air to the indoor environment while minimizing energy losses. They reduce the heating and cooling costs by transferring heat between the indoor and outdoor air during the ventilation process.

Mechanical ventilation is generally applied in four different methods to impact indoor pollutant concentrations: mixing ventilation, displacement ventilation, personalized ventilation, and a hybrid air distribution system. Mixing ventilation supplies the room with fresh air at high flow rates from the upper parts of the room.[98] Displacement ventilation distributes cool air at a low velocity near the floor to create an upward draft due to thermal plumes in various parts of the room.[98] Personal ventilation provides fresh air directly to occupants breathing zone at the 'personal scale', such as at office desks or hospital beds, where the inhaled air may not be contaminated with pollutants from the room.[98,99] Hybrid distribution systems combine mixing ventilation and displacement ventilation to overcome the shortcomings of either system, such as room depth penetration.[98] Mechanical ventilation is the predominant method for ventilating commercial buildings in the developed world and can involve pollutant filtration systems including activated carbon, a

medium used for ozone removal. Further detail on activated carbon for ozone removal is provided in section 2.4.3.1.

Natural ventilation is the movement of air between the indoor and outdoor environment through doors, windows, and other large openings. Building designs that seek natural ventilation have increased in recent decades due to the purported benefits of maintaining indoor temperature stability and a more comprehensive and simpler, energy-saving scheme.[100] While natural ventilation may have some benefits, ozone mitigation is almost non-existent. Open windows, a way of providing natural ventilation to the indoor environment, significantly increase indoor ozone levels, especially when outdoor concentrations are high. This can be explained simply as natural ventilation has increased ventilation rates with practically zero ozone mitigation, resulting in increased indoor ozone concentrations relative to mechanical ventilation and infiltration.[101]

2.2. Indoor ozone removal mechanisms

When outdoor ozone penetrates the indoor environment, indoor removal mechanisms play a key role in reducing and transforming indoor ozone. Ozone removal in the indoor environment occurs through three routes: heterogeneous surface removal, homogenous gas-phase removal, and exfiltration/ventilation.

2.2.1. Heterogenous surface removal

Building materials, furniture, and human skin oils can be significant sinks for ozone, through the irreversible heterogeneous surface reactions between ozone and compounds trapped on surfaces, typically quantified by a constant of proportionality called

the *deposition velocity*.[29,102,103] The deposition velocity is a function of the transport of ozone to the material surface and the uptake on the surface and can vary depending on surface geometry, fluid dynamics close to the surface, and the reaction surface.[104]

Surface removal of ozone often follows the Criegee mechanism, a reaction between the unsaturated bonds present in many organic compounds that are cleaved by ozone and replaced by a carbonyl group. These carbonyl groups have a finite lifetime and can either be detrimental to occupant health or be the catalyst for a secondary reaction that may lead to the formation of compounds that are detrimental to occupant health. A variety of research has been performed to quantify ozone removal to surfaces, from lab-scale experiments to field measurements. Ozone removal to building materials have been quantified for various types of drywall, insulation, green building materials, carpets, furniture, terpenoids sorbed on surfaces, and skin oils desquamated from occupants onto indoor surfaces.[22,33,35,36,42,50–52,67,94,102,105–113] Field experiments have quantified ozone decay in residential homes: Wang and Morrison (2010) characterized deposition velocities and reaction probabilities in 5 homes in Rolla, MO, finding that reaction probabilities ranged from 9.4×10^{-8} to 1.0×10^{-4}, similar in magnitude to modeled and lab-scale experiments. Deposition velocities were quantified per material surface in relation to secondary emission rates from surface reactions using a field chamber with an open bottom and it was found that a correlation can be made between ozone flux to the surface and secondary emission rate.[114,115] While surface reactions can be a major form of ozone removal in the indoor environment (on par with exfiltration and ventilation), gas-phase removal with some indoor VOCs and gaseous compounds can compete with air exchange

and generate harmful byproducts that are important for understanding a potentially important pathway for human exposure to air pollution.

2.2.2. Homogenous gas-phase removal

Ozone is an inorganic, reactive, gaseous molecule that can interact with surface-sorbed and gas-phase compounds and alter indoor chemistry, but gas-phase reactions have to compete with the level of air exchange between indoor and outdoor environments.[38] The air exchange, coupled with the mixing ratio of the room, can determine the competitiveness of homogeneous interactions between indoor pollutants. Transport due to indoor air exchange can also reduce concentrations of indoor pollutants if outdoor concentrations are low, which can subsequently influence the rate at which indoor ozonolysis can occur.[29] But, in cases where the compound of interest is of outdoor origin, such as ozone, the opposite can occur: transport due to air exchange may increase the concentration of a pollutant of outdoor origin and alter indoor chemistry.

The gas-phase interaction between ozone and common indoor compounds, such as terpenes, and therefore, their removal, have been characterized in lab-scale experiments. Gas-phase ozone removal from homogeneous reactions with terpenes, aromatic alkenes found in plants, foods, and some cleaning products, have shown to be on par with air exchange rates.[116] When ozone and terpenes interact, they can form known airway irritants such as formaldehyde, acrolein, methacrolein, methyl vinylketone, as well as some unknown irritants.[43,117–120] Ozonolysis with terpenes may also form hydroxyl (OH) radicals, a molecule that is highly reactive and can further alter indoor chemistry.[121] The

terpene-ozone gas-phase interactions are of particular interest because of the ubiquitous nature of terpenes in the indoor environment and ozone-terpene reaction rates are on par with common air exchange rates, but as ventilation rates increase, gas-phase chemistry is less likely to occur and surface chemistry and exfiltration/ventilation become the major indoor ozone removal mechanisms.

2.2.3. Removal due to exfiltration and ventilation

Exfiltration and ventilation are common processes of removing gases, particulate matter, and other pollutants, from the indoor environment. Like infiltration, exfiltration is the air leakage out of buildings through cracks, leaks, and unintentional openings in the building envelope. Exfiltration pathways are like infiltration pathways; they are narrow and tortuous, and a portion of indoor ozone can interact with building materials while leaving the indoor environment. Ventilation, on the other hand, is the purposeful movement of air between the indoor and outdoor environments and can be through natural and mechanical ventilation, detailed in section 2.1.2. Ventilation systems are used to reduce concentrations of indoor-generated pollutants, and if the concentration of ozone in the indoor environment is higher than that outdoors, ventilation can reduce indoor ozone concentrations. But ventilation during elevated outdoor ozone periods can be detrimental to the indoor environment without appropriate ozone mitigation in the ventilation systems: indoor ozone concentrations are generally lower than outdoor ozone and as ventilation rates increase, elevated outdoor ozone is introduced to the indoor environment with a net increase in indoor ozone levels. Of the four ventilation strategies (exhaust, supply, balanced, and

energy recovery) exhaust ventilation systems with closed doors/windows are the most effective at reducing indoor ozone concentrations as they exhaust indoor air and deliver fresh air only through infiltration pathways, allowing outdoor ozone to react with the building envelope prior to entering the indoor environment.[101,122] But this might introduce secondary pollutants to the indoor environment through surface ozonolysis with the building envelope.

2.3. Ozone byproduct formation

Indoor removal mechanisms for ozone are important in reducing the impact of ozone on the inhaled air breathed by occupants, but surface and gas-phase removal has the potential for secondary byproduct formation that needs to be accounted for. As mentioned in section 2.2.1, ozonolysis works through the Criegee mechanism, a reaction mechanism between ozone and unsaturated groups that form functional carbonyl groups that can either be harmful to health or be the reagent for a secondary reaction that forms compounds harmful to occupant health.

In the indoor environment, ozone/terpene reactions are important in indoor chemistry due to the ubiquity of terpene emission sources in the indoor environment and the speed at which these reactions can take place relative to air exchange.[29,116] These reactions are also important as they can generate a significant quantity of hydroxyl radicals (OH), secondary VOCs, and secondary organic aerosols.[29,43,70,71,74,117–120,123–128] OH in the indoor environment is of particular importance as it is known to be a catalyst for secondary reactions in the indoor environment that may produce harmful products to occupant health.

Weschler and Shields (1996) showed elevated OH concentration from ozone reactions with various terpenes and showed OH can initiate oxidation of saturated organics at rates 2-5 orders of magnitude faster than ozone reactions.[123] Sarwar et al. (2002) modeled OH formation from homogeneous ozone reactions finding that indoor hydroxyl radical levels are primarily controlled by indoor reactions of alkenes with ozone or nitric oxide with hydroperoxyl radical.[124] Forester and Wells (2011) performed chamber studies to determine if water vapor affected the OH formation in ozone-terpene reactions including in pine oil cleaning (POC) products. OH yields measured in this study were 64 ± 8%, 64 ± 6%, and 76 ± 6% for α-terpineol, limonene, and α-pinene, respectively, and the OH yield for POC products was 51 ± 6%. Relative humidity did not affect OH formation.[125]

Secondary volatile organics can also be formed from ozone-initiated terpene reactions or the potentially subsequent OH reaction product. Atkinson and Arey (2003) outlined common secondary VOCs formed from ozone-terpene reactions in the atmosphere, most commonly, formaldehyde, an irritant in the indoor environment that can cause cancer at high doses.[129,130] Destaillats et al. (2006) studied oxidation products of ozone-terpenoid reactions in a 198-L Teflon-lined bag and found increases in oxidation products such as formaldehyde, acetaldehyde, acetone, glycolaldehyde, formic acid, and acetic acid.[74] In a study of ozone reactions with terpenes in common products used for cleaning (orange oil-based degreaser, pine oil-based general-purpose cleaner, and plug-in scented-oil air freshener), Singer et al. (2006) found that VOCs such as formaldehyde and acetone were elevated in the presence of elevated ozone (~120 ppb) and the cleaning product.[119] Investigations of ozonolysis of terpenes show carboxylic and dicarboxylic acids

as reaction products, which could be a reason for the formation of secondary organic aerosols due to their high polarity and low vapor pressure.[131,132]

Secondary organic aerosol (SOA) formation from homogeneous ozone/terpene reactions is an important process to consider in indoor environments due to the potential impact on occupant health.[133–135] SOAs are formed in the atmosphere through the coagulation and condensation of low vapor pressure, oxidation products and they play an important role in many environmental processes; aerosols scatter and absorb solar radiation, impact cloud formation, and provide sites for heterogeneous chemical reactions in the atmosphere.[136,137] In the indoor environment, the formation of SOAs in the ultrafine particle range can have detrimental effects on respiratory health and function.[80,82,83,138] During periods with elevated ozone and terpenes, the potential for SOA formation increases: Weschler and Shields (1999) studied the homogenous interaction of ozone and selected terpenes, d-limonene, α-terpinene, and α-pinene, to form SOAs in adjacent identical offices and discovered that particle formation can be observed for each terpene system, with the greatest being ozone/d-limonene interactions.[38] Sarwar et al. (2004) studied SOA growth from ozone-terpene reactions of 5 terpene-containing consumer products and learned that homogeneous reactions between ozone and terpenes will increase fine particle mass concentration in the indoor environment.[139,140] Sarwar and Corsi (2007) studied SOA formation from gas-phase ozone/limonene reactions, observing that at low air exchange rates, particle size distributions shift towards larger particle diameters and particle mass concentration increase with higher outdoor ozone concentrations, higher

outdoor particle concentrations, higher indoor limonene emission rates, and lower indoor temperatures.[118]

Unsaturated organic compounds sorb onto indoor surfaces that can act as reaction sites for ozone: ozone decay to indoor surfaces occurs at a higher rate than most homogeneous ozone reactions and be on par with ozone removal due to air exchange.[116] Indoor ozone surface reactions may occur on most surfaces, including building materials, paint, carpets, furniture, and human skin oils, and these reactions can generate secondary pollutants, like those of homogeneous reactions. Morrison and Nazaroff (2002) studied ozone interactions with carpets, finding that surface reactions produced C_1-C_{13} n-aldehydes and several unsaturated aldehydes.[50] Wang and Morrison (2006) studied secondary emission rates of aldehydes from ozone-surface reactions in four homes and discovered that upon exposure to ozone, formaldehyde and C_3–C_{10} saturated aldehydes, especially nonanal, were emitted as byproducts of ozone-initiated surface reactions.[114] Secondary organic aerosols may also be formed from ozone-surface reactions: ozone reactions with surface sorbed terpenes from consumer products as well as squalene, desquamated from humans onto surfaces, have been shown to produce secondary organic aerosols.[35,36,40,109] Ozone in the indoor environment can pose many risks, either from direct inhalation or from inhalation of its reaction products, and removal of ozone before or within the indoor environment is paramount to occupant health, comfort, and productivity.

2.4. Air cleaning strategies for ozone removal

Air cleaning mitigation technologies can be described as either *active*, requiring non-trivial energy for pollutant removal, or *passive*, where removal requires no added energy outside of normal building operations. Building scale cleaning through HVAC systems, room cleaning through portable air cleaners, and breathing zone ventilation and air cleaning are examples of 'active' cleaners as they all require energy to remove pollutants from the indoor environment. Examples of passive mitigation technology are functionalized surfaces, such as paint, vegetation, or other reactive surface material. These surfaces require no energy to trigger the removal of pollutants through deposition and surface reaction.

2.4.1. Passive ozone removal

Passive mitigation technology is often based around natural ventilation, functionalized surfaces, vegetation, or other reactive surface material and can exist in the indoor environment or outdoors, in the vicinity of the building where they may treat air brought indoors.[94,111,141–143] In the last two decades, passive removal material (PRM) has been sought as a potentially effective method of reducing the concentration of indoor pollutants. Sekine and Nishimura (2001) developed a board-like air-cleaning material consisting of activated carbon particles and manganese oxides and evaluated it for reductions in formaldehyde concentration, discovering that the board not only reduced indoor formaldehyde concentrations but increased the loss of formaldehyde from other building materials.[143] Kunkel et al. (2010) tested the passive removal of ozone through

activated carbon and gypsum wallboard panels. They found that the ozone decay rate in an unoccupied 34.5 m^3 bedroom was 2 – 7 h^{-1} for activated carbon and 2 – 3 h^{-1} for gypsum wallboard and with sufficient panel area and positioning, an ozone removal effectiveness of over 80% may be possible.[142] In a six-month field study of three green building materials (perlite-based green ceiling tiles, recycled carpet, and recycled gypsum wallboard) and an activated carbon mat for ozone removal capability, Cros et al. (2012) found that for all materials, except the recycled carpet, ozone removal sustained throughout the study period. The activated carbon mat and the green ceiling tile had the highest ozone deposition velocity at 2.5 – 3.8 m h^{-1} and 2.2 – 3.2 m h^{-1}, respectively.[144] Through a Monte Carlo simulation to assess the impact of PRMs on ozone, Gall et al. (2011) showed improvement in indoor-outdoor ozone ratios for homes with PRMs vs. those without. But to reach a removal effectiveness above 50%, PRMs must encompass a large portion of the indoor surface area and enhanced air speeds are required to drive pollutants to the PRM surface, which may cause discomfort to indoor occupants.[94]

In the urban environment, passive removal of ozone through urban vegetation has been a purported method of improving the quality of urban air. Through a large-scale modeling effort to characterize urban ozone fluxes to green roofs in the Chicago area, Yang et al. (2008) attributed ~50.5 kg ha^{-1} y^{-1} of ozone removal to green roofs.[145] Biraldi et al. (2019) modeled the impact of urban forests on urban ozone concentrations using the 'i-Tree Eco' model and found that ozone removal potential ranged from about 58 – 140 g $plant^{-1}$ yr^{-1}.[146] Bottalico et al (2016) also modeled ozone removal to vegetation in Florence,

Italy, and found that ozone removal due to urban vegetation was substantial in absolute terms, but relatively modest when compared to overall pollution levels.[147]

While urban vegetation may provide removal sites for ozone in the urban environment, it may not appreciably alter the concentration of ozone in the urban canopy layer. In a study of pollutant removal to urban forests in the city of Chicago, McPherson et al. (1994) estimated maximum reductions in hourly ozone concentrations of only 5.2 % with an unrealistic, 100 % forest coverage.[148] While urban ozone removal to vegetation may be modest, one unexplored role of vegetation is to act as an ozone reaction and transformation site for air entering the indoor environment. Specifically, green roofs might present an opportunity for this phenomenon to take place: as air travels across the green roof surface, there may be heterogeneous uptake of ozone to the green roof surfaces or to particles suspended from the green roof surfaces, before entering the building heating, ventilation, and air conditioning (HVAC) units and brought indoors. The suspended biotic particles from green roofs may also be trapped on HVAC filters and serve as a secondary reaction/transformation site for ozone.

2.4.2. Active ozone removal

2.4.2.1. Building scale ozone removal

HVAC units are one common method of removing air pollutants of indoor and outdoor origin in buildings, generally through filtration of outdoor and recirculating air supply. Physical filtration techniques using fibrous and membrane filters can be used to remove PM of both outdoor and indoor origin. As air passes through the filter, a portion of

particles suspended is trapped on the fibrous membrane and filters through particle sieving, impaction, interception, and Brownian diffusion mechanisms. The fraction of particles removed through the filter is the filter removal efficiency, often quantified by the minimum efficiency reporting value (MERV).[149] In a survey of small and medium commercial buildings in California, 97% of the filters used had filters with a MERV rating of 8 and lower, and more than half of the buildings used MERV 4 filters.[150] Increasing the MERV rating of filters in the building mechanical systems can improve the removal of PM but increases pressure drop and building energy demand.[88] Walker et al. (2013) found a significant increase in energy use (> 5%) due to an increase in pressure drop when using a MERV 16 or higher filters.[151] Increasing filtration efficacy in ventilation air for the 'excellent' approval based on 12 IAQ parameters as determined by the Hong Kong government were found to increase the operational cost by 5%.[152] Improvements in air quality can potentially offset the costs of higher MERV filtration; Zaatari et al. (2013) found that improving filters from a MERV 8 to MERV 13/14 can increase the clean air delivery rate (CADR) of the system, which offsets the cost of higher energy consumption by a factor of 2.9 - 3.8.[88]

Ozone removal in HVAC units is predominantly through sorbent-based air cleaners that may be impregnated onto filter fibers or installed as a granular media-packed bed and is usually composed of activated carbon or charcoal. Activated carbon filters can be installed as pre-filters where they have shown removal efficiencies of 60-70% within 2 months.[153] Shields et al. (1999) studied ozone removal due to charcoal filters after 5 to 7 years of operation and found removal efficiencies ranged between 60% and 95% depending

on the lifetime of the filter.[154] Another study found that activated carbon filters can provide ozone removal efficiencies up to 98.3% but the reaction dynamics can permanently change the composition of the filter.[155] While there is promise in the use of activated carbon as an ozone mitigation medium, their viability is dependent on the HVAC operational periods: Aldred et al. (2016) evaluated ozone removal efficiencies across 12 cities in 5 different climate zones and found that removal efficiencies varied between ~1% and ~43% for activated carbon filters, where increases in removal efficacy were dependent on HVAC operational times.[156]

Ozone removal through mediums in building scale ventilation systems can have secondary effects: ozone removal via the Criegee mechanism on filters leads to carbonyl formation and ozonolysis products, including formaldehyde, acetaldehyde, acetone, and 4-oxopentanal are elevated downstream of filters laden with particles from vegetation and diesel emissions.[66,73,157] Two oxidation byproducts, formaldehyde and acetaldehyde, were found in air downstream of filters after ozonolysis.[73] If reactive organics such as terpenes and isoprene are present on HVAC filters, ozone-surface reactions can lead to the formation of secondary organic aerosols.[35,36,158]

2.4.2.2. Room air cleaners for ozone removal

Room air cleaners (RAC) are another method for improving indoor air quality, but their effectiveness can vary depending on the type and performance characteristics of the air cleaner. Although RACs are designed to reduce pollutant exposure in the indoor

environment, the process by which they remove pollutants can vary across air cleaners. For indoor PM, air cleaners may mechanically draw air through fibrous or membrane filters, use electrostatic precipitation to induce an electrostatic charge to trap particles without impeding airflow, or ionize the air to charge and remove particles into a collector. The efficiency of the methods used by different air purifiers can have a variety of effects, and in some cases, produce harmful byproducts. The most widely used method to characterize the performance of RACs for particle air cleaning is the method described in the American National Standards Institute (ANSI)/Association of Home Appliance Manufacturers (AHAM) AC-1-2020 protocol.[159] This protocol sets the guidelines for CADR of air purifiers using a measured decay rate of particles in a sealed chamber with the air purifier turned on compared with the air purifier turned off. Since the CADR metric captures the total volume of cleaned air delivered per unit time, it is used to size the RAC to the volume of the space.

Air cleaners that use air ionization technology generally do not lend well to testing via the CADR metric due to the reliance on an external fan for airflow and/or claims of agglomeration, deposition, and other chemical removal processes that may occur throughout the specific space served by the ionization RAC. Ionization technology can also create potentially harmful by-products. In a review of available literature on ion generation and its implications to indoor air quality, many ion generators produce ozone and can increase ozone-initiated reactions that may form secondary volatile organic compounds (SVOC) and secondary organic aerosols (SOA) in the ultrafine particle (UFP) range.[160]

For gas-phase pollutants such as ozone, the most common removal methods are sorption/desorption and chemical reaction methods such as photocatalytic oxidation (PCO). Activated carbon and charcoal are filter mediums that RACs can use to treat ozone, as described in section 2.4.2.1, as well as high concentrations of VOCs in indoor air. Sidheswaran et al. (2012) studied the removal of common indoor VOCs (toluene, benzene, o-xylene, 1-butanol, limonene, undecane, and formaldehyde) due to activated carbon filters and found removal efficiencies of roughly 70% to 80% from a steady concentration of 20-30 ppbv.[161] Laguerre et al. (2020) and Stinson et al. (2022) performed in-situ measurements of the impact of activated carbon ventilation filters on NO_x, ozone, and VOC concentrations at a near-roadway school.[162,163] They found that the carbon scrubber removed 2.4 ± 0.4 g h^{-1} of VOCs, a substantial reduction in indoor VOC source strength. Ozone removal to the air-cleaning system was also found to be on par with or greater than reactive deposition to indoor surfaces; removal rates through the air cleaning system at an air exchange rate of 2.5 h^{-1} were similar to indoor surface removal loss rates, ~2.3 h^{-1}. Another study looked at the effect of activated carbon on benzene, toluene, ethyl benzene, and xylene (BTEX) and found that removal efficiencies for BTEX were between 75% and 94% depending on temperature and relative humidity.[164] This study also found higher removal efficiencies for hybrid activated carbon – photocatalytic oxidation systems, ~100% removal, and there was no dependency on relative humidity.[164] Fifteen air cleaners using five different methods of air cleaning were tested to treat sixteen common indoor VOCs and sorption filtration, the mechanism used in activated carbon, was found to be the most effective off-the-shelf commercial technology for the removal of VOCs.[165]

While sorption filtration is the most effective mitigation technology for ozone and VOC removal, photocatalytic oxidation has seen recent use in portable air cleaners due to the potential of minimal pressure drop needed to treat almost all organic, gaseous indoor compounds and microbes.[165,166] But, the removal efficiency for these pollutants and pathogens depends on the functional group of compounds and the residence time of the air moving through the PCO air cleaner.[149,167,168] Photocatalytic oxidation (PCO) is the process of a light-mediated reaction of gases and biotic particles adsorbed to a titanium oxide photocatalyst.[149] The drawback of PCO technology is the potential for incomplete oxidation, which can introduce byproducts that are more detrimental than the compounds the PCO air cleaner is cleaning.[169] Hodgson et al. (2007) showed the production of formaldehyde, acetaldehyde, formic acid, and acetic acid in the use of ultraviolet photocatalytic oxidation (UVPCO) of a mixture of 27 characteristic indoor VOCs.[169] While the use of PCO technology can improve problems related to pressure drop, their effectiveness in reducing concentrations of gaseous compounds such as ozone still needs to be investigated.

2.4.2.3. Breathing zone ventilation and air cleaning

Breathing zone ozone removal through ventilation or air cleaning is a relatively novel topic, few studies have been performed on pollutant removal at the breathing zone scale relative to other removal methods. The most common method studied is personal ventilation, where fresh, clean air is delivered to the occupants breathing zone with enough momentum to penetrate the thermal boundary layer formed by the human thermal plume

and decrease the concentration of indoor pollutants inhaled. Bauman et al. (1993) was an early study of a 'personal ventilation' study to evaluate the thermal comfort of occupants using a desktop task conditioning system, finding that local thermal control can be achieved for a wide range of thermal conditions by adjusting air trajectory and supply volume.[170] Tsuzuki et al. (1999) studied three different task/ambient conditioning systems; a 'Personal Environmental Module' (PEM), used in US offices, a 'ClimaDesk' (CDESK), used in European offices, and a floor-mounted 'Task Air Module', for thermal comfort control and ventilation air delivery. The PEM provided cooling for the whole body and better pollutant removal efficiency more effectively than the other two methods.[171]

Melikov (2002) experimentally investigated five potential personal ventilation methods for a typical office space: a 'Personal Environments Module' (PEM) consisting of two nozzles mounted at the two back edges of the desk, a Computer Monitor Panel (CMP) mounted to the top of the computer monitor delivering air horizontally toward the manikin, a Movable Panel (MP) positioned in above of the manikin directing air downward toward the manikins face, a Vertical Desk Grill (VDG) mounted at the front of the desk delivering air upward toward the manikin, and finally, a Horizontal Desk Grill (HDG) mounted to the front of the desk delivering air horizontally towards the manikins' body. A personal exposure (PE) effectiveness was used to assess the performance of the tested personal ventilation devices, finding that high airflow rates coincided with increases in PE effectiveness until a threshold value was reached where higher flow rates were ineffective in impacting PE effectiveness. The VDG had the highest PE effectiveness of the tested devices, 0.6, at an airflow rate below 15 l s^{-1} under both isothermal and non-isothermal

conditions. It was also found that the amount of exhaled air re-inhaled by the manikin was small for all tested PV devices and the temperature of inhaled air decreased for all PV devices, with the VDG providing the lowest temperature in inhaled air. The impact of personalized ventilation systems on perceived air quality and sick building syndrome (SBS) was studied by Kaczmarczyk et al. (2002) finding that fresh, outdoor air through the personal ventilation system at roughly 20° C can significantly increase perceived air quality and improve occupant productivity and comfort.[172] Personal ventilation studies have been performed to evaluate the types of air terminal devices (ATDs); the dynamics of personal ventilation jets including the influence of nozzle geometry, fluid regime, and temperature fluxes; and the impact of room airflow dynamics.[99,173–193]

Munhič and Butala (2005) studied the delivery of fresh air close to the occupant and found that personal ventilation systems can decrease tracer gas concentration within the first minute of system operation.[194] Pantelic et al. (2015) studied the impact of personal ventilation versus mixing ventilation using inhalation intake factor for droplets released by coughing roughly 1 to 4 meters away from a thermal manikin. The personal ventilation system was substantially better than mixed ventilation at reducing inhalation intake fraction for cough drops regardless of distance and orientation. Intake fractions for personal ventilation were lower relative to mixed ventilation, by roughly 41 and 99 %.[195] Personalized ventilation can be a supplement for traditional methods of reducing airborne infectious transmission risk and can improve the personal exposure index, a metric similar to the air quality index but at the personal scale, when flow rates increase.[174,175] There is also potential for wearable personal ventilation devices; Bolashikov et al. (2013) tested the

impact of a wearable personal ventilation device relative to mixed ventilation in terms of reductions of a tracer gas, R134a, used to simulate pollution/airborne pathogen-laden nuclei in the breathing zone.[176] They found that wearable personal ventilation devices can increase the portion of clean air inhaled by up to 94% depending on the clean air delivery rate, nozzle geometry, initial velocity, and direction of jet.[176]

There exists little work concerning personal ventilation (PV) systems on the pollutant ozone. Two studies have investigated the impact of PV on ozone in the breathing zone. Russo and Khalifa (2010) performed a CFD analysis on the impact of ozone entering the breathing zone through personal ventilation systems and the potential reaction with d-limonene emitted from the floor below a modeled occupant. Three cases were modeled: no PV, a PV system with a single round jet, and a novel low-mixing co-flow nozzle. The co-flow nozzle had the highest level of ozone in the breathing zone, followed by the PV system with a single round jet and the no PV system. For d-limonene and its hypothetical reaction product, the inverse was observed; the co-flow had the lowest concentration of both compounds in the breathing zone, followed by the PV system with a single round jet and the no PV system.[196] A similar study was performed by Russo and Khalifa (2011) on the impact of personal ventilation in removing squalene oxidation products from the breathing zone, finding that a PV system can reduce inhalation exposure to the reaction products by a factor of four.[197] To my awareness, there are no studies on the impact of air cleaning directly in the breathing zone on ozone concentrations inhaled and none evaluating the impact of the various air cleaning methods at scale, on breathing zone concentrations.

Empirical studies evaluating the impact of air cleaning in the breathing zone are lacking, in part, due to the lack of air cleaning devices that specifically target the breathing zone. A study evaluating breathing zone filtration in an office environment found that after installation of a breathing zone filtration system, symptoms related to poor indoor air quality such as sick building syndrome, lethargy, and low productivity were significantly reduced.[198] Gore et al. (2014) developed a novel temperature control air cleaning device targeting the breathing zone and found that the total magnitude for reductions of particle size greater than 0.5 μ was > 99%.[199] Another study compared the removal of particles in the breathing zone between a temperature-controlled laminar airflow (TLA) device that delivers clean air to the breathing zone and room air cleaners.[200] The TLA provided substantial improvements in particle number concentration reductions in the breathing zone when compared to room air cleaners.[200]

In summary, there are no studies on the impact of air cleaning directly in the breathing zone on ozone concentrations inhaled and none evaluating the impact of the various air cleaning methods on breathing zone concentrations. The goal of this work is to close this gap and quantify the effectiveness of breathing zone air cleaning relative to other ozone mitigation and removal methods for the indoor environment.

2.4.3. Research summary

For this Ph.D., four studies have been planned or performed to evaluate the impact of passive and active air cleaning methods on occupant inhalation of ozone, a gaseous compound detrimental to human health. The first study, described in section 3, evaluates

the ability to measure ozone fluxes through gradient approximations at the rooftop scale and measure CO_2 uptake and evapotranspiration for green and urban surfaces in North Portland, OR. The second study, presented in section 4, is a chamber study to measure ozone uptake resistances of green roofs and green roof substrates and a comparison between green roofs and standard rooftops in terms of passive removal of ozone. The third study, described in section 5, investigates the influence of rooftop type on loaded matter on rooftop air handling unit (AHU) filters in terms of primary volatile organic compounds (VOC) emissions, ozone removal, and VOC emissions in the presence of ozone. The fourth study, described in section 6, is a systematic evaluation of the effectiveness of various air cleaning methods on the inhaled quality of air. Sections 3, 4, 5, and 6 are presented as separate manuscripts that have either been published or are organized for potential future publication.

3. Economical methods of pollutant deposition measurements at the rooftop scale and local-scale CO_2 exchange and evapotranspiration between urban green and hard surfaces

3.1. Introduction

Direct measurements of ozone deposition using high frequency, eddy covariance instruments can be cumbersome and expensive to deploy; there are only a handful of flux towers around the world with the ability to make ozone eddy flux measurements.[201] Dry deposition of ozone to vegetation occurs through surface-mediated reactions via plant gas-exchange pathways and on leaf cuticles or other plant material, soils, and water. Uptake within the plant canopy predominantly occurs via stomatal openings as cuticular uptake of ozone is a few orders of magnitude lower than stomatal uptake.[202] Therefore, scalar relationships between ozone fluxes and CO_2, H_2O, or heat fluxes above urban vegetation canopies may provide a more economically feasible measurement technique to quantify ozone deposition to urban vegetation.

Plant stomatal CO_2 uptake has also been utilized to suggest urban vegetation as a carbon sink in the urban environment; a strong relationship exists between annual CO_2 emissions measured in urban areas and urban vegetation cover fraction.[203] Nowak and Crane (2002) estimated the carbon storage capabilities of urban trees in the U.S., finding that urban trees stored approximately 700 million tons of carbon with a gross sequestration rate of 22.8 million tC $year^{-1}$.[204] Brack (2002) modeled the impact of trees in Canberra, Australia to carbon sequestration, predicting that trees within the city may store 300,000

tons of Carbon between 2008 and 2012.[205] Getter et al. (2009) measured carbon sequestration to eight green roofs in Michigan and four in Maryland finding that green roofs stored roughly 162 g C m^{-2} in aboveground biomass.[206] Heusinger and Weber (2017) measured CO_2 uptake for a green roof in Berlin, Germany, finding that net ecosystem exchange for CO_2 is −313 g CO_2 m^{-2} $year^{-1}$, equivalent to −85 g C m^{-2} $year^{-1}$.[207] Konopka, Heusinger and Weber (2021) measured net CO_2 uptake for 5 years at the same rooftop in Berlin, Germany. They found that green roofs showed a net carbon uptake for each of the 5 years of measurement, with an average of −141.1 g C m^{-2} y^{-1} and an average measurement uncertainty of ±15.5 g C m^{-2} y^{-1}.[208]

These removal estimates allow for the removal of atmospheric pollutants to be commonly cited as a potential urban ecosystem service of vegetation, but there is little support for it empirically.[209] Velasco et al. (2013) studied the role of vegetation in urban CO_2 fluxes in Singapore, finding that that vegetation sequesters 8% of the total emitted CO_2 in a residential neighborhood, but when incorporating soil respiration, there is a net biogenic emission contributing to 4 % of the total CO_2 flux.[210] The impact of evergreen vegetation on residential CO_2 flux was studied in Singapore and Mexico City, where biogenic emissions from greenery contribute to -1.4% to 4.4% of the total suburban CO_2 flux.[211] In Korea, the annual reduction of CO_2 emissions from cities due to urban vegetation is between 0.5 (Seoul) to 2.2 % (Kangleung).[212] The influence of Sedum-dominated green roofs on CO_2 concentrations was studied by Agra et al. (2017), where they found that while night-time CO_2 uptake occurred, it did not fully compensate for high day-time CO_2 emissions from green roofs during the arid season.[213] Li et al. (2010) systematically studied

the CO_2 uptake by green roofs through field measurements, chamber experiments, and numerical simulations, finding only reductions of ~2% in average CO_2 concentration, similar to that observed for other air pollutants such as ozone.[214,215]

The first effort of this work sets out to measure CO_2/H_2O exchange to a site incorporating both urban green and hard surfaces for a full year through eddy-flux measurements. This measurement is separated by seasons and representative surface morphology (associated with two broad categorizations of urban surfaces: "green" and "hard" surfaces). The urban green surfaces include a green roof, a soccer field, and trees northwest of the measurement location and the urban hard surfaces includes a white rooftop, a roadway, and a parking lot east-northeast of the measurement site. This first effort has been submitted for publication at *Urban Climate*. A second effort uses the micrometeorological data and CO_2/H_2O flux data collected in this first effort to evaluate the use of the atmospheric gradient method (AGM) and the modified-Bowen ratio method (MBR) for ozone deposition measurements at the rooftop scale.

3.2. Material and methods

3.2.1. Site Description

Measurements of CO_2/H_2O exchange and meteorological parameters are made on the rooftop of a big-box retail store in north Portland, OR. The rooftop is comprised of three extensive green roof sections varying according to substrate depth (~3600 m^2 of total green roof area) and a 'white' roof section (~5400 m^2) covered only in a white waterproof membrane, shown in Figure 1b, totaling a combined rooftop area of 9,000 m^2. The green

roof design varies by section and is comprised of a scoria-dominated substrate over a capillary fabric and waterproofing membrane. The plant community is a mixture of succulent and herbaceous plants that are both planted and introduced; dominant species include *Erodium cicutarium, Plectritis congesta, Phedmus takesimensis, Sedum rupestre* 'Angelina', *Trifolium repens, and Vulpia sp.* As much as 20% of the roof coverage is classified as rock/gravel. Three artificial soccer fields were directly northwest of the rooftop site, considered as part of urban 'greenery' at the field site. A roadway and two parking lots are present to the east-southeast of the rooftop, considered as part of urban "hard" surfaces. A major interstate highway (I-5) is present to the west of the building. This highway is located over 500 meters from the measurement location and its impact on site air quality is expected to be modest as pollution from traffic typically reaches urban background levels within ~500 meters.[216]

Field measurements occurred between October 2018 to October 2019. During November 2018 and December 2018, minor repairs were conducted to the rooftop site to manage minor leakage of water into the skylights of the building. While regular, controlled irrigation was not performed during this study, maintenance personnel performed roof leak tests before 3 storm events in February, April, and May 2019.[217]

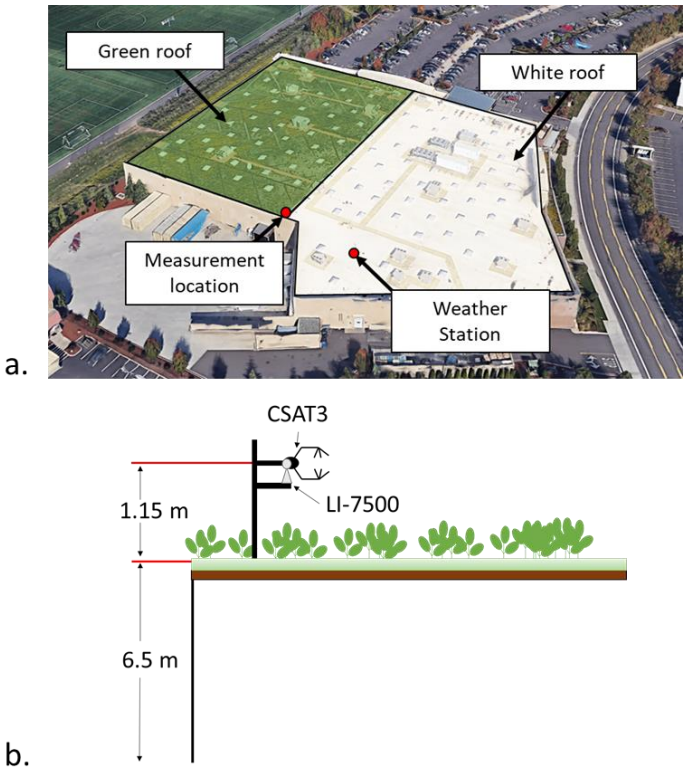

Figure 1. a. Outline of the measurement location and field site **b.** Field set up for CO_2/H_2O fluxes and meteorological data on the rooftop site. The average height of the mixture of plants is approximately 0.2 m.

A three-dimensional sonic anemometer (Campbell Sci., CSAT3) measured velocity and temperature fluctuations at a measurement rate of 10 Hz. The sonic anemometer is placed such that the center of the axis in the z-direction is 1.15 m above the green roof surface, based on Heusinger (2017), and is oriented such that the head is aligned with N (= 0°), shown in Figure 1b.[207] An open-path CO_2/H_2O gas analyzer (LI-COR, LI-7500) measured CO_2/H_2O fluctuations at a height of 1.15 m and a measurement rate of 10 Hz to match the sonic anemometer, shown in Figure 1a. The concentration and meteorological data are averaged over a 30-min period.[218] All monitoring equipment and the switching valve are enclosed in a ventilated, acrylic enclosure to protect the instruments from wind,

rain, and heat. A weather station located on the white roof portion (Figure 1b) captured site precipitation (mm), air temperature (°C), RH (%), and net radiation (W m^{-2}).

A single ozone monitor (2B Tech, 106L) measured ozone concentration at heights of 1.15 m and 1 m above the rooftop every 2 s. An automated Solenoid valve controlled by a measurement and control datalogger (Campbell Scientific, CR-1000) alternated between the heights at 10-min intervals. The concentration at each height is interpolated and averaged over a 30-min period.[218] All monitoring equipment and the solenoid valve were enclosed in a ventilated, acrylic enclosure to protect the instruments from wind, rain, and heat.

Velocity fluctuations in the x, y, and z-direction are used to determine the friction velocity, similar to the approach by Bryan et al. (2012), where shear stresses measured by a sonic anemometer are used to determine the wall shear stress and subsequently the friction velocity.[219] Temperature fluctuations in combination with velocity fluctuations in the z-direction are used to determine heat flux over the rooftop.

3.3. Theory and calculations

3.3.1. Eddy correlation technique

The eddy correlation (EC) technique, also known as the eddy covariance technique, is a direct, non-intrusive measurement of the flux of a pollutant. The EC technique measures the turbulent flux by calculating the covariance of the fluctuating vertical component of velocity (w') and the fluctuating concentration of the pollutant (C').

$$F_O = \overline{w'C'} \quad (1)$$

Prior work has shown the validity of using this technique in conjunction with wind and seasonal data to understand the influence of local sources on measured CO_2 fluxes.[220–225] Vesala et al. (2008) studied the influence of complex urban terrain on turbulent exchange of CO_2, sensible and latent heat fluxes, and used wind data to partition fluxes to vegetation, roads, and urban areas with high building cover. Järvi et al. (2012) measured CO_2 fluxes from an urban site from 2006 to 2010, partitioning their measurement by seasons and wind directions.[225] Disadvantages associated with flux partitioning via wind sector analysis are the lack of quantitative information about the influence of local sources on total CO_2 fluxes and the limited value for sites with complex heterogeneous surface morphology.[203] But the inclusion of footprint models that utilize meteorological data combined with landcover classifications may provide more value in understanding the influences of measured fluxes.[203,223,226–228] Eddy correlation measurements in urban areas are specifically challenging because of the complexity of the urban surface morphology, the heterogeneity of urban carbon sources, and the limited sites where a tall tower may be installed.[203,226] Measurements from this study should be considered as local-scale measurements of CO_2/H_2O partitioned according to seasonal conditions and wind data.

3.3.2. Aerodynamic gradient method

The AGM assumes that turbulent transport is analogous to molecular diffusion and involves an eddy-diffusivity term for the gas, K_c. The vertical flux is described by the following equation:

$$F_O = K_c(\mathrm{z}) \times \frac{dC}{dz} \qquad (2)$$

where $\frac{dC}{dz}$ is the concentration gradient with respect to height and K_c is related to the aerodynamic resistance:

$$R_a(z_1 : z_2) = \int_{z_2}^{z_1} \frac{dC}{K_c(\mathrm{z})} \quad (3)$$

where z_1 and z_2 represent two adjacent measurement heights (z_1>z_2). By combining equation 2 and 3, the only resistance assumed between the two measurement heights is the aerodynamic resistance which can be used to calculate v_d as shown in equation 4:

$$F_O = -\frac{\Delta C_\mathrm{o}}{r_a(z_1 : z_2)} = -v_d \times C_\mathrm{o} \quad (4)$$

where ΔC_o (μg/m^3) is the change in concentration between an upper position, z_1 (m) and the lower position, z_2 (m), r_a (z_1: z_2) (s/m) is the aerodynamic resistance between $z_1$and z_2, and all other terms are as defined previously.

3.3.3. Modified Bowen Ratio

The modified Bowen ratio (MBR) is like the flux-gradient theory, but the eddy diffusivity is derived from measurements of another scalar, such as sensible heat, CO_2, and H_2O. For this study, both CO_2 and H_2O fluxes are evaluated for their accuracy in applying the MBR method. The application is as follows:

$$K_c(\mathrm{z}) = K_s(\mathrm{z}) = -F_s \times \frac{\Delta z}{\Delta C_s} \quad (5)$$

where $K_s(\mathrm{z})$ is the eddy diffusivity of the scalar, F_s is the eddy flux measurement of the scalar, ΔC_s is the concentration gradient of the scalar over the same height difference as the ozone measurement.

We can combine equations 2 and 5 to give:

$$F_O = F_s \frac{\Delta C_o}{\Delta C_s} = -v_d \times C_o \quad (6)$$

3.4. Data Analysis

The flux associated with CO_2/H_2O can be to a large area and is determined by local wind conditions, fluxes derived from wind directions 150° to 290° (S/SW) are excluded as the surface morphology did not allow for clear delineation between urban green surfaces and urban hard surfaces. Although the fluxes were parsed to include the rooftop type, CO_2 and H_2O flux cannot be attributed fully to the green roof or white roof as that would only be met in ideal conditions, such as an infinite rooftop surface.[229] Fluxes from wind directions from -60° to 10° (W/NW) are associated with the green surfaces (the green roof and the park) and wind directions from 30° to 110° (E/SE) are associated with urban "hard" surfaces.

Processing of the 10 Hz eddy flux raw data is performed by the EddyPro Version v7.0.6 with 30-minute averaging, double coordinate rotation, corrections for density in the presence of heat and water vapor, and spectral corrections.[230–232] Spectra and co-spectra is filtered for quality according to automated tests developed by Vickers and Mahrt (1997).[233] Quality flags, a data quality classification marker using a steady-state test and integral turbulence characteristics, are calculated for all fluxes based on the Foken et al. (2003); fluxes that attain a combined flag value of "6" or lower are deemed appropriate for rooftop flux analysis.[234,235] The flux footprint is calculated for each 30-minute period according to the analytical footprint model for scalar fluxes presented by Kormann and Meixner (2001)

and similar to Heusinger (2017).[235,236] Due to the size of the green roof and white roof, the mean 70% footprint isoline (~40 m) is entirely within the fetch of the green and white roof (~50-60 m). But as there may have been influence from local anthropogenic sources within 90% footprint isoline, the measured fluxes represent the exchange between the rooftop and the surrounding surfaces within an urban biosphere.[235,237–239] The footprint length is expected to vary with atmospheric conditions; smaller footprints are expected during the unstable, daytime periods and larger footprints are expected during stable, nocturnal periods.[235]

3.4.1. Statistical analysis and uncertainty propagation

Shapiro-Wilk tests are used to check the normality of CO_2 flux, ET, and ozone flux datasets across the full test period as well as datasets separated by wind direction (associated with green and hard surfaces). Shapiro-Wilk tests with output p-value < 0.05 are ignored but all datasets and subsets (seasonal and green/hard surfaces) are found to be normally distributed. A chi-square test for independence is performed between CO_2 flux, ET, and weather data (precipitation (mm), air temperature (°C), RH (%), and net radiation (W m^{-2})) from the weather station. Both ET and CO_2 measurements are dependent on local weather patterns. Quality of eddy covariance measurements is performed using the EddyPro Version v7.0.6 based on a method specified by Foken et al. (2003).[234] A 95% confidence interval is determined for each dataset and is displayed as gray bars in the figures below.

3.5. Results and discussion

3.5.1. CO_2/H_2O exchange at the rooftop field site

CO_2 and H_2O mole fractions, CO_2 fluxes, and evapotranspiration (ET) for the full study averaged across a 24-hour period are shown in Figure 2. The mean CO_2 mixing ratio at the rooftop is 437 ± 33 ppm and the mean H_2O mole fraction is 13.4 ± 6.1 mmol mol^{-1}. Across both surface types, the mean CO_2 flux is 5.4 ± 7.3 μmol m^{-2} s^{-1}, and the mean ET is 0.01 ± 0.02 mm h^{-1}, shown in Figure 2b. Aggregating across the year, the CO_2 flux is relatively constant throughout the day, in the expected range for urban CO_2 fluxes, roughly 0 – 15 μmol m^{-2} s^{-1}, lacking an obvious diurnal trend as observed in some prior studies.[210,240,241] This is expected given the location of these measurements and the flux footprint that includes urban surfaces that contain feeder streets to a parking lot that lack morning and evening rush hour traffic patterns that are shown to influence urban CO_2 measurements.[241–245] Evapotranspiration (ET) at the field site follows a diurnal pattern; a positive, higher flux during the daytime and lower/non-existent flux at night.[246] The Kormann and Meixner (2001) model is used to generate the footprint associated with the measured flux, and shown in Figure 2c.[236] Wind directions between 150° to 290° (S/SW) are excluded as they would not allow for a clear delineation between urban greenery and urban hard surfaces. The 70% footprint isoline is located almost entirely within the rooftop, apart from the roadway and parking lot adjacent to the field site. The footprint length can vary due to atmospheric conditions, where the nighttime flux footprint can encompass non-rooftop surfaces, therefore, measured fluxes cannot be attributed to strictly rooftop surface exchange.

3.5.2. Influence of local traffic-related emissions

The 90% flux footprint encompassed the full Walmart parking lot (Figure 2c), the adjacent parking lot, the roadway between the two lots, and multiple soccer fields which saw high activity on spring and summer weekends. The measurement location is within 115 m of a well-traveled roadway and traffic-related emissions may affect flux measurements.[216] Heusinger and Weber (2017) evaluated the effect of aircraft emission plumes located close to their 90% footprint isoline and did not find an increase in CO_2 flux due to increases in flights from the airport.[207] A similar assessment of local anthropogenic carbon emission sources cannot be performed at the field site as a quantitative measurement of the continuous daytime pattern of cars, trucks, and general traffic at the field site location is not performed. Data associated with 'green' and 'hard' surfaces may also have been influenced by varying local traffic patterns; the 90% footprint associated with hard surfaces (E/NE) encompasses a roadway and two parking lots and the 90% footprint associated with green surfaces (W/NW) covers soccer fields, a few trees, and potentially a small portion of the Walmart parking lot. Seasonal data may have been influenced by land cover classifications; wind directions for dry seasons are predominantly from the W/NW direction, over green surfaces, and wet and transitional seasons are predominantly from E/SE direction, over hard surfaces, and a markedly different emission source. Traffic-related emissions are therefore more likely to influence CO_2 flux measurements during the wet season than during the dry season. Seasonal rates of ET may also be dependent on land surface classification, as explained in section 4.3, urban greenery has a noticeably different ET profile than urban hard surfaces.

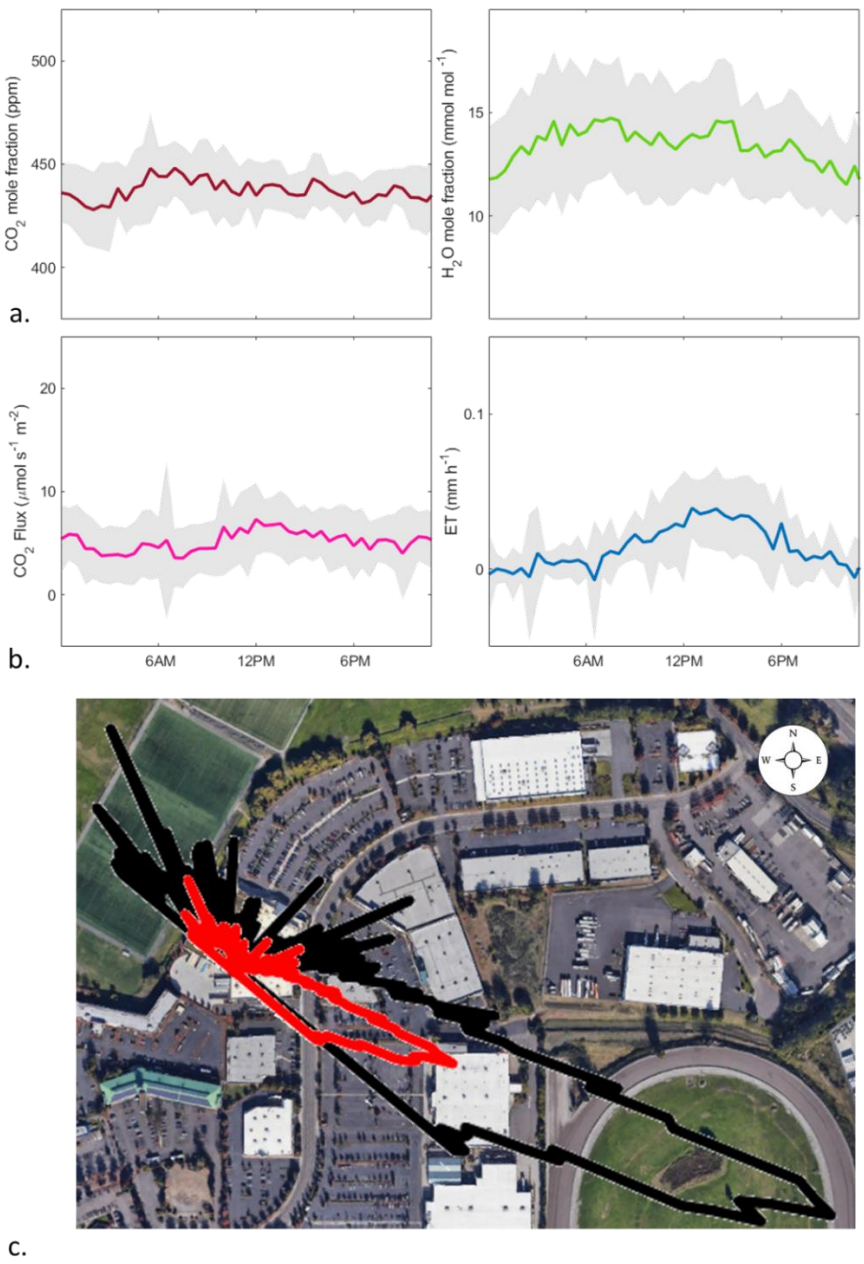

Figure 2. a. Rooftop CO_2 and H_2O mole fractions from the rooftop field site aggregated across the measurement period (Oct 2018 – Oct 2019). **b**. Rooftop CO_2 fluxes and ET for the rooftop field site aggregated across the measurement period (Oct 2018 – Oct 2019). Gray areas in both figures represent a 95% confidence interval. **c.** 70% (red) and 90% (black) footprint isoline overlay associated with the measurement period. Footprint estimation is based on the Kormann and Meixner (2001) analytical model. Wind directions from 150° to 290° (S/SW) are excluded due to the surface morphology not being representative of the rooftop.

3.5.3. Seasonal variation of CO_2/H_2O exchange at the rooftop field site

Site precipitation (mm), air temperature (°C), RH (%), and net radiation (W m^{-2}) from the field weather station are shown in Figure 3a. Seasons for this study are described as 'wet' (October - March), 'transitional' (April - May), and 'dry' (June - September) seasons.[247] The wet season corresponds with higher precipitation periods and relative humidity as well as lower air temperature and net radiation. As expected, drier months coincided with periods of lower precipitation and relative humidity as well as higher net radiation. Wind directions for dry periods are predominantly over greener surfaces and wind directions for wet and transitional periods are over a parking lot and roadway, potential anthropogenic emission sources for CO_2.

The seasonal variation of CO_2 and ET for the study period is shown in Figure 3b. Generally, CO_2 emissions in the dry season are low, with a mean of 0.85 ± 1.98 µmol m^{-2} s^{-1} and the highest CO_2 flux is in the wet season, 6.51 ± 2.63 µmol m^{-2} s^{-1}. CO_2 fluxes for the transitional period are 2.02 ± 3.68 µmol m^{-2} s^{-1}. These measurements match well with urban biosphere measurements of seasonal CO_2 fluxes, with higher fluxes expected in winter months which are usually wetter and colder and lower fluxes in the dry, summer months.[237–239] The transitional (April and May) and dry (June, July, and August) periods are generally associated with higher photosynthetic activity, which can impact the net carbon transport in the urban biosphere and reduce total CO_2 flux in the urban environment.[238]

Evapotranspiration (ET) followed an expected diurnal pattern, with higher rates in the middle of the day and lower at night. ET during the wet, transitional, and dry seasons are, 0.25 ± 0.41 mm d^{-1}, 0.71 ± 0.54 mm d^{-1}, and 0.48 ± 0.68 mm d^{-1}, respectively. During the wet seasons, components that drive ET such as the air temperature and net radiation are low, leading to little ET on the rooftop and surroundings.[248,249] As temperature and net radiation increase, ET increases and is evident in the transitional period. During the dry period, there is little precipitation, a potential precondition for ET, therefore there is lower ET relative to the transitional period.

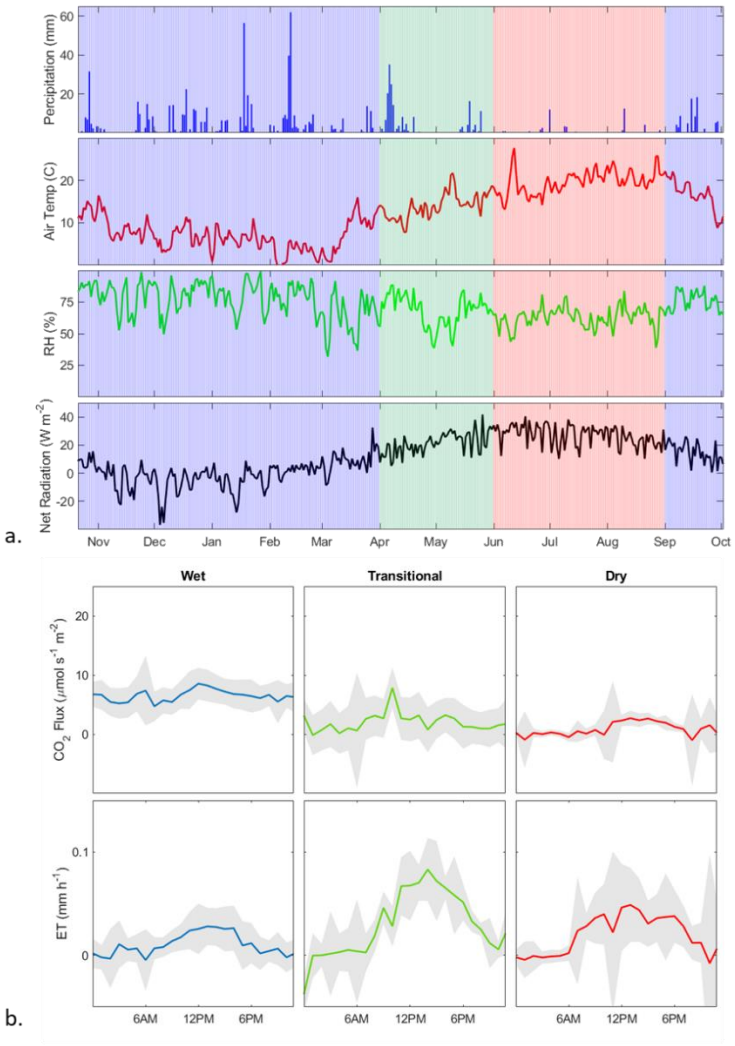

Figure 3. a. Precipitation (mm), Air Temperature (°C), RH (%), and Net Radiation (W m^{-2}) for the study period. Colors represent wet (blue), transitional (green), and dry (red) seasons. **b.** Seasonal CO_2 and evapotranspiration for the rooftop field site aggregated daily across the measurement period (Oct 2018 – Oct 2019).

3.5.4. CO_2 and H_2O exchange for urban green and hard surfaces

Urban green and hard surfaces are determined based on surface morphology; green surfaces are surfaces that have plants, trees, and other forms of vegetation whereas parking lots, roadways, and surfaces with no vegetation are categorized as urban hard surfaces.

Because of regional meteorological trends, wind directions associated with the urban hard surfaces are roughly three times more abundant than wind directions associated with the green surfaces; 881 30-minute periods (23% of the measurement period) are associated with the urban hard surfaces, and 304 30-minute periods (8% of the measurement period) are related with the green surfaces.

CO_2 fluxes and ET for green and urban hard surfaces are shown in Figure 4. Average green surface CO_2 fluxes are much lower than urban hard surfaces, 0.64 ± 1.55 μmol m^{-2} s^{-1} and 8.63 ± 6.78 μmol m^{-2} s^{-1}, respectively. The 90% footprint isoline for measurements of wind directions associated with green surfaces encompassed the green roof as well as the artificial soccer field directly northwest. The urban hard surface 90% footprint measurements encompassed a white rooftop, a roadway, and a parking lot; these marked differences in the nature of the surface are plausible explanations for the differences in observed CO_2 flux.

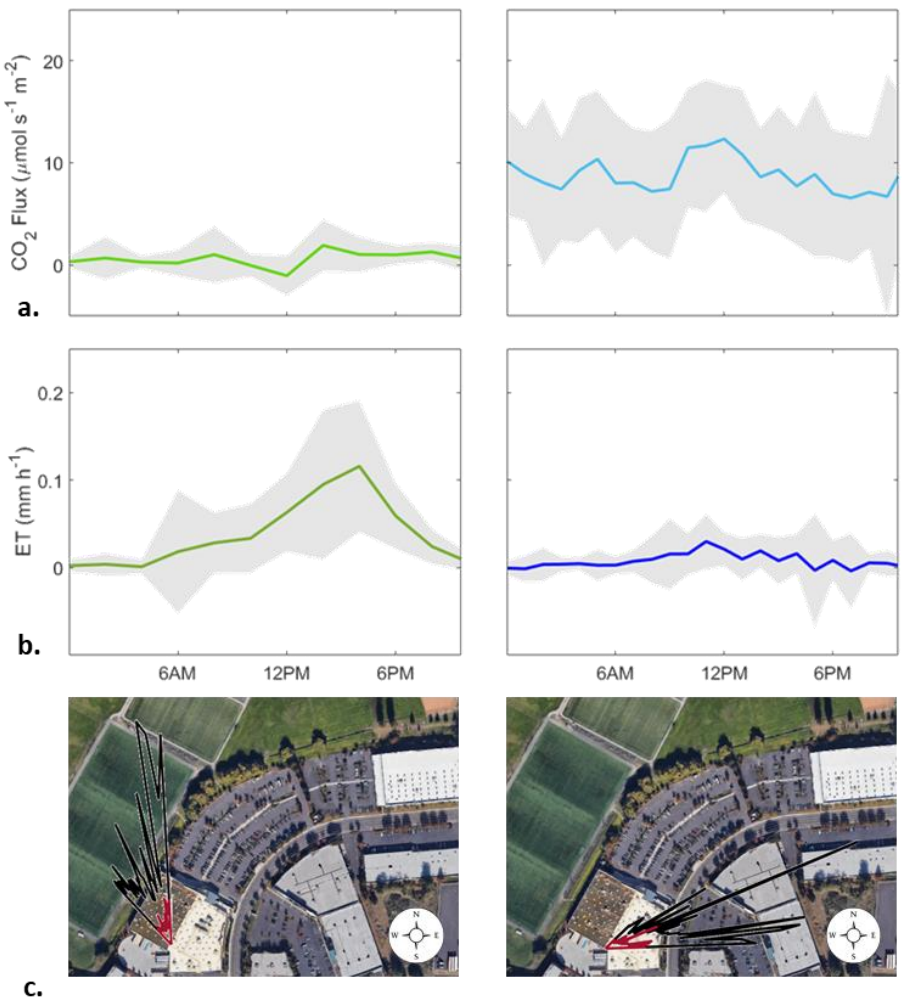

Figure 4. Hourly green (left) and hard (right) surface **a.** CO_2 fluxes and **b.** evapotranspiration aggregated over the study period (Oct 2018 – Oct 2019) **c.** Green and hard surface 70% (red) and 90% (black) along wind footprint isoline.

Heusinger and Weber (2017) reported a net carbon uptake of -85 g C m^{-2} yr^{-1} for green roofs and Konopka, Heusinger, and Weber (2021) reported a net average carbon uptake for green roofs across 5 years of -141 g C m^{-2} yr^{-1} [207,208]. CO_2 uptake to urban green surfaces is not observed in our measurements; net carbon atmospheric exchange for the green and hard surfaces are 241 ± 570 g C m^{-2} yr^{-1} and 3260 ± 2570 g C m^{-2} yr^{-1}, respectively. Velasco et al. (2013) showed that vegetation and soil together can act as a net

source of CO_2 in a tropical climate, similar to the positive carbon flux measured for wind directions associated with urban greenery measured in this study.[210] Sedum-dominated green roofs during arid periods have been shown to increase local CO_2 concentrations, potentially explaining the positive flux measured in this study.[213] While urban greenery may store carbon during the first few years of installation, as the vegetation matures, the net carbon sequestrate reaches an equilibrium where decomposition of organic matter equals carbon sequestration.[206,250] The difference in net carbon atmospheric exchange between wind directions associated with green and hard surfaces is most likely due to the differences in potential carbon emission sources between the two wind directions. Transport-related CO_2 emissions from a roadway and two parking lots may be the reason for an order of magnitude difference between urban greenery and urban hard surfaces.

The incorporation of large trees can indirectly affect urban CO_2 flux via local cooling through shading and transpiration.[210] Increased cooling in the urban environment leads to lower demand for air conditioning resulting in reductions in greenhouse gas emissions from lower indoor cooling energy demand.[251] Measured evapotranspiration, a proxy for urban cooling,[252] is on average higher for urban green surfaces relative to urban hard surfaces, 0.96 ± 0.95 mm d^{-1} and 0.19 ± 0.93 mm d^{-1}, respectively. Higher evapotranspiration rates can reduce urban temperatures by 0.5 to 4.0 °C and is correlated with reducing the effects of urban heat island.[252–254] Heusinger and Weber (2017) reported Bowen ratios, the ratio of sensible heat fluxes to latent heat fluxes and a measure of the urban heat island effect, for green roofs to be much lower than normal urban levels, but highly variable and dependent on ambient meteorology and substrate water availability.[235]

3.5.5. Comparison of eddy covariance to the AGM and MBR methods

A part of this study is meant to compare the rooftop measurement techniques for scalar fluxes, such as CO_2 and H_2O fluxes, and apply the AGM and MBR methods to ozone fluxes as given by Wu et al. (2015).[255] Eddy correlation fluxes of CO_2 and H_2O were measured throughout the measurement period, from October 2018 to October 2019, and closed-path CO_2 and H_2O fluxes were measured only between March 2019 to October 2019. A comparison of EC and AGM measurements of CO_2 and H_2O fluxes made from March 2019 to October 2019 are shown in Figure 5a and 5b. Linear regression is applied using MATLAB R2020b 'fitlm' function between the measured CO_2 and H_2O fluxes using the AGM method and measured fluxes from the EC method, shown in Figures 5c and 5d.

For CO_2 fluxes, the AGM was somewhat correlated with the EC method ($R^2 = 0.52$) whereas for H_2O fluxes, the diurnal profile between the two methods was unlike, and a linear regression showed a poor fit ($R^2 = 0.24$). The AGM assumes homogeneous surface conditions, which cannot be met at the field site, and that the mixing length at the measurement height is smaller than the length scale over which mean gradients are measured, which may not have been met with upper and lower measurement locations at 1.15 m and 1 m, respectively.[256,257] Most urban measurement locations do not meet the required conditions to appropriately apply the AGM accurately without introducing large errors, in part due to the complex morphology, inhomogeneity, and proximity to sources and sinks.[257–259] Specific adjustments, such as removing counter gradients, and the application of a 'mixed layer' analogy can be utilized to potentially improve the accuracy

of the measurements.[258,260,261] The MBR, a method that requires similar assumptions as to the AGM, cannot be applied as, similar to the AGM method, these assumptions may not be met at the field site. Also, the MBR assumes that scalar transport within the surface layer is alike, but the dynamic sources of CO_2 and H_2O above a plant canopy, such as soil heterotrophic and root respiration and plant autotrophic respiration, do not coincide with sources of ozone above vegetation. Ozone fluxes measured using the AGM or MBR method are likely to be inaccurate overestimates of the removal to urban greenery.[255]

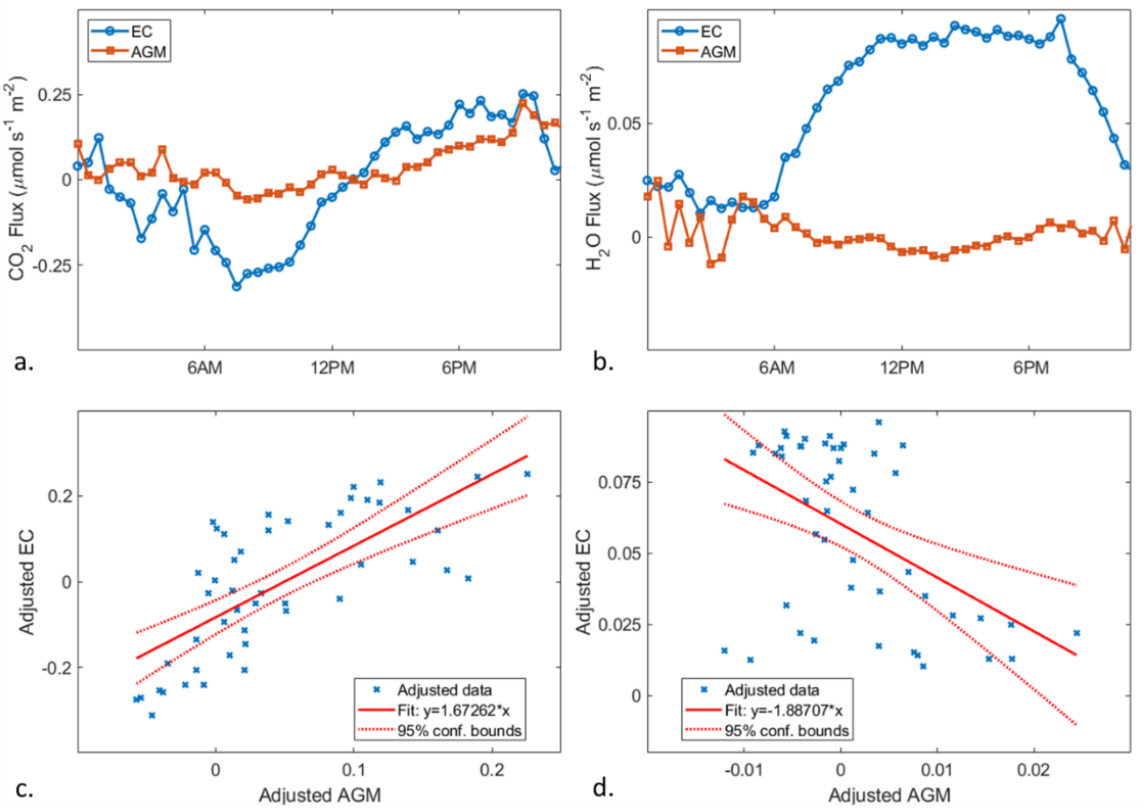

Figure 5. a. CO_2 fluxes measured through the EC (blue) and AGM (red) methods. **b.** H_2O fluxes measured through the EC (blue) and AGM (red) methods. **c.** Linear regression for CO_2 fluxes measured through the EC method and the AGM method, $R^2 = 0.52$. **d.** Linear regression for H_2O fluxes measured through the EC method and the AGM method, $R^2 = 0.24$.

3.5.5.1. Potential improvements to AGM and MBM methods

A potential solution to improve the accuracy of the AGM is to remove counter gradients that are associated with the upward motion of local eddies. The AGM assumes that the flux of a pollutant is strictly downwards, therefore the upward gradients due to turbulent motion can introduce large errors that need should be controlled.[260] Another potential improvement to the accuracy of the gradient method is to apply a 'mixing' layer

analogy instead of the standard Monin-Obukhov similarity theory (MOST) flux-gradient relationships. Due to the impact of local anthropogenic sources, it can be argued that the measurements were conducted within the urban roughness sublayer. The MOST relationships fail in this roughness sublayer, a layer that is roughly from the top of the canopy to two canopy heights. But turbulence in the roughness sublayer may be characterized by coherent structures whose characteristic properties may resemble more of a plane mixing layer between two flows, one below the canopy and one above the roughness sublayer.[258,260,261] This allows the potential use of a mixing length formulation for the scalar profile within and above an urban canopy.[260]

3.6. Conclusions

For the measurement period, the mean CO_2 flux is 5.39 ± 7.26 μmol m^{-2} s^{-1} and the mean evapotranspiration (ET) is 0.01 ± 0.02 mm h^{-1}. Average ET was measured to be higher on urban green surfaces than on urban hard surfaces, 0.96 ± 0.95 mm d^{-1} and 0.19 ± 0.93 mm d^{-1}, respectively. Average urban hard surface CO_2 fluxes are higher than the average green surfaces, 7.74 ± 6.65 μmol m^{-2} s^{-1} and 0.60 ± 1.57 μmol m^{-2} s^{-1}, respectively. While not as emissive as urban hard surfaces, urban greenery has a positive emission flux, matching previously reported results on the impact of urban vegetation on urban CO_2 levels.[209–212,214] The contribution of urban vegetation to human health has been well documented, but the impact on urban CO_2 levels may be more modest.[209,262–266] Over 90% of total CO_2 fluxes measured in this study were from urban hard surfaces (which includes a parking lot and a roadway, potential fossil fuel emission sources), matching prior work

on urban biogenic and anthropogenic CO_2 flux measurements.[220,237,239,267,268] This may imply that reductions in abiotic urban CO_2 emission sources such as fossil fuel combustion, may realize a larger impact on urban CO_2 levels than increasing urban vegetation cover alone.

Site conditions did not completely meet the requirements to apply the AGM, as well as the MBR method, and ozone measurements made through these methods are therefore inaccurate. The AGM assumes homogeneous surface conditions and the length scale over which mean gradients are measured is larger than the length scale of turbulence, which may not have been met at the field site. The MBR method assumes that the behavior of scalar fluxes in the constant flux layer above the vegetation canopy is similar, but heterotrophic and autotrophic sources of CO_2 from vegetation may not be related to the photochemical reaction process that leads to ozone formation above vegetation.[269,270] While EC methods are one approach to capturing local-scale flux measurements, this study highlights the need for further study of approaches for measuring mass deposition or emission within the urban landscape.

4. The potential for rooftops to passively remove ozone prior to entering the indoor environment

4.1. Introduction

Tropospheric ozone plays an important role in climate and atmospheric chemistry, but in the urban and indoor environment, it can be detrimental to human health.[4,29] In the U.S.A., increases in ozone concentrations are predicted to result in over 2,200 additional premature deaths annually by the 2050s.[271] One strategy for reducing the health impacts of ozone exposure is to remove ozone from indoor environments, where 45-75 % of total exposure occurs.[272]

Methods of removing ozone in the indoor environment can be roughly categorized as passive or active air cleaning. Energy consumptive air cleaning technology such as building scale cleaning through HVAC systems, room cleaning through room air cleaners, and breathing zone ventilation and air cleaning are examples of active cleaners which require non-trivial energy to remove pollutants from the indoor air. Passive air cleaning technology requires no energy, outside of energy that would otherwise have similarly been input for building operation, for pollutant removal and has been suggested as a method of improving indoor air quality without increasing building operational costs.[94,142,143] Proposed passive mitigation technology is often based on natural ventilation, functionalized surfaces, vegetation, or other reactive surface material and can exist in the indoor environment or outdoors in the vicinity of the building, cleaning the air that enters the indoor environment.[94,111,141–143] Building rooftop surfaces utilizing vegetation, such as

green roofs, near indoor ventilation systems may provide removal sites for outdoor ozone in the air entering the indoor environment.

Urban scale studies have evaluated the potential of vegetation as a passive air cleaning strategy; large-scale dry deposition models show vegetation can be a sink of ozone in the urban environment. Wesely (1986) showed dry deposition over lush vegetation is roughly 40 times more efficient than over urban land.[273] Applying the UFORE/i-Tree model to estimate total dry deposition, Nowak et al. (2006) and Nowak et al. (2014) showed public urban trees removed 205,100 and 523,000 tons of ozone across 55 cities.[274,275] Yang et al. (2008) modeled the dry deposition of ozone to green roofs in the Chicago area, finding ozone removal is roughly ~50.5 kg ha^{-1} yr^{-1}.[145] Using the i-Tree Eco model in Strasbourg, France, Selmi et al. (2016) showed that 63 % of total ozone deposition in the urban environment is to agricultural areas, urban forests, and parks.[276]

Dry deposition models often take data from limited sites or utilize data from plant chamber studies which may not be representative of the local and urban fluid mechanics, canopy structure, length of photosynthetic activity of urban vegetation, and microclimates within the urban area of interest.[274,277] While dry deposition of ozone to urban vegetation may occur, the impact on urban ozone concentrations is modest.[209] Average percent improvement in air quality due to ozone removal by trees across 14 U.S. cities during peak seasonal photosynthetic activity is 0.61 % and annual ozone reduction in urban areas due to tree cover across 55 U.S. cities is 0.36 %.[275,278] Removal of ozone due to urban forests in the city of Florence, Italy is modest, 1.5 % on average, when compared to overall

pollution levels within the city.[279,280] Sicard et al. (2018) reviewed the impact of green roofs and urban forests on urban ozone concentrations, finding that while local reductions to ozone measured via passive samplers above and below urban forest canopies can be upwards of 40 %, modeled percent improvement due to removal of ozone to trees and shrubs is less than 2% in cities.[277,281] Under ideal conditions, modeled removal of ozone to green roofs at the rooftop scale was predicted to be approximately 1.3%.[215]

Passive ozone removal may also have secondary products that should be accounted for. Ozone-initiated reactions with conventional and green building materials have shown the potential to generate secondary volatiles and organic aerosols.[282–285] Ozone interaction with vegetation and/or biogenic volatile organic compounds (BVOCs) can produce compounds with detrimental health effects that should be considered.[117,128,286] Carslaw et al. (2015) modeled the role of outdoor biogenic volatile organic compounds (BVOCs), typically emitted from vegetation, in the formation of secondary organic aerosols (SOAs) inside office buildings, finding ambient biogenic emissions where ozone concentrations are elevated contribute substantially to indoor particulate matter.[34] Rooftop surfaces may impact loading on ventilation filters as well, offering reaction sites for ozonolysis along the ventilation pathway to the indoor environment. Prior work shows increases in oxidation by-products, such as acetaldehyde, downstream of loaded ventilation filters in the presence of ozone.[287–289]

This study is split into two efforts; the first effort sets out to measure the dry deposition of ozone to the green roof and green roof substrate samples through resistance

uptake theory in a chamber environment, varying temperature and light conditions. A second effort is performed in comparing the ozone removal effectiveness of various rooftop surfaces: three building materials; brick, concrete slab, grey tiles, two glass types; new and dirty, and vegetation. This second effort includes the chamber measurements of ozone uptake resistances to the green roof and green roof substrate as well as micrometeorological measurements of aerodynamic components from a rooftop field site that contains a green roof.

4.2. Methods

4.2.1. Chamber Flux Experiments

Chamber experiments, shown in the schematic in Figure 6, were conducted to calculate ozone surface flux specific to the vegetation from the rooftop via experiments similar to those conducted by Simmons and Colbeck (1990).[290] Two cylindrical chambers (diameter = 20.3 cm, height = 20.3 cm) were constructed from acrylic following a similar design as Almand-Hunter et al. (2015): an open-bottom chamber and a closed-bottom control chamber.[291] Tests were conducted by measuring the decay of ozone following elevation to ~350 ppb using a corona discharge ozone generator (Eleoption, B01M8IC3EK). An ozone monitor (2B Tech, 106L) was used to measure ozone concentrations in the chamber every 10 seconds. Following Gall et al. (2015), the deposition velocity, v_d, was calculated by a numerical solution to a mass balance on the chamber.[292] A closed-bottom chamber was used to measure background deposition velocities to acrylic chamber surfaces. The air-exchange rate for the chambers was

measured using a CO_2 tracer decay experiment in the absence of vegetation and averaged 0.196 min^{-1}.

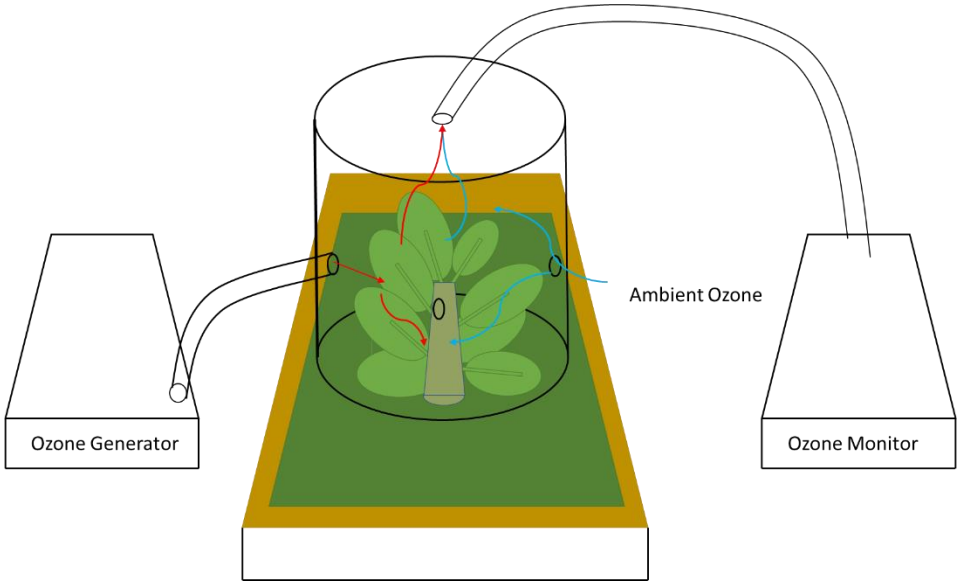

Figure 6. Chamber set up of isolated ozone fluxes over green roof material

One 25.4 cm x 25.4 cm green roof sample and a soil substrate material, removed from a green roof in north Portland, OR, were selected for laboratory measurements of ozone surface flux. Soil moisture was varied by adding and mixing incrementally higher water to the green roof and soil substrate trays and allowing them to saturate overnight. The resulting volumetric water contents determined using a soil moisture sensor (Decagon, EC-5) were, 12, 18, and 25 m3 m^{-3} for the green roof samples, and 3, 4, 7 m3 m^{-3} for substrate sample replicates. Light conditions were varied between 1.2, 14.3, and 100.9 uE for the green roof sample and 1.2, 12.7, and 89.8 uE for the bare substrate sample. The air temperature and relative humidity (Onset, S-THB-M002), substrate temperature (Onset, S-TMB-M006), photosynthetically active radiation (PAR) (Onset, S-LIA-M003), and solar

radiation (Onset, S-LIB-M003) were also monitored throughout the various experiments. Additional experiments were conducted to separate the boundary layer resistance by using potassium iodide (KI), like Almand-Hunter et al. (2015) and Pape et al. (2009).[291,293] However, in these tests, we coated the vegetation itself with a KI solution (100 grams of pure KI dissolved in 125 mL of deionized water) and then immediately conducted an ozone decay test.

4.2.1.1. Chamber Flux calculations

For chamber studies, the deposition velocity and subsequently the surface resistance of the green roof and substrate material was calculated by subtracting the inverse of the deposition velocity calculated to the green roof sample coated with KI from the non-coated green roof deposition velocity as shown in equation 7. The coated sample provides an estimate of transport and boundary layer resistances.

$$r_c = \frac{1}{v_d} - \frac{1}{v_{dKI}} \quad (7)$$

where v_d is the ozone deposition velocity for the green roof sample and v_{dKI} is the ozone deposition.

4.2.2. 'Big leaf' resistance uptake theory

It is generally impractical to describe in explicit detail the microphysical route by which ozone travels from the bulk atmosphere to the surface. The transport of a pollutant to the surface is continuous and can be exceptionally complex, involving atmospheric turbulent transport, the properties of the pollutant, and the nature of the surface. The time

scales that are associated with the uptake of a pollutant can be anywhere from seconds to minutes, hours, or weeks depending on the atmospheric and physiological conditions. Instead, the process can be simplified with the assumption that the dry deposition of ozone can be calculated as the product of the local concentration of ozone and the vertical dry deposition flux. The heterogeneous interaction of ozone and the green roof can be modeled as a downward flux, F_O (μg m^{-2} s^{-1}):

$$F_O = -v_d \times C_o \quad (8)$$

where v_d is a constant of proportionality known as the deposition velocity (m/s) and C_o is the concentration (μg/m^3) of ozone at a measurement height.

A multi-layer big leaf model separates the deposition velocity into transport and surface resistances, shown in equation 9.[256,294,295]

$$v_d = \frac{1}{r_t} = \frac{1}{r_a + r_b + r_c} \quad (9)$$

where r_t is the total resistance (s m^{-1}), r_a is the aerodynamic resistance (s m^{-1}), r_b is the quasi-laminar boundary layer resistance (s m^{-1}), r_c is the canopy or surface resistance (s m^{-1}). The formulation for aerodynamic resistance is provided from our current understanding of the Monin-Obukhov similarity theory.[296–298]

$$r_a = \frac{1}{k * u_*}\left[\ln\left(\frac{z-d}{z_o}\right) - \Psi_H(\delta)\right] \quad (10)$$

where $\Psi_H = \begin{cases} 2 \times ln\left(\frac{1+(0.95\times[1-11.6(\delta)]^{0.5})}{2}\right), -2 < \delta < 0 \\ -7.8 \times \delta, 0 < \delta < 1 \end{cases}$

The quasi-laminar boundary layer resistance is given by equation 11:

$$r_b = \frac{2 \times Sc^{2/3}}{k * u_*} \quad (11)$$

where Sc is the Schmidt number, the ratio of momentum diffusivity (kinematic viscosity of air) to molecular diffusivity of ozone, $\frac{v}{D_{O_3}}$. The friction velocity, u_*, is given by the relation $u_* = \left(\left(\overline{w'u'}\right)^2 + \left(\overline{w'v'}\right)^2\right)^{1/4}$, k is the dimensionless von-Kárman constant taken to be 0.4, δ is the stability parameter given as $\delta = \frac{z_r - d}{L}$, z_r is the measurement height, d is the zero-plane displacement height, taken as $d = \left(\frac{2}{3}\right) \times (Element\ Height)$, L is the Monin-Obukhov length given by $L = -\frac{{u_*}^3}{k\left(\frac{g}{T}\right)\left(\frac{\overline{(w'T')}}{\rho c_p}\right)}$ and z_o is the roughness height taken as $z_o = 0.1 \times (Element\ Height)$.[299,300]

The surface resistance of an urban surface, r_c, can be composed of multiple uptake pathways in parallel or in series, including stomatal and cuticle uptake, soil uptake, uptake to surfaces coated with water, uptake to stone/brick, and/or uptake to other functional materials. The specific parallel uptake pathways in which ozone may degrade, react, and transform at the surface level are outside of the scope of this study. Instead, a material surface resistance, either from field measurements or derived from literature, is used to characterize the processes that occur to remove ozone deposited on material surfaces.

A hypothetical deposition velocity can be constructed for ozone deposition to rooftops using transport resistances (r_a and r_b) measured from the rooftop field site and

surface resistances derived from literature. Four common building materials and four types of vegetation common to the urban environment are chosen to evaluate ozone deposition to rooftop surfaces, shown in Table 1.

Table 1. Surface resistances for common building materials and vegetation derived from prior published measurements [215,290,301–303]

Material	Surface Resistance (s m^{-1})	Reference
Building material		
Brick	50	Simmons and Colbeck (1990)
Concrete Slab	250	Simmons and Colbeck (1990)
Grey Tile	290	Simmons and Colbeck (1990)
Clean glass	2010	Simmons and Colbeck (1990)
Urban Vegetation		
Green roof	390	Ramasubramanian et al. (2018)
Green roof substrate	350	Ramasubramanian et al. (2018)
Lush vegetation	400	Wesely (1989)
Grass	~100	Wesely (1989), Padro (1996), McMahon and Denison (1979)

4.3. Results

4.3.1. Chamber experiments to measure ozone removal to green roofs

Chamber experiments were performed on a green roof and bare substrate samples taken from the green roof, shown in Figure 7. Light and soil moisture conditions were varied across low, medium, and high conditions. The photosynthetic active radiation (PAR) was 1.2, 14.3, and 100.9 μE m^{-2} s^{-1} for the green roof substrate and 1.2, 12.7, and 89.8 μE m^{-2} s^{-1} for the substrate. The upper limit here is low compared to full sunlight day in the summer in Portland, OR, and was limited by the lamps available that did not also appreciably alter the sample air and surface temperature. The moisture conditions, ranging from 0.03 to 0.07% volumetric water content (VWC) for the soil substrate were low relative to the conditions experienced by the green roof sample. Surface resistances measured in the laboratory ranged from 360 s/m to 435 s/m and fell in the 60th-70th percentile of field measurements. This implies that rooftop vegetation, comprised of sedum and herbaceous species, appears to have surface resistance like that of urban vegetation.

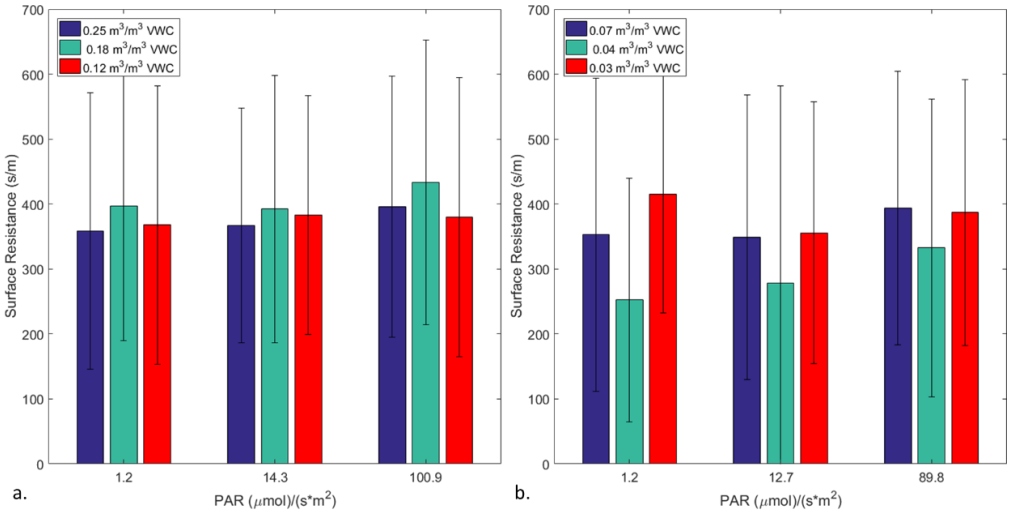

Figure 7. a. Surface resistances from chamber experiments of varying light (uE) and soil moisture (m^3/m^3 VWC) for a sample from a green roof sample. **b.** Surface resistances from chamber experiments of varying light (uE) and soil moisture (m^3/m^3 VWC) for a bare substrate sample.

The green roof sample had slightly higher overall average surface resistance compared to the bare substrate sample, although the difference is within the range of measurement uncertainty. Higher PAR also appeared to lead to a higher surface resistance for most water conditions, again within the range of uncertainty associated with triplicate measurements (Figure 7). Plant and substrate behavior with low water content (red bar, Figure 7) is variable. Interestingly, the driest green roof sample was neither the highest nor lowest surface resistance. In contrast, the driest conditions when substrate alone was tested had the highest surface resistance, implying that substrate water content was key in limiting ozone uptake. For *Sedum* species specifically, a wide range of stomatal conductance of water vapor has been reported under varying light, water, and temperature conditions, with the greatest resistances attributed to periods of drought stress during which the plants enter into the water-efficient crassulacean acid metabolism, or CAM photosynthesis.[304] This is

not evident in our green roof sample, which we speculate to be a result of the presence of exposed substrate in our green roof sample that offered a parallel uptake pathway to that of the high surface resistance stomatal pathways during periods of low water content. Nonetheless, further experiments for different coverage and environmental conditions are needed to specifically evaluate this potential response for sedums.

4.3.2. Ozone removal to rooftops via the resistance uptake model

Ozone deposition velocities to green surfaces and urban hard surfaces are calculated based on resistance uptake theory and are shown in Figure 8a. Aerodynamic and boundary layer resistances are calculated based on turbulence components measured at a local rooftop in north Portland, Oregon, as described in Section 3.2.

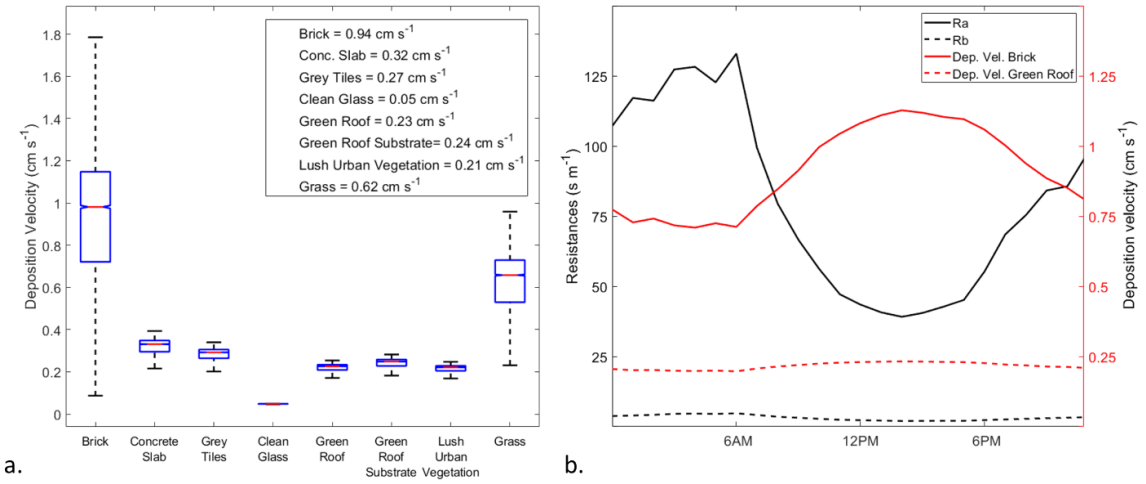

Figure 8. a. Deposition velocities for eight common building and rooftop surfaces: three building materials; brick ($r_c = 50$ s m^{-1}) concrete slab ($r_c = 250$ s m^{-1}), grey tiles ($r_c = 290$ s m^{-1}), clean glass ($r_c = 2010$ s m^{-1}), a green roof sample ($r_c = 390$ s m^{-1}), a green roof substrate sample ($r_c = 350$ s m^{-1}), mid-summer lush urban vegetation in an urban environment ($r_c = 400$ s m^{-1}) and grass ($r_c = 100$ s m^{-1}) **b.** Transport resistances r_a (s m^{-1}) and r_b (s m^{-1}) and its impact on the deposition velocity (cm s^{-1}) for brick and green roof surfaces.

Mean deposition velocities for modeled building materials are: 0.94 ± 0.31 cm s^{-1} for brick, 0.32 ± 0.05 cm s^{-1} for concrete slab, 0.27 ± 0.04 cm s^{-1} for grey tiles, 0.05 ± 0.001 cm s^{-1} for clean glass, 0.23 ± 0.03 cm s^{-1} for green roofs, 0.24 ± 0.02 cm s^{-1} for green roof substrate, 0.21 ± 0.02 cm s^{-1} for lush urban vegetation in mid-summer, and 0.62 ± 0.15 cm s^{-1} for grass. Removal of ozone to building materials is based on material chemical makeup and surface characteristics. Materials containing clay, such as brick, are known to have high reaction probabilities and consume ozone readily with negligible byproduct formation, most likely due to the reaction catalyzed by metals in clay.[102,305] Lamble et al. (2011) studied deposition velocities to green building materials including clay paint, clay wall plaster and porcelain clay tile, finding that clay-based materials promising, with high

deposition velocities and low product yields.[284] Glass is known to have low reaction probability, $\gamma \approx 10^{-8}$, therefore ozone deposition to glass is almost non-existent.[102]

The surface resistance for green roofs and green roof substrate is based on chamber experiments of ozone removal to vegetation taken from a green roof in north Portland, Oregon, and is similar in magnitude to prior work on ozone removal to vegetation.[290,301,303,306] The mean deposition velocity for the green roof (0.22 ± 0.03 cm s^{-1}) and green roof substrate (0.24 ± 0.02 cm s^{-1}) is similar to that of other common building materials (concrete slab and grey tiles) and prior measurements of deposition velocities to vegetation.[307] The impact of urban vegetation such as green roofs on the rate of removal of common outdoor pollutants such as ozone is lower than other building materials such as brick and other clay-based materials. There may also be secondary effects to ozone removal on green roof surfaces; e.g., gas-phase biogenic emissions from vegetation participate in oxidation chemistry that can contribute to increased particle counts in the indoor environment.[34]

Deposition velocities for building materials as a function of transport resistances is plotted in Figure 8b. The rooftop transport resistance is calculated based on resistance uptake theory where the transport resistance, $r_t = r_a + r_b$, where r_a is the aerodynamic resistance and r_b is the boundary layer resistance described in section 3.2. Aerodynamic and boundary layer resistances are high during nocturnal, stable periods and low during the unstable, daytime periods, though for ozone, boundary layer resistances are negligible relative to the aerodynamic resistance. Peak ozone concentrations, generally occurring in

the afternoon, coincide with low transport resistances during the daytime allowing for increased deposition velocities if surfaces are optimized to uptake pollutants during those periods. A mean surface resistance for green roofs and brick is used to calculate the diurnal deposition velocity shown in Figure 8b. Urban greenery follows a dynamic uptake process where stomatal and cuticular uptake of ozone occurs during periods of high photosynthetic activity and only cuticular interactions, an uptake potential a few orders of magnitude lower than stomatal uptake, occur during periods of low photosynthetic activity.[202] Sedum species, commonly used on green roofs, shift from C3 to CAM during arid periods, where gas exchange occurs at night, therefore stomatal uptake pathways are not available during daytime periods.[213,308,309] This suggests that even if transport resistances are minimized, sedum-dominated green roofs would have high surface resistance (i.e. slow uptake at the surface) at the times of day when ozone is elevated; this finding highlights that the dynamics of plant metabolism in combination with air pollutant dynamics are important considerations for studies investigating plant interaction with air pollution.

4.4. Conclusion

Green roof-ozone surface resistances were measured in chamber scale studies with varying light and soil moisture conditions. Surface resistances measured in the laboratory ranged from 360 s m^{-1} to 435 s m^{-1}, similar in magnitude to prior work for ozone surface resistances of vegetation.[290,301,303,306] Rooftop deposition velocities are modeled via the 'resistance uptake' model where the aerodynamic and boundary layer resistances are derived from field measurements and the surface resistances are acquired from prior

measurements of ozone deposition to building materials and vegetation. Brick, a material containing clay that is known to be reactive with ozone, had the highest deposition velocity of materials included in this study, at 0.94 ± 0.31 cm s^{-1}. Green roofs (0.23 ± 0.03 cm s^{-1}), green roof substrate (0.21 ± 0.02 cm s^{-1}), and lush urban vegetation (0.62 ± 0.15 cm s^{-1}) had removal on par with other building materials. While there may be benefits to stormwater management and urban heat island effect, the passive impact of green roofs relative to other common building materials in affecting concentrations of ozone in ventilation air is not expected to be greater than the building rooftop materials that would be exposed if the green roof was not present.

One additional outcome of this modeling is emphasizing the point that even if a rooftop surface has very low surface resistance (i.e. its ability to uptake ozone is idealized), ozone removal from the urban atmosphere is a multi-step, serial process. That is, if a surface is very reactive, ozone removal is then limited by transport, where overall ozone removal to rooftop surfaces is defined by the turbulence characteristics above the rooftop. Further studies may be performed to quantitatively understand drivers of rooftop turbulence and its impact on ozone transport at the rooftop scale. These data would allow for a more complete understanding of the transport and passive removal of ozone in ventilation air and provide insight for practitioners in designing green buildings for healthier indoor environments.

5. Impact of green and white roofs on air handler filters and indoor ventilation air

5.1. Introduction

Green roofs may affect local rooftop air handling units via loading of biotic matter on HVAC filters, which can potentially remove ozone or act as a source for volatile organic compounds (VOCs) to the indoor environment. Since outdoor air intake for buildings is frequently sited on rooftops, the particle-laden rooftop airflow may trap green roof particles onto rooftop filtration systems. Filters loaded with particles can impact the quality of air brought indoors; prior work has characterized ozone removal to loaded HVAC filters from office spaces[60], residential and commercial filters[65], dusty and sooty filters[62], and to green roof and white roof filters[310]. Ozone removal by residential and commercial filters can vary depending on the type of filter as well as the particle loading on the filters. Zhao et al. (2007) found removal efficacies for clean filters varied from 0% to 9% but the removal efficacies for loaded filters increased up to 41%.[65] The type of particle loading may also contribute to removal efficacies; removal for filters located on standard rooftop types was 5-15% while removal for filters taken from a green roof was 10-25%.[310]

Filters loaded with particles can also be emission sources for a variety of compounds in indoor air. As filter operational times increase, surface area for sorption/desorption processes increases due to increases in particle loadings.[311] A study of VOC emissions from HVAC systems from Berlin, Germany, found concentrations of formaldehyde and acetone increased in used filters as compared to unused filters, and acetone concentrations increased with increases in particle loadings.[311] Dust accumulated

on filters have been shown to release carboxylic acids, aldehydes, terpenes, and nitrogen-containing organic compounds.[63,64] Fungal and bacterial growth on filters may contribute to increases in VOC emissions to supply air. A field study of a multi-story office building found indoor VOCs related to the fungal metabolic processes and traced the source to fungal loading of filters.[312]

Heterogeneous chemistry can also occur on filters, in some cases generating harmful byproducts that may then be emitted to the indoors. One driver of this chemistry is ozone, which can enter a building via infiltration or outdoor air supply and subsequently be transported to a filter. Ozone removal via the Criegee mechanism leads to carbonyl formation; a linear correlation can be made between carbonyl generation and ozone removal, when normalized for organic carbon mass on filters.[66,157] Ozonolysis products, including formaldehyde, acetaldehyde, acetone, and 4-oxopentanal are elevated downstream of filters laden with particles from vegetation and diesel emissions.[73]

If around local vegetation, matter composed of whole or fragmented abiotic and biotic matter, maybe trapped on filters which can variably produce isoprene and terpenes, organic compounds that are reactive with ozone. [313314,315] Some products, including formaldehyde, are emitted in proportion to the RH level.[161] If these reactive organics are present on HVAC filters, surface reactions with ozone can lead to the formation of secondary organic aerosols.[35,36,158] Formaldehyde and acetaldehyde, two oxidation byproducts, were found in air downstream of filters after ozonolysis, indicating that ozone reactions of filters can contribute to toxic products in supply air.[73]

In this section, loaded filters are collected from a rooftop, a Walmart retail store in north Portland, OR, with vegetated (green roof) and non-vegetated (white roof) areas to investigate the effect of surrounding rooftop type on filter loading and the ensuing impact on VOC and particle emissions from filters. VOCs in the absence of ozone (primary VOC emissions), ozone removal rates, and emissions in the presence of ozone are identified in a laboratory chamber apparatus. These analyses are conducted for filters collected from the field site during the fall and winter seasons. Despite the growing body of evidence linking HVAC filter quality to indoor air, to my knowledge, this is the first study to characterize the VOC fluxes in the absence and presence of ozone and report ozone removal rates for filters across various temperatures, RH conditions, and multiple seasons.

5.2. Methods

5.2.1. Filter Collection

Loaded filters (hereafter described as "green" and "white" roof filters) were collected from air handling units (AHUs) after operation for three-month periods occurring from October 2018 – January 2019 (Fall season) and January 2019 – March 2019 (Winter season). Samples of filters (area of 17.35 cm^2) for analysis were randomly cut from an intact filter, using sterilized stainless-steel scissors, from a filter taken from the AHU filter bank. An unused filter of the same make (AAF PerfectPleat, HC M8) was acquired from maintenance personnel immediately after the filter collection period. Filters were immediately sealed and stored in a polyethylene bag at -15˚ C freezer until tested for ozone removal and VOC emissions.

5.2.2. Filter chamber-oxidation analysis

Filters were tested for ozone removal and emissions of VOCs in the presence and absence of ozone in the apparatus shown in Figure 9**.** Filtered and humidified compressed air is injected into a temperature-controlled filter cartridge assembly. The chamber apparatus uses an activated carbon filter (Ingersoll-Rand, IRAC40) before humidification and a HEPA filter (ETA Filters, HC01U-4N-B) after the humidifier, the latter necessary as we observed an elevated background particle number due to the humidification. Humidification is regulated using a 1000 mL gas-washing cylinder (Wilmad Lab Glass, LG-3765-130) filled with distilled water and a needle valve to control the flow into the humidification cylinder. Ozone generation is controlled using a shortwave (185 nm) UV photochemical ozone generator (AnalytikJena, SOG-1). A dilution flow is used to provide adequate flow to the instruments, 2 LPM, while maintaining a filter face velocity of 1.1-1.3 cm s^{-1}, chosen for consistency with prior bench-scale laboratory analysis[310,316]. Filters are placed in a PFA filter holder (Savilex, PFA 225-1712) inside a temperature-controlled stainless steel chamber. A 12-Bit combined temperature and relative humidity (RH) sensor (Onset, S-THB-M008) is used to measure the temperature and RH of the air. Ozone is measured using a UV ozone analyzer (Dasibi, 1003-AH). Particle counts (0.02 – 1 μm) are measured using a P-Trak Ultrafine Particle Counter (TSI, P-Trak Ultrafine Particle Counter 8525).

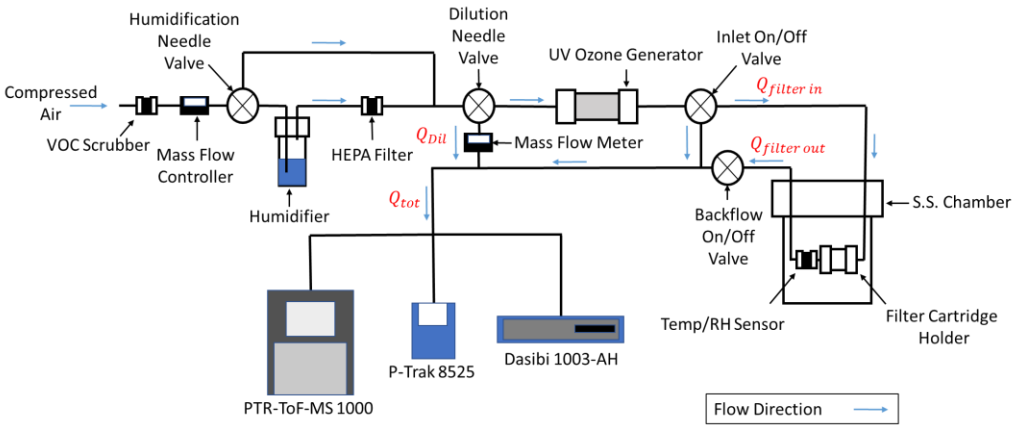

Figure 9. Filter chamber set up for primary emissions, ozone deposition, and emissions in the presence of ozone.

Primary VOC emissions and VOC emissions in the presence of ozone were measured using a proton transfer reaction – time of flight – mass spectrometry (Ionicon, PTR-TOF-MS 1000) with H_3O^+ as the primary reagent ion (O_2^+ and NO^+ signal intensities were respectively less than 5% and 1% of $H_3{}^{18}O^+$ and water cluster ($(H_2O)H_3O^+$) intensities around 1-2% of $H_3{}^{18}O^+$). Drift tube conditions were T_{drift} = 60°C, P_{drift} = 2.20 mbar, U_{drift} = 600 V, which resulted in electric field strength to number density ratio E/N = 135 Td (Townsend, 1 Td = 10-17 V cm^2). The mass axis calibration was performed using three peaks: NO^+ (m/z = 29.9974), $C_3H_7O^+$ (m/z = 59.0497) and a $C_6H_4I_2$ fragment (m/z = 203.944) via an internal standard continuously injected into the drift tube via a heated permeation device (Ionicon Analytik GmbH, PerMaScal). Mass spectra were stored in 30 s intervals. The inlet was held at 60°C and the supplemental inlet flow to the drift tube was set at 150 mL min^{-1}.

A peak list of compounds of interest was chosen based on the potential for emissions from biotic matter and precursors for byproduct formation and oxidation

byproducts[317–326] and shown in Table 2. Putative IDs of these compounds are: methanol (m/z 33.03), acetaldehyde (m/z 45.03), formic acid (m/z 47.01), acetone (m/z 59.04), acetic acid (m/z 61.03), isoprene (m/z 69.07), and monoterpenes (m/z 137.12).

Table 2. Compounds of interest, estimates of high, center, and low m/z ratios, k-Rates, and the references for the compounds

Label	Low	Center	High	k Rate	Studies of emissions in biotic matter
methanol H+	32.94492	33.03226	33.083	2.33	Potard et al. (2017), Abis et al. (2018), Malekina et al. (2007), Fall and Benson (1996), Greenberg et al. (2012), Bamberger et al. (2010)
acetaldehyde H+	44.9517	45.03294	45.10137	3.36	Potard et al. (2017), Abis et al. (2018), Malekina et al. (2007), Greenberg et al. (2012), Bamberger et al. (2010), Kim et al. (2010), Bourtsoukidis et al. (2014)
formic acid H+|Ethanol H+	46.95714	47.01464|47.04885	47.07214	2.00|2.26	Kesselmeier et al. (1998), Sanhueza and Andreae (1991), Laothawornkitkul et al. (2009), Kim et al. (2010), Bourtsoukidis et al. (2014)
acetone H+	58.98423	59.0439	59.11739	3	Potard et al. (2017), Abis et al. (2018), Malekina et al. (2007), Greenberg et al. (2012), Bamberger et al. (2010), Kim et al. (2010), Bourtsoukidis et al. (2014)
acetic acid H+|IPA H+	60.96115	61.02890|61.06169	61.12779	2.00|2.35	Kesselmeier et al. (1998), Sanhueza and Andreae (1991), Potard et al. (2017), Malekina et al. (2007), Greenberg et al. (2012), Laothawornkitkul et al. (2009), Kim et al. (2010)
Furans H+|Isoprene H+	68.94755	69.00049|69.06986	69.16727	2.00|1.94	Potard et al. (2017), Abis et al. (2018), Malekina et al. (2007), Greenberg et al. (2012), Bamberger et al. (2010), Laothawornkitkul et al. (2009), Kim et al. (2010), Bourtsoukidis et al. (2014)
terpenes H+	136.84425	137.1325	137.3355	2.5	Potard et al. (2017), Abis et al. (2018), Malekina et al. (2007), Greenberg et al. (2012), Bamberger et al. (2010), Laothawornkitkul et al. (2009), Kim et al. (2010), Bourtsoukidis et al. (2014)

5.2.3. Experimental protocol

Loaded and unused field filter samples were cut into flat circular samples of diameter of 47 mm and placed in the filter holder. The filter sample is compressed between two mating PFA surfaces and the operative area exposed to airflow (ozone free or containing ozone) was 17.35 cm^2. Before each experiment, the filter cartridge is cleaned and passivated at 200 ppb ozone for 12 hours to remove any confounders due to cartridge handling. Three relative humidity and three temperature conditions were tested for the fall season filters: 20%, 50%, and 80% RH and 15 °C, 23 °C, and 31 °C, respectively. Temperatures were chosen to characterize the behavior of filters across realistic outdoor temperatures. The range was selected to span >10 ◦C, as a rule of thumb (Arrhenius equation) predicts will lead to a doubling of the reaction rate, while considering limitations of our laboratory setup to maintain elevated and lowered chamber concentrations for the duration of each experiment. High and low temperature and RH conditions were tested in duplicates for the fall season. The median condition, 50% RH and 23 °C, was tested in triplicates for the fall and winter seasons. A flow rate of 1.2-1.4 L min^{-1} of air is sent to the filter cartridge, resulting in a face velocity of 1.1-1.3 cm s^{-1}. Measurements were split into two 2.5 h segments for each filter; the first segment was to measure filter primary VOC emissions and downstream particle concentration and the second segment to measure filter ozone removal efficiencies, secondary organic aerosol formation, and VOC emissions in the presence of ozone. For each 2.5 h segment, the inlet concentration was measured for the first 0.5 h, the outlet concentration was measured for the next 1.5 h and finally, the inlet concentration was measured again for 0.5 h. For the first 2.5 h segment, ozone levels were

<2 ppb and during the second segment, ozone was injected, with filter holder inlet levels ranging 170-190 ppb. Experiments were run in duplicate, except for the median temperature and RH conditions (23 °C and 50% RH) for the fall and winter data set, which was run in triplicate. The averaged concentrations reported here are the time average of the final 30 minutes of the 1.5 h outlet measurement. This period met the steady-state conditions for ozone, <2 ppb change over 10 mins[327].

5.2.4. Volatile organic source and sink strength quantification

Primary VOCs were calculated according to the following equation:

$$\overline{F_{filter}} = \left[\left[\left(\frac{\overline{C_{i,\,tot_{out}}} \times Q_{tot_{out}} - \overline{C_{i,\,in}} \times Q_{dil_{out}}}{Q_{filter\ out}} - \overline{C_{i,\,in}}\right) \times \frac{Q_{filter\ out}}{A}\right] \times \alpha\right] - \overline{F_{background}} \quad (12)$$

where subscripts 'out' and 'in' represent the flow through the filter chamber and flow bypassing the filter chamber, respectively. The mean primary VOC flux from the filter (µmol m^{-2} h^{-1}) is $\overline{F_{filter}}$, $\overline{C_{i,\,tot_{out}}}$ is the mean total outlet concentration of compound i (ppb), $Q_{tot_{out}}$ is the total flow during the respective outlet period (L min^{-1}), $\overline{C_{i,in}}$ is the mean inlet concentration of compound i (ppb), $Q_{dil_{out}}$ is the dilution flow during the outlet measurement period (L min^{-1}), $Q_{filter\ out}$ is the flow measurement at the outlet of the filter (L min^{-1}), A is the area of the exposed filter (m^2), α is the unit conversion factor to convert from units of ppb L m^{-2} min^{-1} to units of µmol m^{-2} h^{-1} and depends on the molecular weight of the specific compound, and finally $\overline{F_{background}}$ is the mean background VOC flux (µmol m^{-2} h^{-1}) in the absence of a filter. Time-averages for $\overline{C_{i,\,tot_{out}}}$ and $\overline{C_{i,in}}$ were taken over the

last 30 minutes of the outlet and inlet period, respectively. $Q_{filter\ out}$ was calculated by subtracting $Q_{dil_{out}}$ from $Q_{tot_{out}}$.

VOC emissions in the presence of ozone were calculated similarly and shown below:

$$\overline{F_{filter_{O3}}} = \left[\left[\left(\frac{\overline{C_{i,\,tot_{out}}} \times Q_{tot_{out}} - \overline{C_{i,\,in_{0ppb}}} \times Q_{dil_{out}}}{Q_{filter\ out}} - \frac{\overline{C_{i,\,tot_{in}}} \times Q_{tot_{in}} - \overline{C_{i,\,in_{0ppb}}} \times Q_{dil_{in}}}{Q_{filter\ in}}\right) \times \frac{Q_{filter\ out}}{A}\right] \times \alpha\right] - \overline{F_{background}} \quad (13)$$

where the second part of the right side of the equation represents the potential change in concentration of compound i (ppb) with respect to the increased ozone concentration. $\overline{C_{i,\,in_{0ppb}}}$ is the mean inlet concentration of compound i at 0 ppb ozone (ppb), $\overline{C_{i,\,tot_{in}}}$ is the mean total inlet concentration of compound i (ppb), $Q_{tot_{in}}$ is the total flow during the inlet measurement period (L min^{-1}), $Q_{dil_{in}}$ is the dilution flow during the respective measurement period (LPM), and Q_{in} is the ozonated inlet flow (L min^{-1}). $Q_{filter\ in}$ was measured through bypassing the filter chamber and calculated by subtracting $Q_{dil_{in}}$ from $Q_{tot_{in}}$.

5.2.5. Ozone removal

The removal of ozone to filters was characterized using fractional removal efficiency provided by

$$\eta = 1 - \frac{\frac{\overline{C_{\iota,\, tot_{out}}} \times Q_{tot_{out}}}{Q_{filter\ out}}}{\frac{\overline{C_{\iota,\, tot_{\iota n}}} \times Q_{tot_{in}}}{Q_{filter\ in}}} \quad (14)$$

where η is removal efficiency (%), $\overline{C_{\iota,\, tot_{out}}}$ and $\overline{C_{\iota,\, tot_{\iota n}}}$ are the mean outlet and inlet ozone concentration in (ppb) and the other variables are previously mentioned. Averages for $\overline{C_{\iota,\, tot_{out}}}$ and $\overline{C_{\iota,\, tot_{\iota n}}}$ were taken over the last 30 minutes of the respective experimental period.

5.2.6. Contribution to ventilation air

The contribution of filter emissions to ventilation air downstream of the filter is provided by a mass balance on a volume of air passing through the air-handler containing a filter[73]:

$$C_{in} = C_{out} + \frac{F_{filter} \times R}{V \times \beta} \quad (15)$$

where C_{in} and C_{out} are inlet (μg m^{-3}) and outlet concentrations upstream and downstream a hypothetical filter, respectively, F_{filter} is the emission flux (μg m^{-2} h^{-1}) converted from units of μmol m^{-2} h^{-1}, R is the ratio of filter media surface area to filter face area (dimensionless), V (m s^{-1}) is the filter face velocity, and β is the unit conversion factor (3600 s h^{-1}). R values can vary depending on the type of filter; pad filter (R=1), pleated filter (R=4), thick pleated filter (R=10), and bag filter (R=19). The contribution of the filter to the indoor concentration is given by $\frac{E \times R}{V}$.

5.2.7. Statistical analysis and uncertainty propagation

Shapiro-Wilk tests were used to check the normality of log-transformed fluxes of selected compounds across seasonal, temperature, and RH datasets. Shapiro-Wilk tests with output p-value < 0.05 were ignored from ANOVA tests. A three-way ANOVA considered the effects of the season (fall and winter), filter type (green and white), trial (non-ozonated and ozonated), and associated interactions on compounds from the seasonal dataset that passed the Shapiro-Wilk tests. Data on unused filters were not included in these analyses, as the season is not an independent variable of unused filters. A three-way unbalanced ANOVA was performed on temperature (15 °C, 23 °C, and 31 °C), filter type (green, white, and unused), and trial and their associated interactions on compounds that passed the Shapiro-Wilk tests for the temperature dataset. A similar three-way unbalanced ANOVA considered the effects of RH (20%, 50%, and 80% RH), filter type (green, white and unused), and trial and associated interactions on compounds that passed the Shapiro-Wilk tests for the RH dataset. A Tukey multiple comparison post hoc test was employed for all three-way ANOVA tests.

A Friedman's test was applied, similar to a one-way ANOVA with repeated measures[328,329], for filter type (green, white and unused) across the two trial conditions (non-ozonated and ozonated) for the selected compounds that did not pass the Shapiro-Wilk normality tests for the fall season dataset. A Dunn's pair-wise post hoc analysis was performed between the ranks of the Friedman's test and a Bonferroni post hoc correction for multiple tests was applied. A p-value ≤ 0.05 was deemed a significant difference among

the variables tested for each dataset. All statistical tests, analyses, and graphs were performed and generated in MATLAB.

Uncertainty for VOC fluxes at each condition was estimated by propagating the difference between the maximum and minimum averaged concentrations across replicates for each selected compound. Propagated uncertainty for ozone removal was calculated using a 2% instrumentation error on inlet and outlet concentrations.

5.3. Results

An illustrative dataset collected from chamber studies is shown in Figure 10, with green roof filter data shown for select VOCs, particle number concentrations, and inlet and outlet ozone levels at 23° C and 50% RH. Results from the experiments on fall filters studied across all temperature and RH conditions are presented in Table 2. VOC fluxes are calculated based on eq. 11 and eq. 12 and normalized to background concentrations. Periods in which the background concentration is higher are due to the filter behaving as a sink and shown as a negative flux in Table 2.

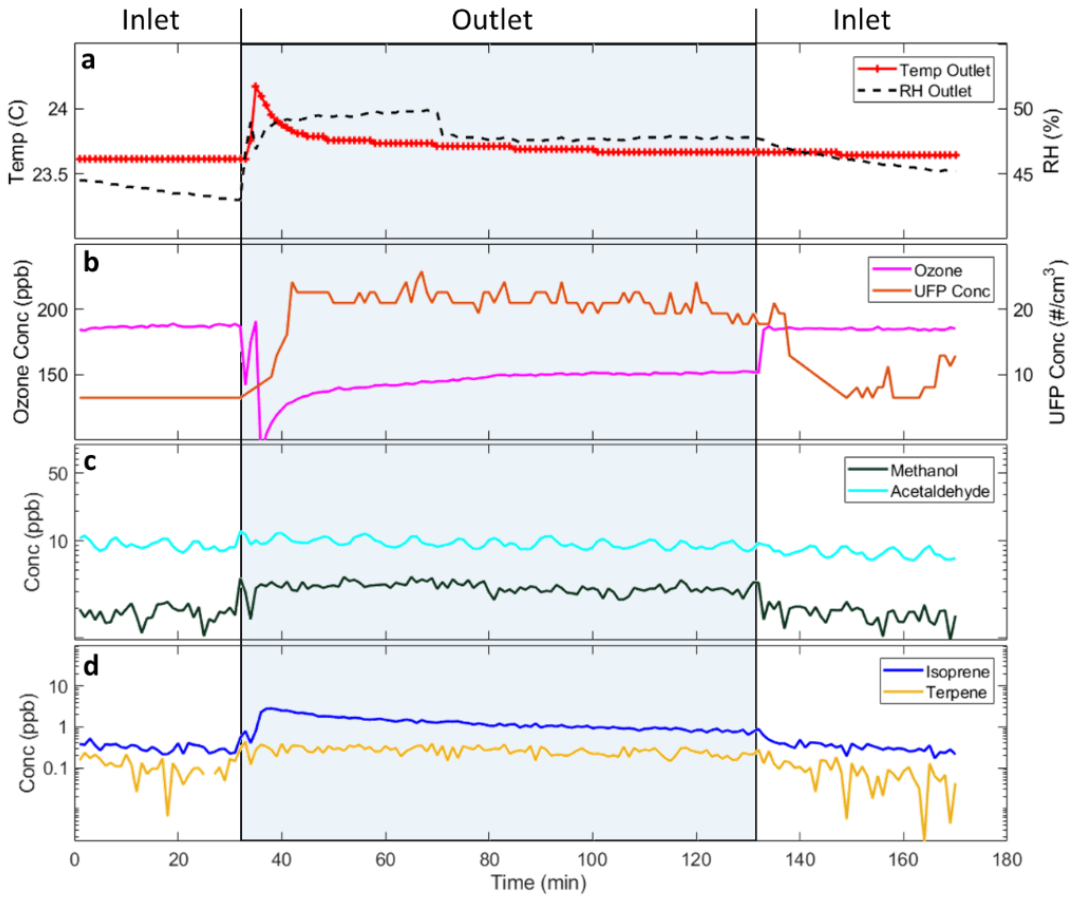

Figure 10. Representative measurements from filter ozonolysis experiment for fall season green roof sample at the 23° C and 50% RH. The inlet concentrations are measured in the first ~30 mins, then ~90 mins of outlet concentrations are measured (shaded area) and finally ~40 mins of inlet concentrations **a.** Temp (C) and RH (%) **b**. Ozone (ppb) and Particle number concentration ($\frac{\#}{cm^3}$) concentration **c.** Methanol (ppb) and Acetaldehyde (ppb) concentrations **d.** Isoprene (ppb) and Terpene (ppb)

Table 3. VOC fluxes (µmol m^{-2} h^{-1}) for unused, white, and green roof filters for high (31 C), median (23 C) and low (15 C) temperature and high (80 %), median (50 %), and low (20%) RH. 'No O_3' represents filter VOC emissions in the absence of ozone and 'High O_3' VOC emissions were emissions presence of ozone.

Temp (C)	RH (%)	Filter Type	Methanol		Acetaldehyde		Formic Acid		Acetone		Acetic Acid		Isoprene		Terpenes	
			No O_3	High O_3	No O_3	High O_3	No O_3	High O_3	No O_3	High O_3	No O_3	High O_3	No O_3	High O_3	No O_3	High O_3
15	50	Unused	0.79 ± 0.99	0.16 ± 0.61	-0.16 ± 0.34	0.22 ± 0.73	0.41 ± 0.78	0.48 ± 0.61	-0.08 ± 0.12	-0.05 ± 0.02	-0.01 ± 0.32	-0.03 ± 0.11	0.00 ± 0.03	0.00 ± 0.04	-0.01 ± 0.37	0.00 ± 0.06
		White	3.61 ± 2.53	0.53 ± 0.52	0.66 ± 1.64	0.48 ± 1.11	0.43 ± 0.40	0.94 ± 1.22	0.19 ± 0.16	0.56 ± 1.08	0.19 ± 0.22	0.65 ± 1.34	0.00 ± 0.06	-0.06 ± 0.16	0.07 ± 0.37	0.04 ± 0.06
		Green	6.84 ± 0.99	2.24 ± 1.13	0.85± 0.44	0.62 ± 0.08	1.31 ± 0.26	1.56 ± 0.87	0.51 ± 0.28	0.43 ± 0.10	0.53 ± 0.14	0.37 ± 0.13	0.05 ± 0.04	0.20 ± 0.36	0.09 ± 0.37	0.05 ± 0.07
23	20	Unused	0.56 ± 0.78	-0.17 ± 3.66	-0.02 ± 1.14	0.10 ± 1.19	-1.44 ± 2.28	-0.44 ± 1.77	-0.17 ± 0.95	0.06 ± 0.93	-0.77 ± 1.41	-0.32 ± 0.56	0.00 ± 0.26	0.00 ± 0.09	-0.18 ± 0.04	-0.02 ± 0.04
		White	7.62 ± 0.50	0.02 ± 3.55	-0.39 ± 1.00	-0.34 ± 0.62	-1.41 ± 2.63	-1.28 ± 2.24	-0.42 ± 0.81	-0.26 ± 0.47	-0.85 ± 1.58	-0.32 ± 0.48	-0.01 ± 0.26	-0.04 ± 0.09	-0.14 ± 0.04	0.00 ± 0.04
		Green	14.56 ± 9.68	0.12 ± 5.21	0.08 ± 1.04	0.24 ± 1.08	-1.58 ± 2.23	-1.65 ± 2.31	-0.08 ± 0.97	0.10 ± 0.81	-0.93 ± 1.45	-0.31 ± 0.61	-0.02 ± 0.27	-0.06 ± 0.13	-0.12 ± 0.04	0.01 ± 0.04
	50	Unused	5.64 ± 1.08	1.08 ± 0.53	1.13 ± 1.20	0.54 ± 1.15	-0.95 ± 1.38	2.83 ± 0.59	0.07 ± 0.12	0.37 ± 0.35	0.03 ± 0.31	0.20 ± 1.08	0.03 ± 0.04	0.00 ± 0.16	0.01 ± 0.01	0.02 ± 0.01
		White	12.02 ± 3.41	2.72 ± 1.66	0.03 ± 0.47	1.21 ± 0.81	-0.14 ± 1.72	3.49 ± 0.62	0.13 ± 0.26	0.58 ± 0.48	0.00 ± 0.46	0.44 ± 0.99	-0.03 ± 0.03	-0.07 ± 0.17	0.03 ± 0.02	0.04 ± 0.01
		Green	10.96 ± 3.09	5.27 ± 5.80	0.71 ± 0.44	1.57 ± 0.84	-0.30 ± 1.43	3.47 ± 0.78	0.34 ± 0.55	0.86 ± 0.78	0.12 ± 0.32	0.77 ± 1.00	-0.02 ± 0.02	-0.06 ± 0.15	0.04 ± 0.13	0.05 ± 0.02
	80	Unused	6.65 ± 4.01	-1.06 ± 0.31	-0.72 ± 0.21	-0.23 ± 0.07	-0.64 ± 0.39	-0.80 ± 0.90	-0.11 ± 0.01	0.06 ± 0.14	0.16 ± 0.01	-0.40 ± 0.12	-0.02 ± 0.05	0.09 ± 0.00	0.01 ± 0.08	0.01 ± 0.01
		White	11.43 ± 8.58	0.52 ± 1.04	-0.11 ± 0.90	0.64 ± 0.58	0.18 ± 0.39	-0.32 ± 1.04	0.18 ± 0.41	0.39 ± 0.26	0.45 ± 0.29	0.14 ± 0.73	-0.08 ± 0.16	-0.07 ± 0.12	0.11 ± 0.07	0.06 ± 0.04
		Green	9.16 ± 3.70	1.05 ± 1.05	-1.40 ± 1.24	0.32 ± 0.29	-1.55 ± 0.60	-1.49 ± 2.57	-0.02 ± 1.36	0.28 ± 0.45	-0.74 ± 1.07	0.30 ± 0.34	0.06 ± 0.30	0.28 ± 0.44	0.08 ± 0.01	0.04 ± 0.01
31	50	Unused	0.12 ± 1.02	-0.75 ± 3.35	1.23 ± 2.34	-0.03 ± 0.16	0.53 ± 1.20	1.34 ± 2.14	0.18 ± 0.35	-0.08 ± 0.03	0.50 ± 1.18	-0.09 ± 0.23	0.01 ± 0.12	-0.01 ± 0.01	0.03 ± 0.03	0.02 ± 0.02
		White	5.52 ± 10.31	-0.04 ± 3.39	-0.15 ± 0.27	-0.16 ± 0.18	-0.83 ± 0.79	0.74 ± 2.38	-0.05 ± 0.12	-0.09 ± 0.05	-0.43 ± 0.37	-0.22 ± 0.24	0.00 ± 0.26	0.00 ± 0.18	0.04 ± 0.11	0.02 ± 0.02
		Green	3.98 ± 1.37	-0.54 ± 3.35	0.08 ± 0.22	0.16 ± 0.16	0.15 ± 0.28	0.53 ± 1.50	0.07 ± 0.13	0.05 ± 0.07	0.04 ± 0.20	0.16 ± 0.15	-0.02 ± 0.07	-0.05 ± 0.29	0.05 ± 0.03	0.04 ± 0.02

5.3.1. Ozone Removal for green, white, and unused filters

Ozone removal across filters varied between 3.5 % ± 2.8 % to 14 % ± 2.8 % depending on the type of filter, temperature, and RH condition, shown in Figure 9. Overall, removal efficiencies were in the range of those previously reported; Abbass et al.[310] found ozone removal efficiencies for green roof and standard rooftop filters were 5 % ± 2.8 % to 14 % ± 2.8 % removal at 21° C across 30% and 70% RH with an inlet ozone concentration of 120 ppb.

White and green filter removal efficiencies increased as a function of RH, while the unused filters did not vary across RH (Figure 11a). Similarly, unused filters did not vary across temperature conditions (Figure 11b), maintaining approximately 7 % ± 2.8 % to 8 % ± 2.8 % removal across all temperature changes. Ozone removal to filters increased as a function of increasing RH, shown in Figure 11a, but effects of temperature (Figure 11b) were within propagated uncertainty. The highest removal was detected at 80% RH at 23° C, which compares well with prior work that reported ozone removal doubles when RH is increased from 24% RH to 80% RH[330]. Removal of ozone to filters has been shown to decrease with time[60,62], but, removal efficiencies have been shown to partially recover after filters were treated with clean, non-ozonated air[60].

5.3.2. Ozone removal across winter and fall seasons

Ozone removal for green roof and white roof filters were higher in the winter season, 6.5 % ± 2.8 % and 8.0 % ± 2.8 % respectively, than those for the fall season, 5.9

% ± 2.8 % and 3.6 % ± 2.8 % respectively, though the differences were within propagated uncertainty, shown in Figure 10c. Green roof filters had similar removal efficiency across the two seasons, but the differences again fell within propagated uncertainty.

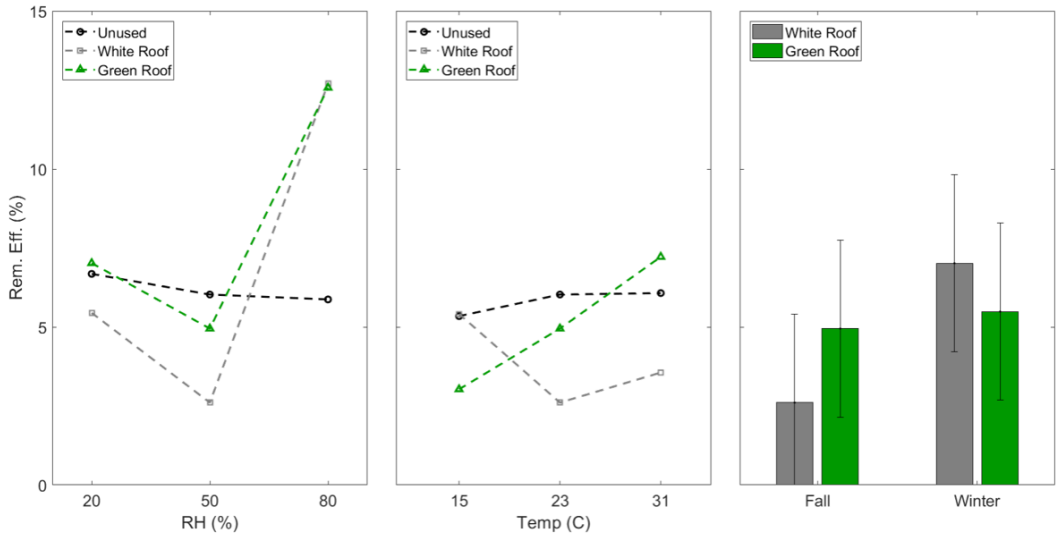

Figure 11. a. Ozone removal efficiency (%) for fall filters as a function of RH (%) **b.** Ozone removal efficiency (%) for fall filters as a function of Temp (C) **c.** Ozone removal efficiency (%) as a function of the season (fall and winter). Unused filters were ignored for the seasonal dataset as seasons have no impact on unused filters. Propagated instrumentation error was calculated to be ± 2.8 % removal efficiency for all tests.

5.3.3. VOC fluxes from green, white, and unused filters

Green and white roof filters were significantly more emissive than unused filters and methanol fluxes dominated the VOC fluxes that were tracked. Compounds of interest for this study were methanol (CH_3OH), acetaldehyde (C_2H_4O), formic acid (CH_2O_2), acetone (C_3H_6O), acetic acid (CH_3COOH), isoprene (C_5H_8) and terpenes ($(C_5H_8)_n$); emission fluxes are reported in full in Table 2. For the fall season at 23° C and 50% RH, methanol emissions from green and white filters are similar in magnitude at 10.96 ± 3.09

and 12.02 ± 3.41 μmol m^{-2} hr^{-1}, respectively, and were significantly more emissive than the unused filters which measured 5.64 ± 1.08 μmol m^{-2} hr^{-1}. Methanol fraction of the total flux of the selected compounds were between 60-100% for green and white filters after background (empty filter holder) emissions were accounted for. Methanol fluxes from filters may be partially a result of the cellulose composition of filters[311]. Cellulose composes many plant and wood walls[331,332] and methanol is a major component of VOC fluxes from plant and wood material[333], potentially explaining the high methanol flux in unused filters. Higher fluxes of methanol from green and white roof filters could be due to numerous reasons, including; local plant leaf emissions of methanol being sorbed and desorbed from filters[320], suspension and entrapment of soil or plant litter, which can include cellulose-containing biotic matter, leading to emissions of methanol[334,335], or anthropogenic sources such as the traffic that could emit methanol that is sorbed onto HVAC filters[336].

Primary fluxes of isoprene and terpenes, which are known precursors for secondary organic aerosol formation, were small across all temperature, RH, and seasonal conditions; 0.07 ± 0.08 and 0.01 ± 0.08 μmol m^{-2} hr^{-1} respectively, relative to other compounds for all filter types. One possible explanation is that since the filters were stored for roughly four months in a polyethylene bag at -15° C freezer, active plant cells trapped in filters may have deteriorated and lost their ability to perform metabolic processes that produce isoprene and terpenes[337,338]. Another potential rationale for the low terpene flux may be

due to these compounds being more strongly sorbed to the filter or dissolved in a reservoir where the mass transfer across the boundary of the reservoir is much slower[339].

Methanol fluxes were lower in the presence of ozone, suggesting methanol consumption during ozonolysis and potential for secondary byproducts. Furthermore, isoprene fluxes increased in the presence of ozone for green roof filters, increasing from 0.15 ± 0.41 to 0.40 ± 0.22 μmol m^{-2} hr^{-1}, and for white roof filters, from 0.17 ± 0.30 to 0.38 ± 0.33 μmol m^{-2} hr^{-1}. We speculate this may result from a few possibilities including; fragmentation of a compound that may lead to a signal at m/z 69.07 or breakdowns and responses of organic matter present on the filter due to oxidation processes that lead to increases in gas-phase isoprene concentrations. Ozone is known to cause death amongst gram-positive and gram-negative bacteria[340] and is suggested in the food industry as a disinfecting agent.[341] This bacterial destruction could introduce isoprene in the gas phase from responses in bacterial metabolic mechanisms.[342–344] Another possibility for isoprene emissions in the presence of ozone could be due to plant cells trapped on loaded filters as some plants are known to emit isoprene as a method of reducing oxidative damage to the plant.[345] Isoprene synthesis has been shown to occur on transgenic tobacco plants to prevent oxidative damage[346] and leaves themselves have been shown to emit isoprene and nitric oxide (NO) during oxidative stress as a protection mechanism.[347]

5.3.4. VOC emissions across the winter and fall seasons

Primary fluxes for selected compounds were higher in the fall relative to the winter seasons. Primary fluxes of methanol at 23° C and 50% RH were higher for fall season filters, 11.49 ± 0.40 μmol m^{-2} hr^{-1}, compared to winter filters, 4.35 ± 0.85 μmol m^{-2} hr^{-1}, and shown in Figure 12a. A filter microbial analysis was performed at the Singapore Centre for Environmental Life Sciences Engineering (SCELSE), where it was found that the fall season had a greater fungal DNA fraction than winter season filters. This difference may explain the higher methanol fluxes for the fall season filters as fungal degradation of plant cell walls have been shown to form methanol[348]. Primary fluxes of acetaldehyde, formic acid, acetone, and acetic acid were low in magnitude across both fall and winter periods.

Fluxes in the presence of ozone exhibited similar seasonal behavior as primary fluxes; higher fluxes of methanol for fall season filters, 3.99 ± 1.26 μmol m^{-2} hr^{-1} in relation to the winter filters, 1.74 ± 0.50 μmol m^{-2} hr^{-1}. Higher fluxes of acetaldehyde, an established byproduct of ozonolysis[50,132,349,350]; was also found in the fall season filters, 1.29 ± 0.94 μmol m^{-2} hr^{-1} versus winter filters, 1.08 ± 0.57 μmol m^{-2} hr^{-1}, shown in Figure 12b. Formic acid, another byproduct of ozonolysis[50,132,349,350], had similar behavior however the differences were within propagated uncertainty. Higher fluxes of methanol and acetaldehyde were found on the fall season green roof sample compared to all other filter samples. Total VOC fluxes of the selected compounds were lower in the presence of ozone but increases in acetaldehyde and formic acid fluxes can have detrimental effects on human

health and function[351,352]. There is also potential for increases in fluxes of compounds not tracked in this study.

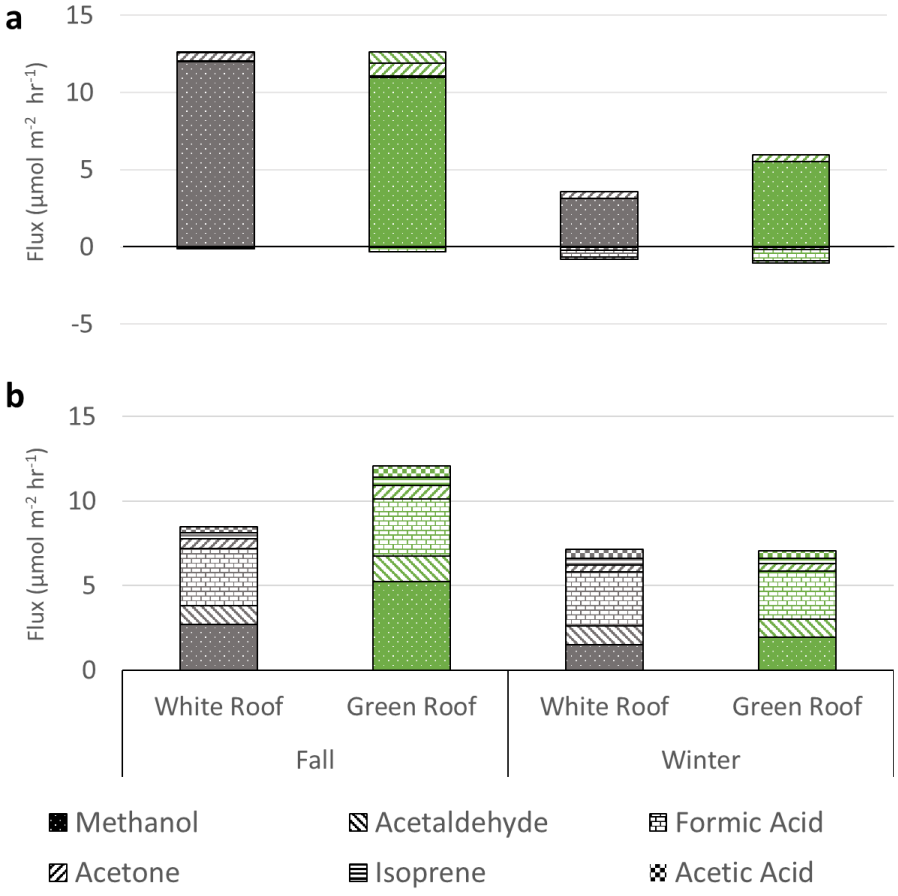

Figure 12. a. Averaged white roof and green roof primary VOC fluxes for selected compounds across seasons at 23° C and 50% RH **b.** Averaged white roof and green roof VOC fluxes in the presence of ozone for selected compounds across seasons at 23° C and 50% RH

5.3.5. VOC Fluxes due to changing temperature and RH conditions

Fluxes for the selected compounds varied highly between filter samples for each temperature and RH condition and shown in Table 3. The temperature was not a statistically significant indicator of VOC fluxes of the selected compounds that passed the

Shapiro-Wilks test criteria. RH was found to be a statistically significant indicator of filter fluxes of formic acid, acetone, and isoprene. Further statistical analysis on filter VOC fluxes as a function of temperature and RH could not be performed due to the non-normality of the dataset. The green roof filter generally had a higher total VOC flux of the selected compounds, with the white roof having a higher total VOC flux under high RH conditions.

5.3.6. Low SOA formation from oxidation processes on filters

The aerosol number formation (ANF) yield was calculated based on equation 4 present in Wang and Waring[35] and the average ANF amongst the green, white, and unused filters across all temperature and RH conditions was, 0.2 ± 1.7 $\frac{\#}{cm^3}/\frac{\mu g}{m^3}$, with the green roof sample at 23° C and 50 % RH being the highest at 0.64 ± 1.2 $\frac{\#}{cm^3}/\frac{\mu g}{m^3}$. For comparison, Waring and Seigel found ANF due to surface reactions and gas phase reactions with d-Limonene was 126-339 $\frac{\#}{cm^3}/\frac{\mu g}{m^3}$ and 51.1-60.2 $\frac{\#}{cm^3}/\frac{\mu g}{m^3}$ [36] and Wang and Waring found ANF varied around 2 $\frac{\#}{cm^3}/\frac{\mu g}{m^3}$ for ozone reactions with surface-sorbed squalene[35]. Low aerosol number fractions are expected given the observation of low concentrations of reactive organics (isoprene and monoterpenes) emitted from filters; we speculate that this implies there exist low concentrations of surface-sorbed monoterpenes on tested filters. For comparison, Waring and Seigel, in a study of the role of surfaces to impact SOA formation from oxidation of d-limonene performed experiments with gas-phase concentrations

between 400 and 600 ppb,[36] whereas average concentrations of monoterpenes downstream loaded and unloaded filter samples varied between 0.2 and 1 ppb in this study.

A thorough study of filter surface properties was not conducted but may be warranted to better understand the fundamental roles of the surface sorbed compounds in the gas-phase filter emissions. Surface environmental scanning electron microscope (ESEM) images and solvent extraction methods are potential ways to better understand the surface properties[310,353] and chemical composition of filter loaded mass, lending further mechanistic insight into what conditions may yield secondary aerosol formation from surface ozonolysis of filters. Future studies could also consider testing filters in-situ, e.g., by generating ozone on-site or immediately after sampling from the field; it is possible that volatile reactive organics were lost in our sample handling and storage.

5.3.7. VOC contribution to the indoor environment

Results of the estimate of the impact of primary emission of VOCs from filters on ventilation air quality (i.e., air downstream a hypothetical filter, emitting at the rate measured in this study) are made using equation 14. A median face velocity, 0.5 m s^{-1} was chosen to represent typical flow rates for a 1 m^2 filter area[73], and a high and low value of 1 m s^{-1} and 0.1 m s^{-1} was chosen to represent high and low HVAC airflow conditions respectively. Low face velocities are on the order of 360 m^3 h^{-1}/(m^2 filter area) and high face velocities are approximately 3600 m^3 h^{-1}/(m^2 filter area). Steady-state contribution to indoor ventilation air for five VOCs for green and white roof filters at various face velocities and ‘R’ values are given in Table 3**.**

Table 3. Increase of VOC level in ventilation air (μg m^{-3}) for fall green and white roof filters without the presence of ozone for different types of filters, pad filter (R=1), pleated filter (R=4), thick pleated filter (R=10), and bag filter (R=19) at 3 face velocities; low, 0.1 m s^{-1}, medium, 0.51 m s^{-1}, and high, 1 m s^{-1}.

Type of filter	Face Velocity (m/s)	Methanol	Acetaldehyde	Formic Acid	Acetone	Acetic Acid
Pad filter	0.10	1.07	0.00	-0.02	0.02	0.47
		0.98	0.09	-0.04	0.05	0.55
	0.50	0.21	0.00	0.00	0.00	0.09
		0.20	0.02	-0.01	0.01	0.11
	1.00	0.11	0.00	0.00	0.00	0.05
		0.10	0.01	0.00	0.01	0.06
Pleated	0.10	4.28	0.01	-0.07	0.08	0.47
		3.90	0.01	-0.07	0.08	0.47
	0.50	0.86	0.00	0.00	0.00	0.09
		0.78	0.02	-0.01	0.01	0.11
	1.00	0.43	0.00	-0.01	0.01	0.05
		0.39	0.03	-0.02	0.02	0.06
Thick Pleated	0.10	10.70	0.04	-0.18	0.21	1.18
		9.75	0.87	-0.38	0.55	1.38
	0.50	2.14	0.01	-0.04	0.04	0.24
		1.95	0.17	-0.08	0.11	0.28
	1.00	1.07	0.00	-0.02	0.02	0.12
		0.98	0.09	-0.04	0.05	0.14
Bag filter	0.10	20.33	0.07	-0.34	0.40	2.24
		18.53	1.65	-0.73	1.04	2.63
	0.50	4.07	0.01	-0.07	0.08	0.45
		3.71	0.33	-0.15	0.21	0.53
	1.00	2.03	0.00	0.00	0.00	0.05
		1.85	0.01	0.00	0.01	0.06

units (μg m^{-3})	
Green roof	
White roof	

A steady-state increase in methanol concentration in ventilation air for various filter pleats under different face velocities is shown in Figure 13. For loaded green roof bag filters (R = 19) operating at low flow rates, the steady-state contribution to the indoor ventilation air is approximately 19 ± 0.5 μg m^{-3} which can be a substantial contribution to the indoor environment given that a typical range of indoor air methanol concentrations is 10 - 30 μg m^{-3} [354].

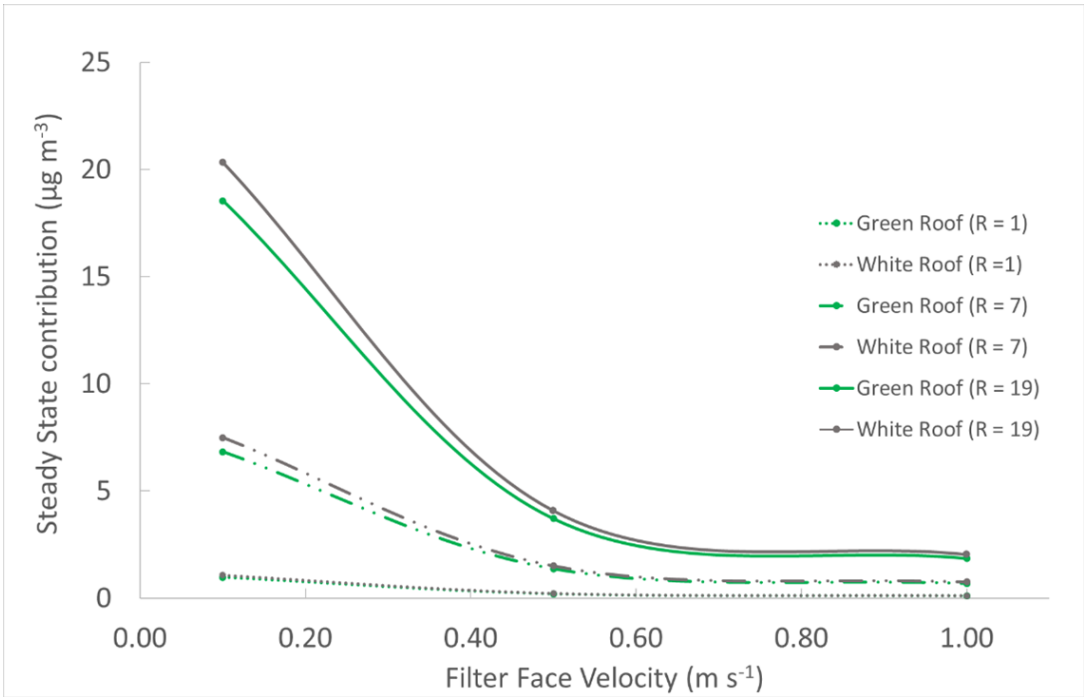

Figure 13. Steady state volatile contribution to the indoor environment for green (GR) and white (WR) roof filters for different filter types; pad filter (R = 1), thick pleated filter (R = 7), and bag filter (R = 19).

For green roof filters from the fall season at 23° C and 50% RH, the measured methanol primary flux was 10.96 ± 3.09 µmol m^{-2} h^{-1} and the respective contribution to the indoor ventilation air is 3.90 ± 0.27, 0.78 ± 0.05, and 0.39 ± 0.03 µg m^{-3} for the low, medium, and high face velocities and pleated filters (R = 4). Similarly, for a fall green roof filter at the same temperature and RH conditions and in the presence of ~180 ppb ozone, the measured flux of formic acid is 3.47 ± 0.78 µmol m^{-2} h^{-1} and the contribution to indoor ventilation air is 1.72 ± 0.38, 0.34 ± 0.08, and 0.17 ± 0.04 µg m^{-3} for pleated filters at low, medium, and high face velocities, respectively. For thick bag filters (R = 19), the

contribution to the ventilation air can be sizeable, 3.48 ± 1.32 μg m^{-3}, relative to measured formic acid concentrations in the indoor environment, approximately 9 μg m^{-3} [355].

5.4. Conclusions

In sum, ozone removal to clean, green roof and standard rooftop filters ranged between 5 % ± 2.8 % to 14 % ± 2.8 %. Contributions of loaded filters to the indoor environment can elevate VOC levels in ventilation air and depend on the filter face velocity and the ratio of filter media to face area. Filter VOC fluxes can vary across seasons and potentially vary due to the local rooftop environment. Fluxes of methanol overshadowed the compounds tracked in this study, including in unused filters suggesting high methanol fluxes are intrinsic to some HVAC filters. Variation of VOC fluxes of other selected compounds between filter samples made it difficult to assess trends due to temperature, RH, or seasonal conditions. Green and white roof filters collected different microbial contents in terms of both absolute and relative abundance suggesting roof type may affect the amount and composition of biotic particles depositing on the HVAC filters. No particle formation was observed due to surface ozonolysis across varying temperatures, RH, and seasonal conditions. Further studies should quantitively characterize the amount and chemical composition of accumulated mass loaded on the filter. These data would contribute to a more complete understanding of the drivers of emissions and chemistry occurring on loaded HVAC filters that may lead to the gas-phase emissions to indoor ventilation air.

6. Effectiveness of cleaning and ventilation technology to exposure of ozone

6.1. Introduction

In general, three strategies can be applied to reduce indoor pollutant concentrations; control of pollutant sources, changes in ventilation rates, or application of air cleaning/treatment technologies. For ozone, source control is generally not a viable mitigation strategy that can be employed by indoor occupants due to the outdoor origin of indoor ozone. Reducing ventilation can reduce indoor ozone levels but with tradeoffs; compounds of indoor origin can accumulate and be elevated to harmful levels. This means that ventilation may not be a viable route in reducing indoor ozone concentrations unless ozone removal mediums are placed in the ventilation pathway. Treatment, indoors or immediately outdoors along the ventilation pathway to the indoor environment, is the main strategy that can be employed to remove ozone in the indoor environment. Yet, there remains a gap in our understanding of the effectiveness of air cleaning of ozone at different scales in impacting the quality of inhaled air.

Several studies have quantified the effectiveness of potential cleaning mechanisms on indoor PM or other compounds.[94,111,142,159,356] Shaughnessy and Sextro (2006) performed a clear and extensive modeling exercise to understand the effectiveness of indoor air cleaning on indoor PM. Utilizing steady-state assumptions, they demonstrated that the effectiveness of air cleaning systems can be modeled by a removal ratio, the ratio of the removal intervention over other losses in the indoor environment.[159] A removal ratio of unity equates to an effectiveness of 50 %, a proposed minimum threshold for air

cleaners. As the removal ratio increases to four, the effectiveness reaches 80 %, the AHAM performance recommendation. Increasing removal ratios further than the AHAM performance recommendation has diminishing effectiveness.[159] An analogous removal ratio can be defined for ozone where only removal and transformation occur along the pathway from the bulk outdoor air to the breathing zone. A few studies have determined the ozone removal effectiveness of some passive and active indoor interventions and are described in section 2.4.

Technologies that can improve indoor air quality by reducing indoor ozone concentrations with minimal energy consumption have become imperative. There exist few studies that have quantified the breathing zone effectiveness of both active and passive methods across the building, room, and breathing zone scales. In addition, there also are no studies that incorporate ozone losses to occupants, a potentially large indoor sink, when evaluating the effectiveness of mitigation systems. This study aims to determine the effectiveness of air cleaning on breathing zone concentrations and occupant intake fractions. The indoor technologies of interest are passive removal in the indoor and outdoor environment, building-scale active removal, room-scale active removal, and breathing-zone scale active removal.

6.2. Methods

6.2.1. Multi-zone breathing zone mass balance

Multiple zone mass balance models have been used to characterize the effects of ventilation, imperfect air mixing, and loss mechanisms on indoor concentrations. Nicas (1996) studied exposure intensity in an imperfectly mixed room utilizing a two-zone mass balance model for an upper and lower layer. Ventilation air enters and room air is exhausted in the upper zone while the lower zone carries the source and sink terms, the exchange between the two zones is the interzonal air exchange rate described by, β.[357] Boetler et al. (2009) applied a two-zone model to breathing zone concentrations from area welding fumes. In this case, one zone contained the source term in the near field as well as the breathing zone of the occupant while another contained the far-field terms such as air exchange with the outdoor environment. An inter-zonal air exchange term, β, is created to describe the exchange between the two zones.[358] Earnest and Corsi (2013) built a model to predict VOC emissions from a cleaning product in an inner and outer zone where an interzonal air exchange rate was used to bridge the exchange between the inner and outer zones. Their results suggest that the effect of buoyancy-driven flow from the human thermal plume plays a substantial role in transport between the near field (inner zone) and the far-field (outer zone) and models based on a single zone may significantly underpredict exposure.[359]

The multi-zone concepts in prior studies of indoor exposure are built upon to evaluate the effectiveness of passive and active cleaning methods on breathing zone ozone concentrations. Ultimately, a three-zone model is used, as described in Figure 14.

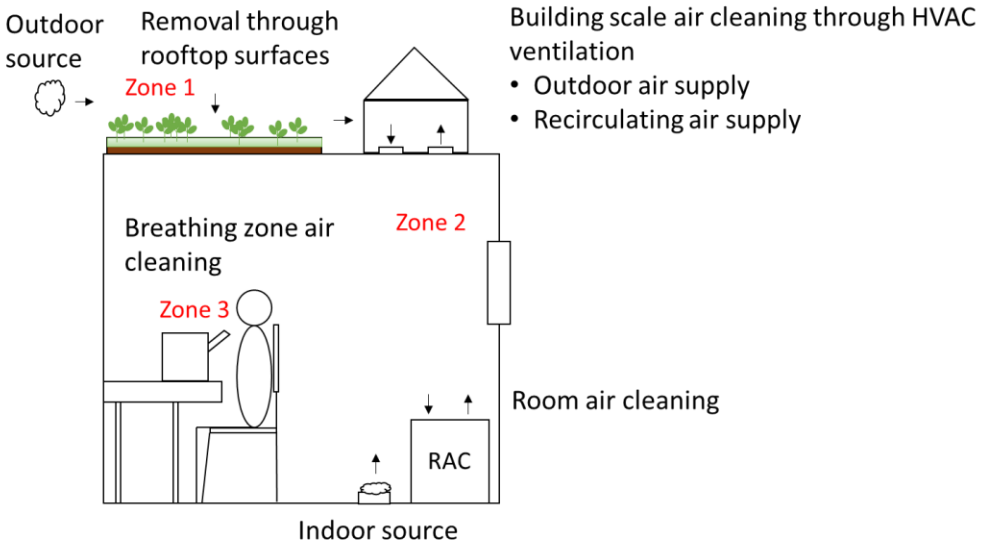

Figure 14. A multi-zone model to characterize the impact of passive outdoor removal mechanisms, building and room-scale air cleaning, and air cleaning at the breathing zone.

6.2.1.1. Zone 1

The first 'zone' is used to describe the removal due to outdoor passive removal mechanisms, in this case, green roofs, and shown in Figure 15. An advection-diffusion equation, shown in equation 16, can be used to model the transport and deposition of ozone onto the rooftop surface.

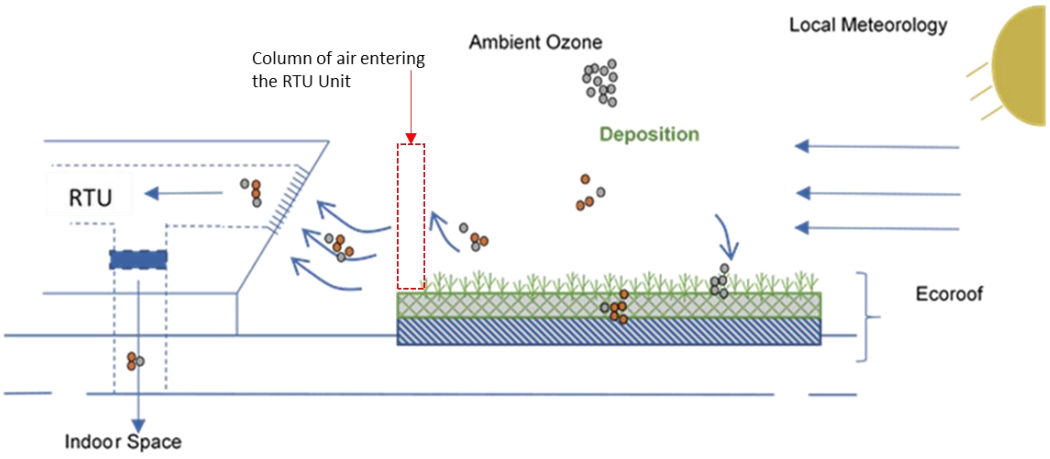

Figure 15. Ozone transport and passive removal by a rooftop surface, in this case, green roofs, near ventilation air supply. The figure is modified from Figure 2 of Ramasubramanian et al. (2018).[215]

The advection-diffusion equation for the first zone is given as:

$$\frac{\partial \overline{C_0}}{\partial t} = -\bar{u}\frac{\partial \overline{C_0}}{\partial x} - \frac{\partial}{\partial z}K_m\frac{\partial \overline{C_0}}{\partial z} - \left[\sum_{i=1}^{n}\frac{v_{di}*A_i}{V}\right] * \overline{C_0} \qquad (16)$$

where $\overline{C_0}$ is the mean ozone concentration, $\bar{u}$ is the mean velocity, K_m is the eddy diffusivity coefficient for mass, v_{di} is the deposition velocity, A_i is the area of the deposition surface, V is the control volume.

The rooftop model space was discretized non-uniformly so that the treatment of the roughness sublayer (RS), shown in equation 18, occurred in one layer while the inertial surface layer (ISL), shown in equation 17, was split into multiple layers over the rooftop similar to prior work.[215] The roughness sublayer is a layer in which the constant flux assumption does not hold, instead, the deposition velocity, v_{di} (m/s), is used characterize the downward flux.[255] The height of the roughness sublayer is typically assumed to be

somewhere between 2 to 5 times the height of the roughness elements, and for our model, we chose 3 times the height of the roughness elements.[360]

$$\frac{\partial \overline{C_0}}{\partial t} = -\bar{u}\frac{\partial \overline{C_0}}{\partial x} - \frac{\partial}{\partial z}K_{mass}\frac{\partial \overline{C_0}}{\partial z} \quad (17)$$

$$\frac{\partial \overline{C_0}}{\partial t} = -\bar{u}\frac{\partial \overline{C_0}}{\partial x} - \left[\sum_{i=1}^{n}\frac{v_{di}*A_i}{V}\right] \times \overline{C_0} \quad (18)$$

An upwind (forward) discretization method was applied to the model and to simplify the discretization. The area for deposition was assumed to be the bottom surface area of the control volume, which allowed for the reduction of the bulk deposition term as shown in equation 19:

$$\frac{v_{di}\times A_i}{V} = \frac{v_{di}}{h} \quad (19)$$

where h is the height of the control volume (m), and all other terms as described previously.

A multi-layer resistance uptake model can be used separate the deposition velocity to aerodynamic, boundary layer, and surface resistances.[256,294,295] The formulations for the aerodynamic resistance, r_a (s/m) and boundary layer resistance, r_b (s/m) are based on universal functions for momentum determined from field measurements of shear above the rooftop and shown in equations 20 and 21.

$$r_a = \frac{1}{k\times u_*\times Sc_t}\left[\ln\left(\frac{z-d}{z_o}\right) - \psi_m(\delta)\right] \quad (20)$$

where $\psi_m = \begin{cases} \ln\left[\left(\frac{1+x^2}{2}\right)\left(\frac{1+x}{2}\right)^2\right] - 2\ \tan^{-1}x + \frac{\pi}{2}, -2 < \delta < 0 \\ -6(\delta), 0 < \delta < 1 \end{cases}$

Here, $x = (1 - 19.3(\delta))^{1/4}$ and Sc_t is the turbulent Schmidt number given as $Sc_t = \frac{K_{momentum}}{K_{mass}} \approx 0.8$.

The quasi-laminar boundary layer resistance is given by equation 19:

$$r_b = \frac{2 \times Sc^{2/3}}{k * u_*} \quad (21)$$

where Sc is the Schmidt number, the ratio of momentum diffusivity (kinematic viscosity of air) to molecular diffusivity of ozone, $\frac{v}{D_{O_3}}$. The friction velocity, u_*, is given by the relation $u_* = \left(\left(\overline{w'u'}\right)^2 + \left(\overline{w'v'}\right)^2\right)^{1/4}$, k is the dimensionless von-Kárman constant taken to be 0.4, δ is the stability parameter given as $\delta = \frac{z_r - d}{L}$, z_r is the measurement height, d is the zero-plane displacement height, taken as $d = \left(\frac{2}{3}\right) \times (Element\ Height)$, and z_o is the roughness height taken as $z_o = 0.1 \times (Element\ Height)$.[299,300]

δ is the stability parameter given by:

$$\delta = \frac{z - d}{L} \quad (22)$$

where L is the Monin-Obukhov length given by:

$$L = -\frac{{u_*}^3}{k(\frac{g}{T})(\frac{H}{\rho c_p})} \quad (23)$$

where g is gravity (m/s^2), T is the temperature (K), H is heat flux (W/m^2), c_p is specific heat (J/(Kg*K)) and ρ is the density (kg/m^3).

The mean velocity and eddy diffusivity profiles may be generated from the Monin-Obukhov Similarity Theory (MOST) shown in equations 24 and 25.[296,298,300]

$$\bar{u} = \frac{u_*}{k}\ln(\frac{z-d}{z_o}) - \psi_m(\delta)) \quad (24)$$

$$K_{mass}(z) = \left(\frac{1}{Sc_t}\right) * \frac{(u_*)(k)(z-d)}{\varphi_m(\delta)} \quad (25)$$

and

$$\varphi_m(\delta) = 1 + 6(\delta)\ for\ \delta > 0\ (Stable\ atmosphere)$$

$$\varphi_m(\delta) = 1\ for\ \delta = 0\ (Neutral\ atmosphere)$$

$$\varphi_m(\delta) = (1 + 19.3(\delta))^{-1/4}\ for\ \delta < 0\ (Unstable\ atmosphere)$$

The model was run until steady-state; defined similarly to Coleman et al. (2008), as ozone levels changing less than 2 ppb over 20 minutes.[361] A grid sensitivity study was performed to define a grid-independent solution, occurring at an x-z grid spacing of 125 x 125 nodes.

6.2.1.2. Zone 2

The second 'zone' characterizes the removal effects of outdoor air exchange, building scale active air cleaning, room-scale passive and active air cleaning, and losses to room surfaces and occupants, shown in Figure 16.

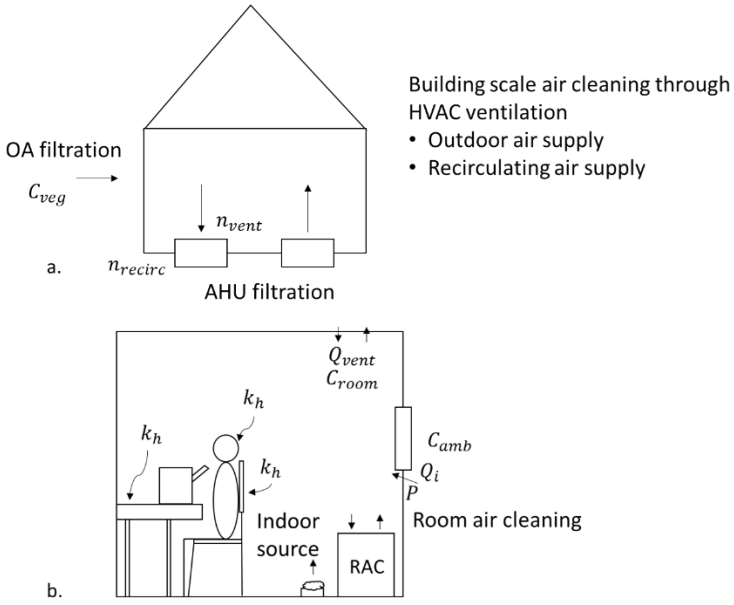

Figure 16. a. Description of cleaning at the building ventilation scale including outdoor air cleaning and recirculation air cleaning. **b**. Description of room-scale air cleaning (RAC), indoor sources, and outdoor penetration.

The second zone can be split into cleaning at the building ventilation scale and cleaning at the room-scale, which can be described using a mass balance similar to that of Figure 2a in Ruan and Rim (2019):[87]

$$V_{Room} \times \frac{dC_{room}}{dt} = [\mathrm{P} \times Q_i \times C_{amb}] + \left[Q_{vent} \times C_{veg} \times (1 - n_{vent})\right] + [Q_{nat-vent} \times C_{amb}] + [Q_{BZtoRM} \times (C_{bz} - C_{room})] + S - C_{room} \times [Q_{recirc} \times n_{vent} + Q_{vent} + CADR_{rac} + V_{Room} \times (k_d + k_h)] \quad (26)$$

where V_{Room} is the volume of the room, C_{room} is the room concentration, P is the penetration factor for the pollutant, Q_i is the infiltration rate, Q_{vent} is the mechanical ventilation flow rate, $Q_{Nat-vent}$ is the natural ventilation flow rate, n_{vent} is the outdoor air

filtration efficacy, n_{recirc} is the recirculation air filtration efficiency, which for this study is equal to n_{vent}, Q_{recirc} is the recirculation flow rate, $CADR_{rac}$ is the clean air delivery rate of room air cleaner, k_d represents any losses to indoor surfaces, and k_h represents any losses to human surfaces. Q_{BZtoRM} and C_{bz} are described in Figure 17 and equation 28.

6.2.1.3. Zone 3

The third zone in the multi-zone mass balance is at the breathing zone scale, shown in Figure 17.

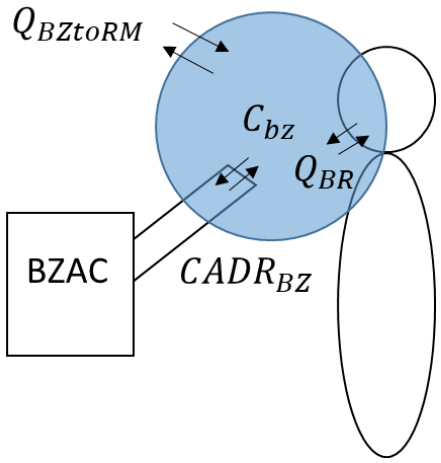

Figure 17. The breathing zone with impact from the room flow rate, losses to occupant skin, breathing zone air cleaner, and the inhalation rate.

The mass balance for the breathing zone can be characterized by:

$$V_{BZ} \times \frac{dC_{bz}}{dt} = [Q_{BZtoRM} \times (C_{room} - C_{bz})] + [Q_{BR} \times (C_{human} - C_{bz})] - C_{bz} \times CADR_{bzac} \quad (27)$$

where V_{bz} is the volume of the breathing zone, C_{bz} is the breathing zone concentration, Q_{BR} is the inhalation flow rate, C_{human} is the concentration of the pollutant emitted from humans, $CADR_{bzac}$ is the clean air delivery rate of breathing zone air cleaner. The surface area for ozone deposition within the breathing zone is much smaller than the surface area of a human, therefore the k_h within the breathing zone is considered negligible. Q_{BZtoRM} is the interzonal flow rate between the breathing zone and the room and is given by:

$$Q_{BZtoRM} = Q_{BR} + Q_{thermplume} + V_{bz} \times \frac{Q_{Nat-vent} + Q_{vent} + Q_i}{V_{Room}} \quad (28)$$

where $Q_{thermplume}$ is the flow rate induced by the thermal plume of the human body and ACH is the air changes per hour of the room.

The breathing zone model assumes ozone losses only to surfaces; NO and organics in the breathing zone are assumed to be non-existent or negligible relative to losses to the skin or air cleaning in the breathing zone. It is assumed there is no source of ozone in exhaled human breath, therefore, there is no C_{human}, making inhalation of breathing zone air a sink within the breathing zone.

The rooftop advection-diffusion model is first solved for various deposition velocities and different surface areas. Then the output concentration at the ASHRAE standard minimum RTU height of 0.75 m is taken as an input value for the room and breathing zone mass balance. These models allow an understanding of the time-dependent transport, removal, and/or transformation process of ozone along its pathway from the

outdoor air to the breathing zone. For this study, steady-state indoor to outdoor ratios and breathing zone to outdoor ratios may also be calculated by setting the accumulation term (dC/dt) equal to zero.

6.2.2. Ozone mitigation effectiveness

The impact of a mitigation method can be evaluated through a clean air delivery rate (CADR) metric. One way to define the CADR metric is a product of the flow rate through a removal mechanism (Q) multiplied by the removal efficiency (η). For HVAC systems CADR is system-specific as the fan and the air cleaner are components of a larger distribution system.[362] For portable air cleaners, CADR is typically measured with a pollutant decay test (ANSI/AHAM AC-1) and CADR may differ depending on the type of cleaner; plant-based systems, ionizers, and photocatalytic air cleaners generally have lower CADR due to the need for longer residence times to remove pollutants. Several studies have evaluated the effectiveness of CADR to indoor PM, and a similar, analogous system can be described for ozone. The theoretical effectiveness of an ozone intervention method may be calculated as:

$$H = 1 - \frac{C_{ac}}{C_{no\ ac}} \quad (29)$$

where C_{ac} is the steady-state concentration with the air cleaner and $C_{no\ ac}$ is the steady-state concentration without the air cleaner.

6.2.3. Steady-state ozone infiltration fraction at the breathing zone scale

A well-mixed mass balance may be applied to track ozone from bulk outdoor air to the breathing zone. When the time interval for changes in the outdoor concentration of a pollutant is much larger than the time interval for changes in the indoor concentration of the pollutant, the indoor concentration can be related to the outdoor concentration through a simple, indoor-outdoor ratio expression.[363] At steady state, with constant air change rates, and absent variable indoor sources, a simple expression can be made for indoor to outdoor ozone concentration ratios that includes only the air exchange rate and ozone losses in the transport to and within the indoor environment.[29] While a steady-state assumption for indoor ozone concentrations is generally not valid, the *ozone infiltration ratio*, the indoor-outdoor ratio specific to an indoor environment, can represent good estimates of ozone levels for time-averaged conditions over hours or days.[364] This ratio can be extended to include the breathing zone, allowing for the inclusion of ozone loss mechanisms within the breathing zone, including; losses to skin, gaseous compounds, personal ventilation, and air cleaning.

Ozone indoor to outdoor relationships have been measured in numerous types of buildings, including public, commercial, and residential buildings.[364] Shair and Heitner (1974) first suggested that if the time interval for changes in the outdoor concentration of a pollutant is long relative to changes in the indoor concentration, then the indoor concentration can be predicted with a simple indoor-to-outdoor ratio. The suggested relationship uses a single-zone, well-mixed assumption and incorporates the air exchange rate, heterogeneous losses to the building envelope and the indoor environment, and losses

to supply and recirculation filters.[363] The impact of air exchange, indoor heterogeneous chemistry, including ozone reactions on surfaces and occupants, indoor homogeneous chemistry, including reactions with NO and organics, on ozone infiltration ratios have been well studied. Nazaroff and Weschler (2021) compiled indoor and outdoor concentrations and indoor/outdoor ratios for measurements in approximately 1500 homes distributed across Asia, Europe, and North America, 500 schools across Asia, Europe, and North America, and 75 offices, mainly in Europe.[364] For residences, median indoor concentrations were 6 ppb; median outdoor ozone concentrations were 22 ppb, and indoor to outdoor ratios (I/O) were 25%.[364] Indoor concentrations and I/O ratios were also lower during the winter months compared to the summer season, during high ozone periods such as the summer season, the I/O ratio is 24%, whereas, during cooler, low ozone seasons, I/O ratios are only 15%.[364] For schools, median indoor concentrations were 6 ppb; median outdoor ozone concentrations were 25 ppb, and indoor to outdoor ratios (I/O) were 28%, relatively similar to I/O ratios for residences. The classroom I/O ratio generally represents median I/O ratios for unoccupied classrooms; occupied classrooms may have different I/O ratios, reported findings for occupied I/O ratios are higher than unoccupied: 38 – 65%.[364] Ventilation may also play an important role in indoor concentrations; Gold et al. (1996) found the I/O ratio rose from 18% to 73 % by opening windows.[365] Offices had similar indoor to outdoor ratios as schools and residences, across six studies reported in Table 3 of Nazaroff and Weschler (2022), mean indoor concentrations were 4.6 ppb, mean outdoor concentrations were 25 ppb and I/O ratios were 19 %.[364]

For this study, steady-state indoor to outdoor ratios and breathing zone to outdoor ratios are based on equations 22 and 23 and are as follows:

$$\frac{C_{Ind\_SS}}{C_{Out_{SS}}} = \frac{\left((1-\eta_v)\lambda_m + P_i\lambda_i + \lambda_n\right)}{\beta_{Room} - \frac{\sum \lambda_{BZtoRM-RM} \times \lambda_{BZtoRM-BZ}}{\beta_{BZ}}} \quad (30)$$

$$\frac{C_{BZ_{SS}}}{C_{Out_{SS}}} = \frac{\left((1-\eta_m)(1-H_{roof})\lambda_m + P_i\lambda_i + \lambda_n\right)}{\left[\frac{\beta_{Room} \times \beta_{BZ}}{\lambda_{BZtoRM-BZ}} - \sum \lambda_{BZtoRM-RM}\right]} \quad (31)$$

where:

$$\beta_{Room} = \eta_v\lambda_r + \lambda_i + \lambda_n + \lambda_m + k_{CADR\_RAC} + k_h + k_d + \sum \lambda_{BZtoRM-RM}$$

$$\beta_{BZ} = \lambda_{BZtoRM-BZ} + \lambda_{BR} + k_{CADR\_BZ}$$

Here, the ventilation and removal rates are normalized to the respective volumes (the room and breathing zone volume). λ_m is the mechanical ventilation rate (h^{-1}), λ_r is the recirculation rate (h^{-1}), λ_n is the natural ventilation rate (h^{-1}), λ_i is the infiltration rate (h^{-1}), $\lambda_{BZtoRM-RM}$ is the inter-zonal exchange rate between the breathing zone and room, normalized to the room volume (h^{-1}), λ_{BR} is the breathing rate normalized to the breathing zone volume, $\lambda_{BZtoRM-BZ}$ is the inter-zonal exchange rate between the breathing zone and room, normalized to the breathing zone volume (h^{-1}), and η_v is the ventilation filtration efficiency. H_{Roof} is the removal effectiveness of the rooftop surface, given by $(1 - \frac{C_{veg}}{C_{amb}})$, and can be solved using equations 17 and 18 for the site of interest. Removal rates are normalized at the room and breathing zone scale: k_{CADR_RAC} is the clean air delivery rate of the room air cleaner normalized to the room volume, k_{CADR_BZ} is the clean air delivery

rate of the breathing zone air cleaner normalized to the breathing zone volume, k_h loss to human surfaces at the room-scale, described earlier, k_d is the loss to indoor surfaces.

6.2.4. Steady-state Intake Fraction in the breathing zone

Another metric, *intake fraction*, also known as the exposure fraction and given as the inhalation rate of a pollutant relative to the emission rate of the pollutant, can be used to better understand the impact of different ozone interventions in improving occupant health. The intake fraction terminology was first introduced by Bennett et al. (2002) as a descriptor for quantifying emissions to occupant intake relationships but these concepts were developed from prior studies.[366] Harrison et al. (1986) described an 'exposure efficiency', defined as the fraction of total emissions likely to reach the occupant, Smith (1993) defined the fraction of released material that enters the persons breathing zone in exposure units (μg/m^3 person-year) as 'exposure effectiveness'.[367,368] Lai, Thatcher, and Nazaroff (2000) introduced the concept of 'inhalation transfer factor', defined as the mass inhaled of a pollutant by an exposed individual per unit pollutant mass emitted from a source, synonymous with the 'intake fraction' definition.[10]

Since its introduction, intake fraction has been used to characterize the impact of a plethora of sources across a variety of pollutants. Marshall et al. (2003) investigated intake fractions for benzene and carbon monoxide across 15 urban cities and found that intake fractions ranged from 0.000007 to 0.000021.[369] Intake fractions for indoor sources can be greater than for outdoor sources; Lai, Thatcher, and Nazaroff (2000) found that indoor

transfer functions, a metric synonymous with inhalation intake fraction, are a few orders of magnitude greater indoors than outdoors.[10] Ilacqua et al. (2007) modeled intake fractions for VOCs across 5 cities and found that intake fractions of VOCs generated in the indoor environment are two to three orders of magnitude higher than VOCs common to the outdoor environment.[11] Hellweg et al. (2009) modeled indoor and outdoor exposure within Life Cycle Assessment (LCA) models by integrating inhalation intake fraction to LCA, finding that intake fractions from indoor emissions are often much larger than intake fractions from outdoor sources.[8] Several other LCA models also incorporate inhalation intake fractions to describe the damage to human health of pollutant emission events.[370–374]

As the time interval for indoor removal of ozone is generally smaller than changes in outdoor concentration, a steady-state intake fraction value can be utilized to understand the relationships between ozone transport, removal, and transformation and occupant health.[363] Several studies have evaluated the steady-state impact of loss mechanisms to intake fraction. Hodas et al. (2016) developed a model for inhalation intake fraction of PM2.5 that considered filtration, particle decay, and other particle loss mechanism.[9] Wenger et al. (2012) studied the steady-state impact of sorption/desorption mechanisms on indoor intake fraction. Compounds with low loss rates, approximately 1×10^{-5} to 5×10^{-2} h^{-1}, contribution to reductions in intake fraction was roughly 0.05% to 5%, respectively, but as loss rates increased to values on par with the ventilation rate, the contributions of removal mechanisms such as adsorption or degradation to inhalation intake fraction

increases.[375] To my knowledge, no specific studies have modeled the impact of air cleaning methods on inhalation intake fraction. Incorporating air cleaning as a removal mechanism along the ozone pathway from the bulk atmosphere to the breathing zone allows us to study the effectiveness of ozone mitigation at various scales to occupant health. The intake fraction can be represented simply as the mass inhaled over the mass of a pollutant:

$$iF = \frac{Q_B \times \int_0^{\infty} C_{bz}(t)dt}{\int_0^{T_\alpha} S(t)dt} \quad (32)$$

where Q_B is the flow rate into and out of the breathing zone, $C_{bz}(t)$ is the breathing zone concentration as a function of time, and $S(t)$ is the emission term as a function of time. T_α is the time related to the source emission event where $T_\alpha \ll t$.

Since ozone is predominantly of outdoor origin, the source term, $S(t)$, as a function of T_α, can be characterized as the whole of outdoor ozone entering the indoor environment through ventilation and infiltration and the inhalation intake fraction may be approximated by the steady-state relationship shown in equation 31:

$$iF_{SS} = \frac{Q_{BR} \times C_{BZ\_SS}}{(\lambda_i + \lambda_n + \lambda_m) \times V_{Room} \times C_{Out\_SS}} \quad (33)$$

By supplementing the breathing zone to outdoor ratio from equation 29, we can find the steady-state intake fraction as a function of ventilation rates, loss terms, and occupancy.

$$iF_{SS} = \frac{Q_{BR}}{(\lambda_i+\lambda_n+\lambda_m)\times V_{Room}} \times \frac{(1-\eta_{roof})(1-\eta_v)\lambda_m+P_i\lambda_i+\lambda_n}{\left[\frac{\beta_{Room}\times\beta_{BZ}}{\lambda_{BZtoRM-BZ}} - \sum \lambda_{BZtoRM-RM}\right]} \quad (34)$$

where all values have been previously described.

6.2.5. Monte Carlo Simulation

To understand the impact of mitigation technologies on steady-state breathing zone concentration and inhalation intake fractions across a variety of ventilation, occupancy, and sink parameters, a Monte Carlo simulation is used, similar to Gall et al. (2011) and Li and Siegel (2022).[94,356] Table 4 shows the baseline parameters used across all tests in the Monte Carlo simulation. Constant values are chosen for the outdoor concentration (70 µg m^3), the area outdoor air flow rate for a classroom-based on ASHRAE 62.1 (0.6 L s^{-1} m^{-2}), the breathing zone volume as defined by OSHA as a hemisphere (9 in. radius), and the breathing rate (0.3 L s^{-1}).[376,377] Three room areas are tested: 50, 100, and 150 m^2 with a room height of 4 m. A value for the thermal plume cross-sectional velocity was randomly selected between 0.01 and 0.2 m s^{-1}, shown in Table 4. Removal rates to indoor surfaces were randomly selected from a normal distribution with a mean of 2.8 ± 1.3 h^{-1}. Similarly, removal rates for occupants were also randomly selected from a normal distribution with a mean of 0.9 ± 0.02 h^{-1}.

Table 5 describes the range of occupancy and ventilation rates tested to understand the sensitivity of inputs to breathing zone concentrations and intake fractions. Two tests were run for increasing occupancy, one with constant mechanical ventilation of 1 h^{-1} and

one with demand-controlled ventilation (DCV) of 5 L s^{-1} per person. For both cases, infiltration, penetration, and natural ventilation rates are randomly selected from a range of values described in sections 6.2.7.2 and 6.2.7.3. and shown in Table 5. Three more tests were run to understand the sensitivity of ventilation values, either via mechanical ventilation, natural ventilation, or infiltration rates, on intake fractions and breathing zone concentrations, where occupancy was held at a constant 25 occupants. For each increment of increasing ventilation parameter, other ventilation values were randomly sampled from the range specified in Table 5. Finally, a test was performed to understand the impact of penetration on breathing zone concentrations and intake fractions. In this case, occupancy was also held constant, at 25 occupants, and ventilation parameters were randomly selected from the range described in Table 5.

To study the breathing zone effectiveness of ozone mitigation techniques, five mitigation methods were chosen: removal through rooftop materials, removal through ventilation filters, removal in the indoor environment through passive and active removal methods, and active removal in the breathing zone, shown in Table 6. When testing one mitigation technique, other mitigation methods were set to zero, except for ozone removal to ventilation filters, where a 5 percent removal efficiency was used to signify the removal to a clean particle filter. Also, for each increment of the mitigation technique, occupancy was held at a constant 25 occupants, and values for penetration, mechanical ventilation, infiltration, and natural ventilation were randomly selected from a range described in Table 5. For the tests described in this section, each increment of the test parameter was simulated

10,000 times and a mean and standard deviation are calculated. The following section serves as a brief review of the range of values used in the Monte Carlo simulation.

6.2.6. Model Parameters

6.2.6.1. Environment description

Indoor environments are dynamic; classrooms, office spaces, kitchens, and residential bedrooms all have different ozone infiltration pathways and removal mechanisms. For example, residences generally do not have mechanical or recirculating ventilation but are more likely to have room air cleaners and higher infiltration rates, depending on the age of the building. Schools and offices are likely to use mechanical or recirculation ventilation with either particle or activated carbon filtration medium, with generally lower infiltration rates than residences. Kitchens are areas where natural gas combustion may be used and therefore, may have higher levels of NO, a compound that reacts rapidly with ozone.[378–380] At a steady-state concentration of 10 ppb NO, ozone removal is fast: $k_{NO} = 16\ h^{-1}$.[364]

The environment of focus for this work will be classrooms. Classrooms are environments where infiltration, natural ventilation, and mechanical ventilation are all utilized and ozone removal rates to indoor surfaces and occupants are well described.[364] To understand the effectiveness of air cleaning on breathing zone concentrations and intake fractions, 3 mock areas of classrooms were chosen, 50, 100, and 150 m^2, with an average room height of 4 m, and a constant occupancy of 25 persons, shown in Table 4.

6.2.6.2. Breathing zone volume

The breathing zone (also known as the inhalation zone) is the volume of air immediately outside a human nostril and mouth where the air is inhaled and exhaled. Brohus and Neilson (1996) found that the breathing zone is a hemispherical volume immediately projected from the tip of the nose, which has been codified by OSHA as a 'hemisphere forward of the shoulders within a radius of approximately six to nine inches'.[376,377] Pantelic et al. (2019) confirmed these findings using CO_2 concentrations measured using a LI-COR CO_2 monitor.[381] Laverge et al. (2014) proposed that the breathing zone is dynamic and dependent on respiration rate, local environmental fluid mechanics, and the position and facial structures of the person.[382] For their analysis of ozone surface reactions near occupant skins, Rim et al. (2018) described the breathing zone as a hypothetical cube of 500 cm^3.[33] Although a dynamic volume is possibly more representative of the breathing zone volume, for simplicity, this study will apply a fixed breathing zone volume based on a hemisphere of radius, 22.85 cm (9 inches) provided by OSHA.

6.2.6.3. The impact of occupant thermal plume

Indoor occupants continuously exchange energy with the indoor environment via radiation, convection, evaporation, and respiration.[383] At average room temperatures this exchange in energy between the occupant and the indoor environment can generate approximately 100 W of energy.[384,385] A temperature gradient is formed that drives buoyant convective flow around an occupant, with a laminar thermal free-convective boundary

layer at the feet to a turbulent flow in the upper body. Several studies have evaluated the flow characteristics around the breathing zone due to the human thermal plume. Murakami et al. (1999) studied the thermal and dynamic effects of wind on human bodies via CFD, finding that a thin layer of warm air is observed around a human body under stagnant or weak conditions.[383] Craven and Settles (2006) characterized the human thermal plume in a uniform-temperature and thermally stratified environment using CFD and through experimental measurements via particle image velocity. They found that buoyancy accelerates the thermal plume upwards, mixing pollutants from the ambient environment into the breathing zone. Plume flow rates above the human were found to be between 20 – 35 LPS, depending on the height from the floor.[386] Rim and Novoselac (2009) investigated airflow and pollutant dynamics in the vicinity of an occupant based on activity, breathing, and ventilation system operation. They found that at 5 cm away from the occupant's mouth, the velocity was approximately 0.1 m s^{-1} but as the manikin started to breathe, breathing jets directly affect the airflow in the breathing zone and the velocity increased to between 0.5 to 0.6 m s^{-1}.[387] In a similar CFD analysis, Rim et al. (2009) reported that the mean velocity magnitude around an occupant is 0.1 m s^{-1}.[388] Salmanzadeh et al. (2012) studied the thermal plume near a sitting, heated manikin in a ventilated cube, finding that the thermal plume significantly affected the airflow pattern in the cubicle and mean velocities in the breathing zone were between 0.1 and 0.25 m s^{-1}.[389] For this study, a mean velocity of 0.1 m s^{-1}, which results in a flow rate of 29 m^3 h^{-1} for an OSHA specified breathing zone volume, is taken as the velocity within the thermal plume and is symmetrically varied between 0.01 to 0.2 m s^{-1} for the Monte Carlo simulation.

6.2.6.4. Indoor losses to surfaces and gas-phase compounds

Ozone losses in the indoor environment predominantly occur to both occupant skin/clothing and other indoor surfaces. For indoor surfaces, the median central estimate of the surface loss rate is around 2 h^{-1}, but indoor surface loss rates are commonly higher than the median central estimate.[364] Lee et al. (1999) measured indoor loss rates to surfaces in 43 residences in Southern California, finding the mean loss rate to surfaces was 2.8 ± 1.3 h^{-1}.[390] Yao and Zhao (2018) performed similar measurements in 15 bedrooms of 14 Chinese residences finding a similar loss rate to indoor surfaces of 2.8 ± 1.1 h^{-1}.[391] For this study, a surface removal rate of 2.8 ± 1.3 h^{-1} is used.

Gas-phase removal via reaction with indoor volatile organics may be quite slow and depends on the reaction rate relative to the air exchange rate. For organics like D-limonene or α-pinene at average indoor concentrations across residences in three major cities, the loss rate through indoor gas-phase reaction was estimated to be between 0.02-0.07 h^{-1} for D-limonene and less than 0.01 h^{-1} for α-pinene.[364,392] Price et al. (2019) estimated a typical of ozone reactivity of 0.11 h^{-1} based on concentrations of volatile organics synthesized across 77 studies of gas-phase organics in residences from developed countries. Removal rates may increase due to occupancy, increase in occupants could increase concentrations of volatile organics which may increase ozone removal in the gas phase. For an empty large classroom, removal due to volatile organics was estimated to be 0.022 h^{-1} but doubled during classes.[393]

Ozone reaction with nitric oxide (NO) in the indoor environment can be quite fast, at 20º C and 1 atm, the second-order rate constant is 1.6 ppb^{-1} h^{-1}. At a steady NO concentration of 10 ppb, the ozone loss rate would be 16 h^{-1}. NO is a product of natural gas combustion in cooking burners and ozone reaction to NO is an important removal mechanism for ozone within a kitchen environment.[380,394] For simplicity in understanding the dynamics of ozone mitigation techniques in impacting occupant health, homogeneous reactions of ozone were considered negligible.

Table 4. Environmental constants and sink/transfer parameters for the school classroom simulation

Variable	Value	Distribution Type
Outdoor Concentration (μg m^{-3})	70	-
Room area (m^2)	50 – 100 – 150	-
Area Outdoor Air Rate (LPS m^{-2})	0.6	-
Breathing Zone Hemisphere Radius (inches)	9	-
Inner zone volume (m^3)	1	-
Breathing flow rate (L s^{-1})	0.3	-
Thermal Plume Cross-Sectional Velocity (m s^{-1})	0.01 – 0.2	Uniform
Room Surface Loss Rate (h^{-1})	2.8 ± 1.3	Normal
Loss Rate to Occupant Skin and Clothing (h^{-1} $person^{-1}$)	0.09 ± 0.02	Normal

6.2.7. Impact of occupancy and potential sources of ozone

6.2.7.1. Indoor losses to occupants

As the occupant density increases, the surface area for ozone reaction with occupants increases, as ozone may react with occupant clothing, skin, and hair.[364] Several studies have measured ozone removal to occupant skin, hair, and clothing. Fischer et al. (2013) measured loss of ozone to reactions on the occupants in the classroom reporting an effective deposition velocity of 16 m h^{-1} and an inferred average loss rate per occupant of 0.09 ± 0.02 h^{-1}.[395] Rim et al. (2018) used computational fluid dynamics models to model ozone reaction dynamics to human surfaces under varying air exchange rates (AER). For

AERs below 5 h^{-1}, ozone deposition velocity to human skin was 8-10 m h^{-1}.[33] Wisthaler and Weschler measured ozone reaction and byproduct formation on human skin lipids, finding ozone deposition velocities ranged from 0.4 – 0.5 cm s^{-1} (14.4 – 18 m h^{-1}).[22] Ozone losses to occupants in a simulated aircraft were smaller than that reported previously, between 0.2-0.23 cm s^{-1} (7.2 - 8.3 m h^{-1}).[396] Deposition velocities to occupants may vary due to compounds on the skin, clothing, and hair, and overall removal rates to occupants are impacted by the available reaction surface area on occupants, which may differ between occupants. Therefore, for this study, an average removal rate per occupant with a geometric mean 0.09 ± 0.02 h^{-1} is used and shown in Table 4.

6.2.7.2. Ventilation and recirculation

The effect of ventilation systems on indoor ozone concentrations have been well studied and described in section 2.4.2. Ventilation and recirculation rates are generally based on occupancy levels, indoor relative humidity, occupant thermal comfort, and outdoor weather conditions and therefore vary between different environments. For this work, mechanical ventilation and the ozone filtration medium are organized like Figure 2a of Rim and Ruan (2018).[87] Ventilation rates are calculated based on outdoor occupant air requirements described in Table 62.2.1. of ASHRAE's ventilation standard 62.1-2019. Per person outdoor air rates are varied between 0.5 to 10.5 L s^{-1} and shown in Table 5.

6.2.7.3. Penetration and Infiltration rate

Infiltration rates may vary based on local weather conditions and indoor-outdoor pressure and temperature differences. Ng et al. (2013) modeled infiltration rates for various reference buildings, including a primary school, quick service restaurant, and a small office. Modeled infiltration rates varied from ~0.1 h^{-1} to ~ 0.9 h^{-1} depending on HVAC system operation; lower infiltration rates were modeled for systems that were operational and higher infiltration was modeled for non-operational systems.[397] Lai et al (2015) measured air exchange rates for infiltration in a large chamber and a student office space, finding infiltration rates ranged from 0.23 to 0.32 h^{-1}.[398]

This penetration factor is a function of local weather conditions and building materials. Zhao and Stephens (2016) measured ozone penetration factors across various infiltration rates in a multifamily apartment unit, finding that penetration factors varied between 0.37 ± 0.04 to 0.74 ± 0.06 with a mean of 0.54 ± 0.10.[399] While infiltration rates may be a function of ventilation; higher rates for natural ventilation and lower rates for mechanical ventilation, for this study, infiltration is assumed to be not dependent on ventilation.[397] Infiltration rates were varied between 0.05 to 0.95 h^{-1} and the penetration factor was varied, between 0.05 to 0.95, shown in Table 5.

Table 5. Occupancy and source test parameters (uniform distributions)

# of people	Outdoor vent. flow rate (L s^{-1} $person^{-1}$)	Infiltration (h^{-1})	Penetration Factor	Natural Vent (h^{-1})
5 - 50	0.5 - 10.5	0.05 - 0.95	0.05 - .95	0.1 - 2

6.2.8. Removal parameters

6.2.8.1. Single-pass removal efficiency for ozone

HVAC filters offer an early line of defense for ozone in the pathway from the bulk atmosphere to the breathing zone. Filters loaded with particles may impact ozone concentrations in the air brought indoors; prior work has characterized ozone removal to loaded HVAC filters in office spaces,[60] residential and commercial filters,[65] dusty and sooty filters,[62] and to green roof and white roof filters[310]. Particle loading on residential and commercial filters can impact ozone removal. Zhao et al. (2007) studied removal efficacies for clean and loaded filters finding clean filters varied from 0% to 9% but for loaded filters, the removal efficacies increased up to 41%.[65] The rooftop surfaces may also impact ozone removal; filters located on standard rooftop types showed removal efficacies between 5-15% and filters taken from a green roof showed removal efficacies between 10-25%.[310] For this study, single-pass removal efficiencies were studied from 5 % to 95 % and shown in Table 6.[153–155,287]

6.2.8.2. Rooftop meteorological variables and surface resistances

Rooftop turbulence components for this model were based on rooftop micrometeorological measurements from Oct. 2018 to Oct. 2019 at a big-box retail store. Field measurements of friction velocity (u_*) and Obukhov length (L) was varied from the 10th to the 90th percentiles to understand the impact of rooftop shear on ozone removal effectiveness. Removal effectiveness was modeled like equation 29, where $C_{no\ ac}$ is the concentration of air entering the indoor environment without outdoor surface removal and C_{ac} is the concentration with outdoor surface removal. The 90th percentile shear condition (low aerodynamic and boundary layer resistance) was used to understand the impact of various potential rooftop materials in impacting ozone removal effectiveness. Ozone surface resistances can vary depending on parallel transport and transformation pathways such as stomatal, cuticular and soil uptake as well as on available compounds and reaction sites on surfaces for ozonolysis. These variations of potential uptake or transport pathways at the surface are outside the scope of this study and bulk surface resistance is used to quantify surface removal. Tested outdoor surface resistances for this study were varied between 10 to 3000 s m^{-1}, shown in Table 6.

6.2.8.3. Recirculation rates

Recirculation is largely applied to reduce heating and cooling loads and rates are generally much higher than ventilation rates; Zuraimi et al. (2006) conducted experiments to understand the impact of recirculation rates on secondary organic aerosols generated from indoor chemistry, running experimental recirculation rates between 11 and 24 h^{-1} for

a constant ventilation rate of 1 h^{-1}.[400] As recirculation of indoor air is typically performed to reduce energy load from heating and cooling air and not for air cleaning, recirculation is not modeled in the Monte Carlo simulation.

6.2.8.4. Passive indoor removal

Passive removal in the indoor environment has been studied and is described in section 2.4.1. Of previously tested materials activated carbon mat had the highest ozone deposition velocity at 2.5 – 3.8 m h^{-1} in one study and 5.3 m h^{-1} in quiescent air in another study.[142,144] The incorporation of passive removal as a first-order removal rate, described as $\beta = \frac{v_d A}{V}$, where v_d is the deposition velocity, A is the available surface area on the PRM material for removal of ozone, and V is the volume of the environment. To model the impact of PRM on room concentrations, a study utilized two surface area conditions (low and high) with surface area to volume ratios of 0.075 m^{-1} and 0.3 m^{-1}, respectively.[94] For this study, removal rates for PRM materials are varied between 0.05 to 10.5 h^{-1}, shown in Table 6, and an area is back-calculated to demonstrate the feasibility of removal to passive removal materials.

6.2.8.5. Portable room air cleaners and breathing zone air cleaning

Relative to studies on building scale pollutant mitigation at the HVAC level, few studies in evaluating the impact of portable air cleaners on indoor pollutant concentrations. But technologies associated with room and breathing zone air cleaning are not specifically different than technologies used at the HVAC scale. The impact of air cleaning through

portable and breathing zone air cleaners is quantified by a $CADR$ metric, given as $CADR = \eta \times Q$ where Q is the flow rate through the device and η is the filtration efficiency. A large number of portable air cleaners utilize activated carbon (AC) filters to remove gas-phase pollutants, but their impact may be modest and estimates of single-pass ozone removal efficiency are generally unavailable. Effective portable room cleaners generally run at high flow rates for particle removal and utilize a relatively thin AC medium placed after the particle filter. Contact times, therefore, are not always optimized for adsorption and degradation processes to occur impacting the filtration efficiency (η) for ozone of the portable cleaner.

Hypothetical filtration in portable and breathing zone air cleaners is assumed to occur through activated carbon-packed beds, with contact times necessary to degrade and remove ozone. $CADR$ for ozone removal is generally not reported therefore values were chosen from reported $CADR$ for particles and the author's best judgment and to explore the impact of a wide range of possible values, even if current technology may be unable to reach those $CADR$ values. $CADR$ for portable room air cleaners varied from 10 to 3000 CFM and $CADR$ for breathing air cleaners from 1 to 19 CFM and shown in Table 6.

Table 6. Passive and active removal test parameters (uniform distributions)

Rooftop Surface Resistance (s m^{-1})	Single Pass filtration efficacy (%)	Indoor Passive Removal (h^{-1})	CADR Room Air Cleaner (CFM)	CADR Breathing Zone Air Cleaner (CFM)
10 - 3000	5 - 95	0.5 - 10.5	10 - 3000	1 - 19

6.3. Results

6.3.1. Rooftop advection-diffusion model

For zone 1 in the mock environment with a rooftop area of 100 m^2, a scenario with a perfectly reactive surface (surface resistance, $r_s = 0$ s m^{-1}) and changing friction velocity, from the 10th to the 90th percentile of field measurements described in section 3, was modeled to understand the impact of turbulence on ozone removal to rooftops (Figure 18a). The stability parameter corresponding to the friction velocity at the percentile increment was also derived from field measurements described in section 3 and rooftop aerodynamic and boundary layer resistances are calculated based on equations 20 and 21. Increasing the friction velocity above the rooftop increased the removal effectiveness of the rooftop surface. Turbulence is inherently essential in the deposition of ozone to vegetation. Contact between parcels of ozone-rich air and surfaces may be enhanced through either shear or buoyancy-derived turbulent forces over complex surface morphology.[298] At an ASHRAE specified minimum height above the rooftop of 0.75 m, maximizing transport to the surface and reaction on the surface ($r_s = 0$ s m^{-1}) only had a modest reduction of ~4.7 % in air entering the ventilation system.

Figure 18b shows the removal effectiveness of various rooftop materials at the 90th percentile friction velocity. Rooftop surface resistances, r_s, were varied between 10 – 3000 s m^{-1} and are shown as rooftop deposition velocities ($v_s = \frac{1}{r_s}$). Reducing surface resistances (increasing deposition velocities) for an intake height of 0.75 m and under ideal atmospheric conditions can have a maximum effectiveness of ~4.7 %. Removal of ozone

to rooftop surfaces must compete with advective and turbulent transport away from the surface, which in some meteorological conditions, can be an order of magnitude greater. Stable atmospheric conditions where transport limitations due to advection are minimized and can potentially increase the deposition of pollutants, but ozone concentrations are generally highest during the daytime, where atmospheric conditions are usually unstable and advection is high.

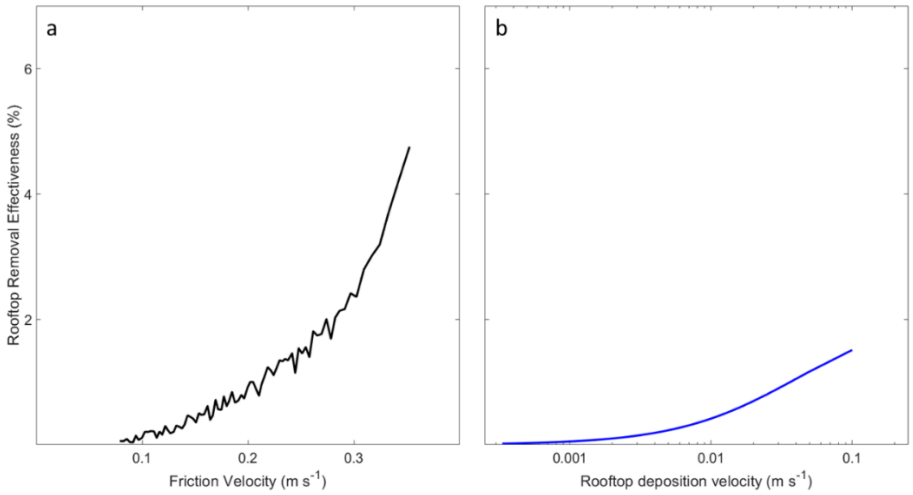

Figure 18. a. Rooftop removal effectiveness as a function of rooftop friction velocity with a complete uptake ($r_s = 0$ s m^{-1}) at a rooftop intake height of 0.75 m. **b.** Rooftop removal effectiveness as a function of rooftop surface deposition velocities at the 90th percentile friction velocity at 3 rooftop intake heights of 0.25, 0.5, and 0.75 m.

6.3.2. Sample multi-zone mass balance model

Room and breathing zone concentrations, as well as intake fractions for a mock environment of an area of 100 m^2, are shown in Figure 19. The impact of ozone loss rates without occupants is shown in Figure 19a. A natural ventilation case with occupants is considered a base case and is shown in Figure 19b. As occupants are introduced to the environment, indoor ozone concentrations are reduced due to occupant surfaces (skin,

clothing, hair, etc.) serving as a sink of ozone in the indoor environment. A slight difference exists between the breathing zone concentration and room concentration due to occupant inhalation. As ozone is not formed in exhaled breath, inhalation serves as a weak sink in the breathing zone, thereby reducing breathing zone concentrations of ozone. As occupancy increases to 40 occupants (Figure 19c), removal due to occupancy increases, further reducing the indoor and breathing zone ozone concentrations but this impact is smaller than increasing occupancy from 0 to 25 occupants.

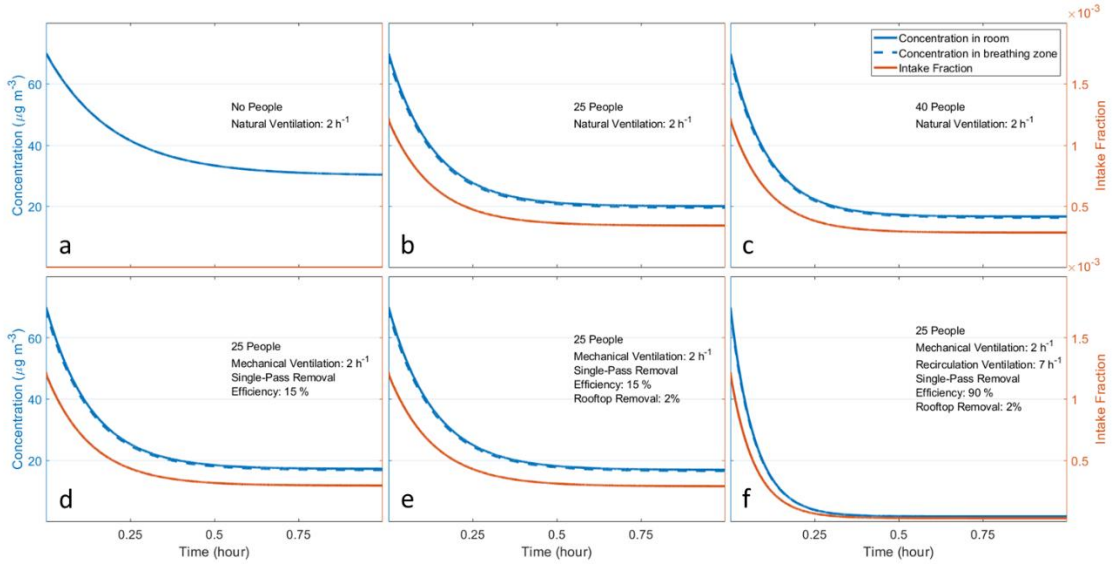

Figure 19. Sample mass-balance model output. Environmental constants are shown in Table 1. **a.** No people, only natural ventilation. **b.** 25 people, only natural ventilation, considered the base case. **c.** 40 people, only natural ventilation. **d.** 25 people, mechanical ventilation, 15 % single-pass removal efficiency of filter. **e.** 25 people, mechanical ventilation, 15 % single-pass removal efficiency of filter, 10 % removal to rooftop surfaces. **e.** 25 people, mechanical and recirculation ventilation, 90 % single-pass removal efficiency of filter, 10 % removal to rooftop surfaces

Figure 19d shows the impact of mechanical ventilation with a loaded particle filter at an ozone removal efficiency of 15% instead of natural ventilation. The impact on

breathing zone and room concentrations are similar to increasing occupants from 25 to 40, an increase in the indoor removal rate of 1.35 h^{-1}. The impact of passive removal at the rooftop scale (Figure 19e) is low, matching previously reported impact of passive ozone removal on ventilation air.[215] Worth noting is that for passive removal of ozone to adventitiously placed surfaces (i.e. those already in place and not intentionally engineered for surface removal) like particle-laden filters and rooftop surfaces may coincide with increases in byproducts downstream of the filter that should be accounted for.[34–36,66,73,157] Finally, introducing higher efficiency mitigation and higher recirculation rates (Figure 19f) substantially impacts breathing zone and room concentrations and intake fractions; breathing zone ozone concentrations and intake fractions dropped by 91 % within 30 mins. Activated carbon filters are known to have removal efficiencies of 90+ % and the impact on breathing zone concentrations and intake fractions is considerable.

Portable room air cleaners and breathing zone air cleaners are intentional sinks that occupants can place in the room and breathing zone respectively, and their impact on breathing zone and room concentrations and intake fractions are shown in Figure 20. A room air cleaner operating at a CADR of 500 CFM (Figure 20a.) reduced the breathing zone concentration and intake concentrations by 22 % from the base case (Figure 19b). Applying a breathing zone air cleaner at a CADR of 8 CFM (Figure 20b.) had a similar effect, reducing breathing zone concentrations and intake fractions by 28% from the base case. While these results show the potential of high CADR cleaners at the breathing zone and room-scale, they may be unrealistic. High CADR air cleaners for ozone or other

gaseous removal are difficult to construct. Ozone removal via activated carbon mediums is dependent on contact time and air cleaners with high airflow may have low contact time if only a thin activated carbon filter is used. A packed activated carbon bed might allow for higher CADR but also necessitates higher static pressure fans which may be energy intensive.

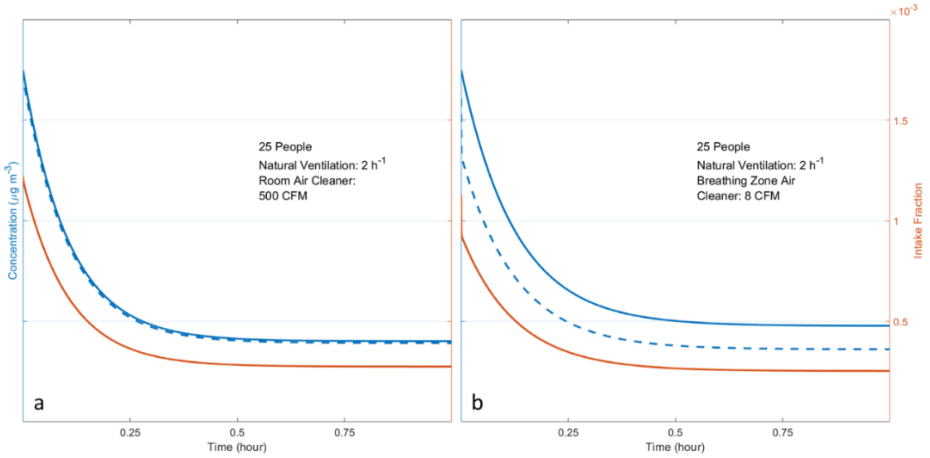

Figure 20. Room volume: 400 m^3, penetration rate: 0.75, infiltration rate: 0.2 h^{-1}, surface removal rate: 2.8 h^{-1}, removal rate on occupants: 0.09 h^{-1} per person, breathing zone volume: 0.02502 m^2 (9 in. radius hemisphere), breathing rate: 0.3 LPS. **a.** 25 people, natural ventilation, room air cleaners at CADR of 500 CFM. **b.** 25 people, natural ventilation, breathing zone air cleaners at CADR of 8 CFM.

6.3.3. Contribution of sources and sinks to breathing zone concentrations and intake fraction

While a dynamic mass balance allows us to model the impact of various sources and sinks on breathing zone concentrations and intake fractions, it can be computationally intensive to study the sensitivity of sources and the effectiveness of source and sink parameters. A steady-state output offers a simpler approach to understanding the dynamics of a two-zone mass balance and its impact on intake fractions. A Monte Carlo simulation was used across parameters shown in Tables 4 and 5. Figure 21 shows the impact source

rates (mechanical ventilation, natural ventilation, and infiltration rates) and occupancy for a mock room area of 100 m^2 on intake fractions and breathing zone concentrations. Breathing zone concentrations were calculated by multiplying breathing zone infiltration ratios by the outdoor concentration.

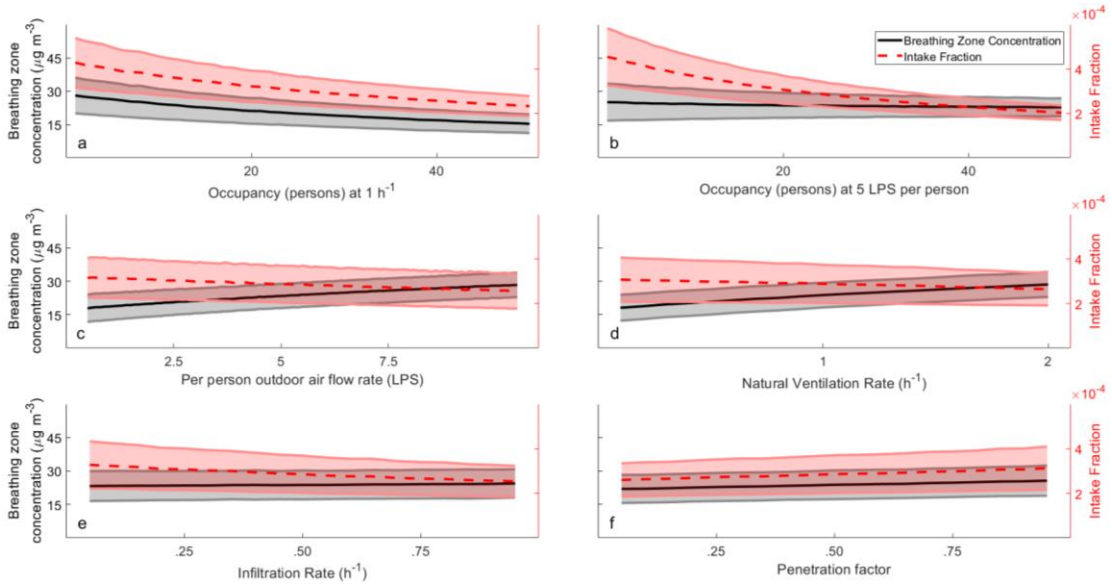

Figure 21. Monte Carlo simulation for changes of source rates and occupancy to steady-state breathing zone concentrations and intake fractions for a mock environment, described in Table 2. All passive and active removal methods were turned off. A minimum removal effectiveness of 5% was used to represent a clean particle filter in the ventilation system. **a.** Occupancy changes from 5 to 95 persons at a constant ventilation rate of 1 h^{-1}. **b.** Occupancy changes from 5 to 95 persons at demand-controlled ventilation of 5 LPS per person. **c.** Changes in per person outdoor air ventilation rates from 0.5 to 29.5 LPS per person **d.** Changes in natural ventilation rates from 0.1 to 4 h^{-1} **e.** Changes in infiltration rates from 0.1 to 1 h^{-1} **f.** Changes in penetration factor from 0.1 to 1

Changes in occupancy are shown in Figures 21a and 21b. For a constant natural ventilation rate of 1 h^{-1} in the mock environment (Figure 21a), occupants act as a sink of ozone in the indoor environment. Ozone removal to occupants was estimated to be 0.09 ± 0.02 h^{-1} per person[364] and increases in occupants decreases the indoor concentration of

ozone. This removal coincides with reductions in intake fraction of ozone but ozone removal to occupants can form ozone reaction products in the room and within the breathing zone that may be harmful.[22,388] When coupling ventilation rates with occupancy such as in demand-controlled ventilation (DCV) (Figure 21b), increases in occupancy increase ozone-rich air into the indoor environment. This, in conjunction with increases in sinks due to increased occupancy, sustains a near-constant breathing zone ozone concentration as occupancy increases. But the implication of maintaining a constant breathing zone ozone concentration while increasing occupant-related sinks is the inhalation of oxidation products from ozonolysis on occupants/indoor surfaces. While this coincides with reducing the exposure fraction, due to increases in the outdoor source flow rate (mechanical ventilation) relative to the inhalation (0.3 LPS), DCV increases absolute occupant exposure to both ozone and ozone reaction products.

Changes in ventilation rates, either via increases in per person outdoor air rates and natural ventilation rates are shown in Figures 21c and 21d, respectively. As ventilation rates increase, mass transfer rates of ozone into the indoor environment increase, increasing occupant exposure to ozone. But this coincides with reductions in intake fraction because the source rate increases relative to the inhalation rate. Increases in infiltration rate also increase ozone concentrations indoors and within the breathing zone, although the impact is modest relative to mechanical ventilation and natural ventilation. Infiltration occurs through air movement within cracks and small openings in the building envelope and is generally smaller than both mechanical and natural ventilation rates. Changes in

penetration factor were also modeled and shown in Figure 21f. As the penetration factor increases, a lower amount of ozone is removed by the building envelope, thereby increasing the intake fraction and exposure to ozone.

6.3.4. Effectiveness of passive and active mitigation methods

Monte Carlo simulations were run to test the effectiveness of passive and active mitigation methods in impacting breathing zone concentrations. Figure 22 shows the breathing zone effectiveness of various mitigation techniques for a room with an area of 100 m^2 and Table 7 outlines the removal values necessary to meet a theoretical threshold effectiveness of 50 %. Passive and active methods tested were removal to ventilation filters, deposition to rooftop surfaces, removal to indoor passive materials, portable room air cleaners, and breathing zone air cleaning shown in Table 6. For each mitigation method, a Monte Carlo simulation was applied where, for each increment of the independent mitigation method, the concentrations were calculated 10,000 times with random sampling of ventilation values (per person OA rate, natural ventilation, infiltration, and penetration factor), thermal plume cross-sectional velocity, losses to surfaces, and losses to occupants shown in Table 4 and 5. Minimum removal efficiency for particle filters of 5 % was used to signify ozone losses to unsoiled, clean particle filters.

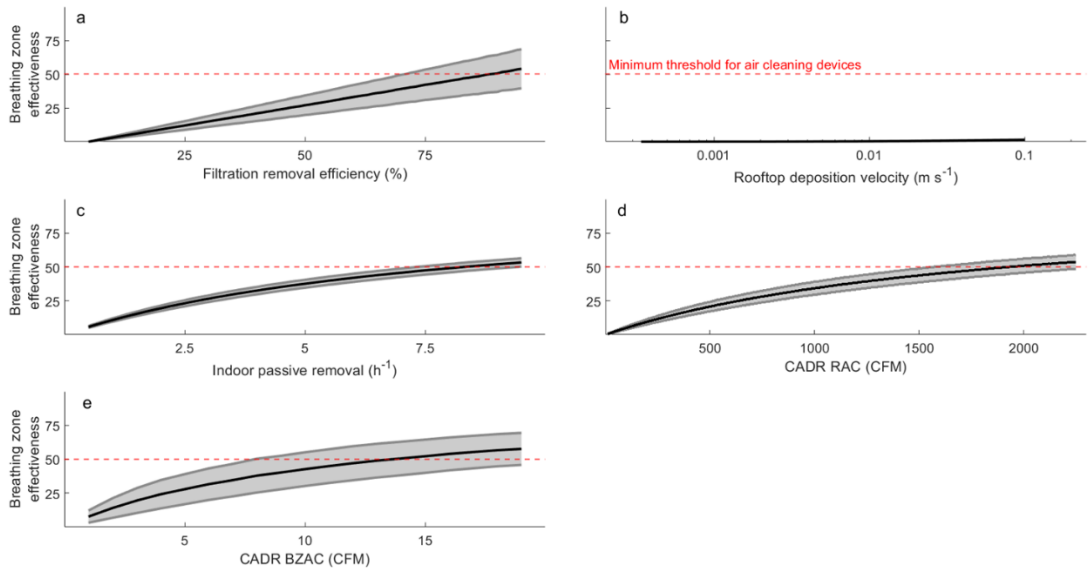

Figure 22. Breathing zone effectiveness of changes in **a.** single pass removal efficiency **b.** rooftop deposition velocity **c.** indoor passive removal rates **d.** room air cleaner CADRs **e.** breathing zone CADRs

Results of the simulation should be considered the theoretical breathing zone effectiveness, the actual impact of removal methods may vary due to air exchange rates, HVAC system cycles and run times, proximity to occupants, and other environmental parameters. The impact of filtration efficiency on the theoretical breathing zone effectiveness, shown in Figure 22a, is linear; the mitigation method is applied at the source and a portion of ozone is removed before entering the indoor environment, therefore, a reduction in breathing zone concentrations is linearly proportional to filtration efficiency. While increasing ozone removal efficiency of HVAC filtration to activated carbon (AC) can provide greater reductions in ozone exposure, energy costs associated with upgrading to AC filtration may increase and the real impact on the indoor environment is dependent on the duty cycle and run time.[156,356] Aldred et al. (2016) modelled the effectiveness of activated carbon filtration in single-family homes incorporating the HVAC system cycles,

where they found that the benefits of carbon filtration were greatest in homes with highly efficient HVAC systems.[156] When incorporating a typical runtime of 20 %, the runtime influenced breathing zone effectiveness (RIBE) would not be able to meet the minimum threshold for air cleaning technologies. Li and Siegel (2021) showed, through a Monte Carlo simulation of the effectiveness of ventilation cycles on particle concentrations, that incorporating runtime into effectiveness calculations provided the closest approximation of the exposure reduction of PM2.5.[356]

A similar analysis can be used for the relationship between rooftop deposition velocity and breathing zone effectiveness, where the impact of the rooftop is on the air brought indoors through the ventilation system. But, since rooftop uptake is shown to be ineffective even with parameters set for optimal removal e.g., transport-limited conditions, the inclusion of HVAC cycling would only further reduce the impact of this approach.[215]

The theoretical effectiveness of indoor passive removal materials is shown in Figure 22c. Shaughnessy and Sextro (2006) showed that the effectiveness of indoor air cleaners to indoor PM can be modeled via the removal ratio; the ratio of the pollutant removal due to the air cleaner over the removal due to other factors in the indoor environment. This removal ratio is based on a single-zone mass balance, where the effectiveness is only calculated to room concentrations and the impact of a separate breathing zone volume near occupants is not included.[159] A similar room-scale removal ratio can be quantified for ozone, but removal rates for ozone to surfaces and occupants in the indoor environment can be much larger than for some particle sizes. For example, in a

sample classroom with an area of 100 m^2 and 25 occupants, shown in Figure 21c, typical surface removal rates in the indoor environment may be 2.8 $h^{-1,}$ and losses to occupants can be approximately 0.09 h^{-1} per occupant.[364] Therefore, the total removal to indoor surfaces (including occupants) is approximately 5 h^{-1} without accounting for losses due to air exchange between the indoor and outdoor environments, occupant inhalation, or other factors. Incorporating the removal to occupants, surfaces, and air exchange, the threshold removal rate to reach a minimum of 50 % effectiveness for a room with an area of 100 m^2 (Table 7) is 8.2 h^{-1}. Gall et al. (2011) modeled the effectiveness of activated carbon cloth and gypsum wallboard under high flow conditions and low and high surface area to volume ratios. Under high near-material airflow conditions, with high surface area to volume ratios, and an air exchange rate of 0.5 h^{-1}, the removal ratio of the activated carbon cloth is approximately 2 and an effectiveness of approximately 67 %.[94] But this analysis did not incorporate losses to occupants, a potentially substantial sink of ozone in the indoor environment. Under quiescent indoor airspeeds, the deposition velocity to activated carbon cloth is 5.3 m h^{-1}.[142] Incorporating occupancy, the area required for effective removal to activated carbon cloth in the sample environment is approximately 620 m^2, which is not achievable in most indoor environments.

The theoretical effectiveness requirements of PRM can also be extended to portable room air cleaners; portable room air cleaners at the room-scale must provide a CADR at the same indoor removal rate as PRM. To meet the minimum threshold effectiveness, room air cleaners, shown in Figure 22d, need to provide approximately 1930 CFM, an extremely

high value. This suggests that effective ozone interventions at the room-scale may not be feasible.

Table 7. Minimum removal values for 50% effectiveness across 3 room sizes (height = 4 m)

Room Area:	50 m^2	100 m^2	150 m^2
Ventilation removal efficiency (%)	75	85	90
Rooftop deposition velocity (cm s^{-1})	-	-	-
PRM (h^{-1})	9.5	8.2	7.8
Air Cleaner CADR (CFM)	1120	1930	2760
Breathing Zone CADR (CFM)	13	14	15

The theoretical breathing zone effectiveness of a novel, hypothetical breathing zone air cleaner is shown in Figure 22e. As the breathing zone volume is small relative to the room, the impact on breathing zone concentrations is substantial. To meet the minimum threshold effectiveness of 50 % in the sample environment, breathing zone air cleaning needs to provide a CADR of 14 CFM, much smaller than what's needed by room-scale air cleaners to impact breathing zone concentrations. But these air cleaners will be ineffective in treating room air, outside of the breathing zone, potentially leading to a greater accumulation of ozone reaction products in the room air compared with other ozone interventions. Estimates of effective CADRs for breathing zone air cleaners are likely to be underestimates due to the potential errors associated with the well-mixed assumption within the breathing zone, described in section 6.3.5. The impact of sinks within the

breathing zone is likely underestimated and the breathing zone volume may be larger than what is estimated in this study, leading to an underestimation of the CADR necessary for effective breathing zone air cleaning.

Also, sinks related to occupant breathing, metabolism, or interaction with the environment can impact the effectiveness of breathing zone air cleaning. For example, occupant surface reaction rates, respiration, thermal plume flow rates, and ventilation air can increase when the occupant is exerting themselves or in motion, which will lead to increases in removal rates of sinks within the breathing zone, reducing the effectiveness of a breathing zone air cleaner. The feasibility of air cleaning technology at the breathing zone scale is also doubtful. Technologies for ozone removal at the breathing zone scale are most likely like that of room air cleaning for ozone therefore, similar issues associated with overcoming low contact or residence times and high static pressures exist.

6.3.5. Potential errors associated with the multi-zone model

The use of the multi-zone model considers a few assumptions that may not be met when applying it to the breathing zone. Generally, multi-zone models use single temperatures for each zone, implying that the air temperature is uniform in the zone.[401] But as occupants represent a heat source in the indoor environment, a temperature gradient exists within the breathing zone that drives the convective transport of pollutants between the indoor environment and the breathing zone. Another assumption commonly used in multi-zone models is that the air in the zone of interest is quiescent and the flow of air through the breathing zone does not impact zone pressure. Errors associated with

neglecting the impact of air momentum within the breathing zone may lead to ignoring recirculation areas that may impact breathing zone concentrations. Finally, multi-zone models also assume that a pollutant is perfectly mixed in a zone, which may not hold for the breathing zone. Since ozone can react on occupant skin and be inhaled by occupants, a concentration gradient exists within the breathing zone. In a CFD analysis of personal exposure to ozone, Rim et al. (2009) found that the thermal plume pulls air up across the occupant surface boundary layer depleting ozone concentrations and enriching ozone reaction products within the breathing zone.[388] In another CFD analysis to understand ozone reactions on occupant surfaces, Rim et al. (2018) found breathing concentrations to be a function of airflow and occupant surface reaction probability, with breathing zone concentrations being reduced by a maximum ~10% due to complete uptake on occupant skin.[33] To properly incorporate the impact of the occupant and proximity of cleaners, a well-defined CFD model is required, which is outside the scope of this effort.

6.4. Conclusions

This study is the first of its kind to evaluate the theoretical effectiveness of passive and active ozone mitigation methods to breathing zone concentrations and intake fractions. Removal at the outdoor air ventilation scale has a positive, linear relationship with theoretical breathing zone effectiveness but the actual effectiveness depends on the duty cycle and run time.[156,356] Ozone mitigation at the breathing zone scale may also be an effective method in reducing breathing zone ozone concentrations and intake fractions but the effectiveness can be influenced by occupant respiration, thermal plume, air exchange,

and other sinks in the indoor environment. With the inclusion of occupancy, the potential for room-scale interventions to effectively treat breathing zone ozone concentrations may not be feasible. As occupants can represent a large sink, air cleaning methods must not only compete, but overcome the combined sinks due to the removal to surfaces, ventilation, and removal to occupants. Removal ratios of indoor interventions can decrease with increasing occupancy, decreasing the effectiveness of room-scale air cleaners. Although increases in source rates (mechanical ventilation, natural ventilation, and infiltration rates) correspond with reductions in intake fractions, they also increase exposure to ozone.

Limitations exist in applying this model; multi-zone model assumptions may not be met within the breathing zone. Ozone removal to occupant skin and clothing may also generate ozone reaction products that could act as secondary reaction sites for ozone within the breathing zone. The proximity of mitigation systems to the breathing zone is an important factor to consider when studying the effectiveness of air cleaners but cannot be quantified without a fully defined CFD model. Finally, chamber measurements and *in situ* studies are warranted to better understand the effectiveness of pollution mitigation systems to inhalation concentrations and occupant health.

7. Conclusion and future work

This dissertation explores the transport, transformation, and control of ozone in the indoor environment. Ozone in the troposphere is predominately a secondary pollutant formed through a photochemical reaction process and our collective exposure to ozone is largely in the indoor environment. This exposure occurs via inhalation which can have both short- and long-term impacts on occupants. Also, when ozone is transported indoors, it may be removed and transformed on indoor surfaces, including on occupants, potentially producing detrimental byproducts inhaled by occupants. Therefore, control and removal of ozone in indoor air, in the outdoor spaces surrounding a building, or in the air transport pathway to the indoor environment, is imperative to reducing breathing zone concentrations and improving occupant health. To understand the impacts of potential mitigation systems, I set out to measure and model various ozone removal mechanisms in the outdoor and indoor environment.

First, I measured ozone removal to green roofs via economical measurements such as the atmospheric gradient method (AGM) and the modified-Bowen ratio (MBR) method. Costs associated with high frequency, direct ozone flux measurements can be substantial, only a few direct ozone flux towers exist around the world. The AGM and MBR methods are more economically feasible for in-situ ozone flux measurements, but their usability at the rooftop scale requires investigation. In conjunction with gradient methods, I measured CO_2/H_2O exchange to a site incorporating both urban green and hard surfaces for a full year through eddy-flux measurements. This measurement is separated by seasons and

representative surface morphology. I found that average evapotranspiration (ET) was higher on urban green surfaces than on urban hard surfaces, 0.96 ± 0.95 mm d^{-1} and 0.19 ± 0.93 mm d^{-1}, respectively. Average urban hard surface CO_2 fluxes were higher than the average green surfaces, 7.74 ± 6.65 µmol m^{-2} s^{-1} and 0.60 ± 1.57 µmol m^{-2} s^{-1}, respectively, and over 90% of total CO_2 fluxes measured in this study are from urban hard surfaces (which includes a parking lot and a roadway, potential fossil fuel emission sources). This suggests that reductions in anthropogenic urban CO_2 emission sources, like fossil fuel combustion, may realize a larger impact on urban CO_2 levels than increasing urban vegetation cover alone.

Measurements of CO_2 and H_2O exchange via the AGM and MBR methods did not track well with the direct measurements of CO_2 and H_2O fluxes using the eddy correlation method. The AGM assumes homogeneous surface conditions and that the length scale over which mean gradients are measured be larger than the length scale of turbulence, both of which may not have been met at the field site. Potential solutions/workarounds may be to remove counter gradients that are associated with the upward motion of local eddies and/or to apply a 'mixing' layer analogy instead of the standard Monin-Obukhov similarity theory (MOST) flux-gradient relationships.

In the second effort of this dissertation, I measured ozone removal to rooftop vegetation through chamber experiments and evaluated the uptake potential of various rooftop surface types. I retrieved rooftop vegetation and substrate samples from the green roof, and measured deposition velocities and the transport limited deposition velocities to

the vegetation and substrate samples. I found that rooftop vegetation, comprised of sedum and herbaceous species, appears to have similar surface resistances to that of urban vegetation. When I tested substrate alone, I discovered that the driest substrate condition had the highest surface resistance, implying that substrate water content was key in limiting ozone uptake. I then used these chamber-scale, measured vegetation resistances and values of surface resistances for other potential rooftop surfaces attained from literature to compare the uptake potential of rooftop surface types. Field measurements of rooftop aerodynamic and surface resistances were calculated from measurements made in the field campaign described in section 3. I found that brick, a material containing clay that is known to be reactive with ozone, had the greatest deposition velocity at 0.94 ± 0.31 cm s^{-1}. Green roofs (0.23 ± 0.03 cm s^{-1}), green roof substrate (0.21 ± 0.02 cm s^{-1}), and lush urban vegetation (0.62 ± 0.15 cm s^{-1}) had removal on par with other building materials. If the rooftop surface's ability to uptake ozone is idealized, ozone removal is transport-limited, where ozone uptake to rooftop surfaces is defined by the turbulence characteristics above the rooftop. But the impact of the rooftop surface on ozone removal is modest, for an area of 100 m^2, rooftop removal effectiveness at the 90^{th} percentile friction velocity was 4.7 %.

In the third research effort, I studied the influence of rooftop surfaces on HVAC filter loadings, ozone removal, and secondary byproduct formation in ventilation air. Measured ozone removal across filters varied between 3.5 % ± 2.8 % to 14 % ± 2.8 % depending on the type of filter, temperature, and RH condition, matching previously reported values of ozone removal to loaded filters. Ozone removal across the two rooftop

types was similar but ozone removal did vary depending on the season. Ozone removal for green roof and white roof filters were higher in the winter season, 6.5 % ± 2.8 % and 8.0 % ± 2.8 % respectively, than those for the fall season, 5.9 % ± 2.8 % and 3.6 % ± 2.8 % respectively, but these differences were within propagated uncertainty. In terms of the impact of primary and secondary VOCs of loaded and unused filters, I discovered that loaded filters can elevate VOC levels in ventilation air to the indoor environment, but this depends on the filter face velocity and the ratio of filter media to face area. Filter fluxes of methanol overshadowed other compounds tracked in this study, including in unused filters, suggesting high methanol fluxes are intrinsic to some HVAC filters. Also, I observed no particle formation due to surface ozonolysis, implying there exist low concentrations of surface-sorbed monoterpenes on tested filters.

For the fourth effort, I set out to model the effectiveness of various mitigation methods on breathing zone concentrations through a Monte Carlo simulation. Inputs to this model were collected from the previous three efforts as well as the literature. The modeled ozone interventions were passive removal via outdoor deposition to rooftops, removal to HVAC filters, removal to indoor PRMs, removal via indoor air cleaners, and removal via breathing zone air cleaning. Through this modeling effort, I determined that the removal to ventilation filters was the most direct method of impacting breathing zone concentrations; breathing zone effectiveness was linearly correlated with ventilation filter removal efficiencies. But, their actual impact may depend on HVAC unit duty cycles and run times.[156,356] I also find that effective ozone removal, as typically defined in the indoor air-

field as at least 50% reduction in concentration at steady-state, at the room-scale may not be feasible; ozone losses to surfaces, occupants, and air exchange with the outdoor environment can be high. Therefore, removal rates necessary for effective indoor interventions are potentially unachievable in most environments. Finally, ozone removal at the breathing zone scale may be promising; the CADR of breathing zone air cleaners to reach a minimum threshold of 50 % was found to be two orders of magnitude smaller than room air cleaners but the feasibility of the necessary contact times and fan static pressures required of such a technology is still doubtful.

7.1. Potential future work

Future work on this topic could include performing further studies of pollutant gradient measurements described in section 3 and the evolution of the model of the effectiveness of various air cleaning mechanisms described in section 6. Concentration measurements at height differences farther than the mixing length associated with the measurement height can provide more accurate gradient measurements of pollutant deposition to rooftops. The mixing length can be estimated as $l \approx \kappa z$ where z is the measurement height and κ is the von-Kárman constant.[402]

Ozone removal can also occur to gaseous compounds such as NO_x and organic compounds and second-order rate coefficients can be described and easily added to the model described in chapter 6. Duty-cycle and runtime coefficients can also be easily added to the multi-zone mass-balance model allowing the depiction of realistic influences on

breathing zone effectiveness. Also, a similar modeling exercise can be performed in evaluating the effectiveness of mitigation systems on indoor PM, a pollutant of both indoor and outdoor origin where indoor exposure also dominates our total exposure. Finally, chamber experiments of combined air cleaning through ventilation filters, room air cleaning, and breathing zone air cleaning in a large environmental chamber can be used to validate the two-zone mass-balance model and more accurately provide measurements of parameters estimated via a Monte Carlo simulation.

8. References

(1) World Health Organization. Burden of Disease from Household Air Pollution for 2012. **2017**.

(2) Wiley, J.; Robinson, J.; Piazza, T.; Garrett, K.; Cirksena, K.; Cheng, Y.; Martin, G. Activity Patterns of California Residents. Final Report. *Survey Research Centre, University of California, Berkeley. California Air Resources Board NL-w AK* **1991**, *17722*.

(3) Klepeis, N. E.; Nelson, W. C.; Ott, W. R.; Robinson, J. P.; Tsang, A. M.; Switzer, P.; Behar, J. V.; Hern, S. C.; Engelmann, W. H. The National Human Activity Pattern Survey (NHAPS): A Resource for Assessing Exposure to Environmental Pollutants. *J Expo Sci Environ Epidemiol* **2001**, *11* (3), 231–252. https://doi.org/10.1038/sj.jea.7500165.

(4) Jones, A. P. Indoor Air Quality and Health. *Atmospheric Environment* **1999**, 30.

(5) Robinson, J.; Nelson, W. C. National Human Activity Pattern Survey Data Base. *USEPA, Research Triangle Park, NC* **1995**.

(6) Wallace, L. The Total Exposure Assessment Methodology Study: Summary and Analysis. **1987**.

(7) Licina, D.; Tian, Y.; Nazaroff, W. W. Inhalation Intake Fraction of Particulate Matter from Localized Indoor Emissions. *Building and Environment* **2017**, *123*, 14–22. https://doi.org/10.1016/j.buildenv.2017.06.037.

(8) Hellweg, S.; Demou, E.; Bruzzi, R.; Meijer, A.; Rosenbaum, R. K.; Huijbregts, M. A. J.; McKone, T. E. Integrating Human Indoor Air Pollutant Exposure within Life Cycle Impact Assessment. *Environ. Sci. Technol.* **2009**, *43* (6), 1670–1679. https://doi.org/10.1021/es8018176.

(9) Hodas, N.; Loh, M.; Shin, H.-M.; Li, D.; Bennett, D.; McKone, T. E.; Jolliet, O.; Weschler, C. J.; Jantunen, M.; Lioy, P.; Fantke, P. Indoor Inhalation Intake Fractions of Fine Particulate Matter: Review of Influencing Factors. *Indoor Air* **2016**, *26* (6), 836–856. https://doi.org/10.1111/ina.12268.

(10) Lai, A. C. K.; Thatcher, T. L.; Nazaroff, W. W. Inhalation Transfer Factors for Air Pollution Health Risk Assessment. *Journal of the Air & Waste Management Association* **2000**, *50* (9), 1688–1699. https://doi.org/10.1080/10473289.2000.10464196.

(11) Ilacqua, V.; Hänninen, O.; Kuenzli, N.; Jantunen, M. F. Intake Fraction Distributions for Indoor VOC Sources in Five European Cities. *Indoor Air* **2007**, *17* (5), 372–383. https://doi.org/10.1111/j.1600-0668.2007.00485.x.

(12) Weschler, C. J. Changes in Indoor Pollutants since the 1950s. *Atmospheric Environment* **2009**, *43* (1), 153–169. https://doi.org/10.1016/j.atmosenv.2008.09.044.

(13) Bernstein, J. A.; Alexis, N.; Bacchus, H.; Bernstein, I. L.; Fritz, P.; Horner, E.; Li, N.; Mason, S.; Nel, A.; Oullette, J.; Reijula, K.; Reponen, T.; Seltzer, J.; Smith, A.; Tarlo, S. M. The Health Effects of Nonindustrial Indoor Air Pollution. *Journal of*

Allergy and Clinical Immunology **2008**, *121* (3), 585–591. https://doi.org/10.1016/j.jaci.2007.10.045.

(14) Perez-Padilla, R.; Schilmann, A.; Riojas-Rodriguez, H. Respiratory Health Effects of Indoor Air Pollution. *The international journal of tuberculosis and lung disease : the official journal of the International Union against Tuberculosis and Lung Disease* **2010**, *14*, 1079–1086.

(15) Hoskins, J. A. Health Effects Due to Indoor Air Pollution. *Indoor and Built Environment* **2003**, *12* (6), 427–433. https://doi.org/10.1177/1420326X03037109.

(16) Pérez-Lombard, L.; Ortiz, J.; Pout, C. A Review on Buildings Energy Consumption Information. *Energy and Buildings* **2008**, *40* (3), 394–398. https://doi.org/10.1016/j.enbuild.2007.03.007.

(17) Husman, T. Health Effects of Indoor-Air Microorganisms. *Scand J Work Environ Health* **1996**, *22* (1), 5–13. https://doi.org/10.5271/sjweh.103.

(18) Crutzen, P. J. Tropospheric Ozone: An Overview. In *Tropospheric Ozone*; Isaksen, I. S. A., Ed.; Springer Netherlands: Dordrecht, 1988; pp 3–32. https://doi.org/10.1007/978-94-009-2913-5_1.

(19) Lelieveld, J.; Dentener, F. J. What Controls Tropospheric Ozone? *J. Geophys. Res.* **2000**, *105* (D3), 3531–3551. https://doi.org/10.1029/1999JD901011.

(20) Haagen-Smit, A. J.; Bradley, C.; Fox, M. Ozone Formation in Photochemical Oxidation of Organic Substances. *Industrial & Engineering Chemistry* **1953**, *45* (9), 2086–2089.

(21) Lippmann, M. HEALTH EFFECTS OF OZONE A Critical Review. *JAPCA* **1989**, *39* (5), 672–695. https://doi.org/10.1080/08940630.1989.10466554.

(22) Wisthaler, A.; Weschler, C. J. Reactions of Ozone with Human Skin Lipids: Sources of Carbonyls, Dicarbonyls, and Hydroxycarbonyls in Indoor Air. *Proceedings of the National Academy of Sciences* **2010**, *107* (15), 6568–6575. https://doi.org/10.1073/pnas.0904498106.

(23) Allen, R. J.; Wadden, R. A.; Ross, E. D. Characterization of Potential Indoor Sources of Ozone. *American Industrial Hygiene Association Journal* **1978**, *39* (6), 466–471. https://doi.org/10.1080/0002889778507791.

(24) W.Leovic, K.; Sheldon, L. S.; Whitaker, D. A.; Hetes, R. G.; Calcagni, J. A.; Baskir, J. N. Measurement of Indoor Air Emissions from Dry-Process Photocopy Machines. *Journal of the Air & Waste Management Association* **1996**, *46* (9), 821–829. https://doi.org/10.1080/10473289.1996.10467517.

(25) Lee, S. C.; Lam, S.; Fai, H. K. Characterization of VOCs, Ozone, and PM10 Emissions from o Ce Equipment in an Environmental Chamber. *Building and Environment* **2001**, 6.

(26) Barrese, E.; Gioffrè, A.; Scarpelli, M.; Turbante, D.; Trovato, R.; Iavicoli, S. Indoor Pollution in Work Office: VOCs, Formaldehyde and Ozone by Printer. *ODEM* **2014**, *02* (03), 49–55. https://doi.org/10.4236/odem.2014.23006.

(27) Weschler, C. J.; Shields, H. C.; Naik, D. V. Indoor Ozone Exposures. *JAPCA* **1989**, *39* (12), 1562–1568. https://doi.org/10.1080/08940630.1989.10466650.

(28) Huang, Y.; Yang, Z.; Gao, Z. Contributions of Indoor and Outdoor Sources to Ozone in Residential Buildings in Nanjing. *IJERPH* **2019**, *16* (14), 2587. https://doi.org/10.3390/ijerph16142587.
(29) Weschler, C. J. Ozone in Indoor Environments: Concentration and Chemistry: Ozone in Indoor Environments. *Indoor Air* **2000**, *10* (4), 269–288. https://doi.org/10.1034/j.1600-0668.2000.010004269.x.
(30) Romieu, I.; Lugo, M. C.; Colome, S.; Garcia, A. M.; Avila, M. H.; Geyh, A.; Velasco, S. R.; Rendon, E. P. Evaluation of Indoor Ozone Concentration and Predictors of Indoor-Outdoor Ratio in Mexico City. *Journal of the Air & Waste Management Association* **1998**, *48* (4), 327–335. https://doi.org/10.1080/10473289.1998.10463684.
(31) Weschler, C. J. Ozone's Impact on Public Health: Contributions from Indoor Exposures to Ozone and Products of Ozone-Initiated Chemistry. *Environmental Health Perspectives* **2006**, *114* (10), 1489–1496. https://doi.org/10.1289/ehp.9256.
(32) Fadeyi, M. O. Ozone in Indoor Environments: Research Progress in the Past 15 Years. *Sustainable Cities and Society* **2015**, *18*, 78–94. https://doi.org/10.1016/j.scs.2015.05.011.
(33) Rim, D.; Gall, E. T.; Ananth, S.; Won, Y. Ozone Reaction with Human Surfaces: Influences of Surface Reaction Probability and Indoor Air Flow Condition. *Building and Environment* **2018**, *130*, 40–48. https://doi.org/10.1016/j.buildenv.2017.12.012.
(34) Carslaw, N.; Ashmore, M.; Terry, A. C.; Carslaw, D. C. Crucial Role for Outdoor Chemistry in Ultrafine Particle Formation in Modern Office Buildings. *Environmental Science & Technology* **2015**, *49* (18), 11011–11018. https://doi.org/10.1021/acs.est.5b02241.
(35) Wang, C.; Waring, M. S. Secondary Organic Aerosol Formation Initiated from Reactions between Ozone and Surface-Sorbed Squalene. *Atmospheric Environment* **2014**, *84*, 222–229. https://doi.org/10.1016/j.atmosenv.2013.11.009.
(36) Waring, M. S.; Siegel, J. A. Indoor Secondary Organic Aerosol Formation Initiated from Reactions between Ozone and Surface-Sorbed D -Limonene. *Environ. Sci. Technol.* **2013**, *47* (12), 6341–6348. https://doi.org/10.1021/es400846d.
(37) Morrison, G. Interfacial Chemistry in Indoor Environments. *Environ. Sci. Technol.* **2008**, *42* (10), 3495–3499. https://doi.org/10.1021/es087114b.
(38) Weschler, C. J.; Shields, H. C. Indoor Ozone/Terpene Reactions as a Source of Indoor Particles. *Atmospheric Environment* **1999**, *33* (15), 2301–2312. https://doi.org/10.1016/S1352-2310(99)00083-7.
(39) Zhou, S.; Forbes, M. W.; Abbatt, J. P. D. Kinetics and Products from Heterogeneous Oxidation of Squalene with Ozone. *Environ. Sci. Technol.* **2016**, *50* (21), 11688–11697. https://doi.org/10.1021/acs.est.6b03270.
(40) Petrick, L.; Dubowski, Y. Heterogeneous Oxidation of Squalene Film by Ozone under Various Indoor Conditions. *Indoor Air* **2009**, *19* (5), 381–391. https://doi.org/10.1111/j.1600-0668.2009.00599.x.

(41) Shu, S.; Morrison, G. C. Surface Reaction Rate and Probability of Ozone and Alpha-Terpineol on Glass, Polyvinyl Chloride, and Latex Paint Surfaces. *Environ. Sci. Technol.* **2011**, *45* (10), 4285–4292. https://doi.org/10.1021/es200194e.
(42) Springs, M.; Wells, J. R.; Morrison, G. C. Reaction Rates of Ozone and Terpenes Adsorbed to Model Indoor Surfaces: Reaction Rates of Ozone and Terpenes Adsorbed to Model Indoor Surfaces. *Indoor Air* **2011**, *21* (4), 319–327. https://doi.org/10.1111/j.1600-0668.2010.00707.x.
(43) Wolkoff, P. Indoor Air Chemistry: Terpene Reaction Products and Airway Effects. *International Journal of Hygiene and Environmental Health* **2020**, *225*, 113439. https://doi.org/10.1016/j.ijheh.2019.113439.
(44) Ham, J. E.; Wells, J. R. Surface Chemistry of a Pine-Oil Cleaner and Other Terpene Mixtures with Ozone on Vinyl Flooring Tiles. *Chemosphere* **2011**, *83* (3), 327–333. https://doi.org/10.1016/j.chemosphere.2010.12.036.
(45) Coleman, B.; Wells, J.; Nazaroff, W. Investigating Ozone-induced Decomposition of Surface-bound Permethrin for Conditions in Aircraft Cabins. *Indoor air* **2010**, *20* (1), 61–71.
(46) Nørgaard, A. W.; Kofoed-Sørensen, V.; Mandin, C.; Ventura, G.; Mabilia, R.; Perreca, E.; Cattaneo, A.; Spinazzè, A.; Mihucz, V. G.; Szigeti, T.; Kluizenaar, Y. de; Cornelissen, H. J. M.; Trantallidi, M.; Carrer, P.; Sakellaris, I.; Bartzis, J.; Wolkoff, P. Ozone-Initiated Terpene Reaction Products in Five European Offices: Replacement of a Floor Cleaning Agent. *Environ. Sci. Technol.* **2014**, *48* (22), 13331–13339. https://doi.org/10.1021/es504106j.
(47) Aoki, T.; Tanabe, S. Generation of Sub-Micron Particles and Secondary Pollutants from Building Materials by Ozone Reaction. *Atmospheric Environment* **2007**, *41* (15), 3139–3150. https://doi.org/10.1016/j.atmosenv.2006.07.053.
(48) Kagi, N.; Fujii, S.; Tamura, H.; Namiki, N. Secondary VOC Emissions from Flooring Material Surfaces Exposed to Ozone or UV Irradiation. *Building and Environment* **2009**, *44* (6), 1199–1205. https://doi.org/10.1016/j.buildenv.2008.09.004.
(49) Morrison, G. C.; Nazaroff, W. W. The Rate of Ozone Uptake on Carpets: Experimental Studies. *Environ. Sci. Technol.* **2000**, *34* (23), 4963–4968. https://doi.org/10.1021/es001361h.
(50) Morrison, G. C.; Nazaroff, W. W. Ozone Interactions with Carpet: Secondary Emissions of Aldehydes. *Environ. Sci. Technol.* **2002**, *36* (10), 2185–2192. https://doi.org/10.1021/es0113089.
(51) Nicolas, M.; Ramalho, O.; Maupetit, F. Reactions between Ozone and Building Products: Impact on Primary and Secondary Emissions. *Atmospheric Environment* **2007**, *41* (15), 3129–3138. https://doi.org/10.1016/j.atmosenv.2006.06.062.
(52) Poppendieck, D.; Hubbard, H.; Ward, M.; Weschler, C.; Corsi, R. L. Ozone Reactions with Indoor Materials during Building Disinfection. *Atmospheric Environment* **2007**, *41* (15), 3166–3176. https://doi.org/10.1016/j.atmosenv.2006.06.060.

(53) Toftum, J.; Freund, S.; Salthammer, T.; Weschler, C. J. Secondary Organic Aerosols from Ozone-Initiated Reactions with Emissions from Wood-Based Materials and a “Green” Paint. *Atmospheric Environment* **2008**, *42* (33), 7632–7640. https://doi.org/10.1016/j.atmosenv.2008.05.071.
(54) Weschler, C. J.; Hodgson, A. T.; Wooley, J. D. Indoor Chemistry: Ozone, Volatile Organic Compounds, and Carpets. *Environ. Sci. Technol.* **1992**, *26* (12), 2371–2377. https://doi.org/10.1021/es00036a006.
(55) Fick, J.; Pommer, L.; Åstrand, A.; Östin, R.; Nilsson, C.; Andersson, B. Ozonolysis of Monoterpenes in Mechanical Ventilation Systems. *Atmospheric Environment* **2005**, *39* (34), 6315–6325. https://doi.org/10.1016/j.atmosenv.2005.07.013.
(56) Fick, J.; Nilsson, C.; Andersson, B. Formation of Oxidation Products in a Ventilation System. *Atmospheric Environment* **2004**, *38* (35), 5895–5899. https://doi.org/10.1016/j.atmosenv.2004.08.020.
(57) Morrison, G. C.; Nazaroff, W. W.; Cano-Ruiz, J. A.; Hodgson, A. T.; Modera, M. P. Indoor Air Quality Impacts of Ventilation Ducts: Ozone Removal and Emissions of Volatile Organic Compounds. *Journal of the Air & Waste Management Association* **1998**, *48* (10), 941–952. https://doi.org/10.1080/10473289.1998.10463740.
(58) Metts, T. A. Heterogeneous Reactions of Ozone and D-Limonene on Activated Carbon. *Indoor Air* **2007**, *17* (5), 362–371. https://doi.org/10.1111/j.1600-0668.2007.00484.x.
(59) Metts, T. A.; Batterman, S. A. Effect of VOC Loading on the Ozone Removal Efficiency of Activated Carbon Filters. *Chemosphere* **2006**, *62* (1), 34–44. https://doi.org/10.1016/j.chemosphere.2005.04.049.
(60) Beko, G.; Halas, O.; Clausen, G.; Weschler, C. J. Initial Studies of Oxidation Processes on Filter Surfaces and Their Impact on Perceived Air Quality. *Indoor Air* **2006**, *16* (1), 56–64. https://doi.org/10.1111/j.1600-0668.2005.00401.x.
(61) Bekö, G.; Clausen, G.; Weschler, C. J. Further Studies of Oxidation Processes on Filter Surfaces: Evidence for Oxidation Products and the Influence of Time in Service. *Atmospheric Environment* **2007**, *41* (25), 5202–5212. https://doi.org/10.1016/j.atmosenv.2006.07.063.
(62) Hyttinen, M.; Pasanen, P.; Kalliokoski, P. Removal of Ozone on Clean, Dusty and Sooty Supply Air Filters. *Atmospheric Environment* **2006**, *40* (2), 315–325. https://doi.org/10.1016/j.atmosenv.2005.09.040.
(63) Hyttinen, M.; Pasanen, P.; Kalliokoski, P. Adsorption and Desorption of Selected VOCs in Dust Collected on Air Filters. *Atmospheric Environment* **2001**, *35* (33), 5709–5716. https://doi.org/10.1016/S1352-2310(01)00376-4.
(64) Hyttinen, M.; Pasanen, P.; Björkroth, M.; Kalliokoski, P. Odors and Volatile Organic Compounds Released from Ventilation Filters. *Atmospheric Environment* **2007**, *41* (19), 4029–4039. https://doi.org/10.1016/j.atmosenv.2007.01.029.

(65) Zhao, P.; Siegel, J. A.; Corsi, R. L. Ozone Removal by HVAC Filters. *Atmospheric Environment* **2007**, *41* (15), 3151–3160. https://doi.org/10.1016/j.atmosenv.2006.06.059.
(66) Zhao, P.; Siegel, J.; Corsi, R. Ozone Removal by Residential HVAC Filters. *Indoor Air* **2005**, 5.
(67) Morrison, G. C. *Ozone-Surface Interactions: Investigations of Mechanisms, Kinetics, Mass Transport, and Implications for Indoor Air Quality*; University of California, Berkeley, 1999.
(68) Apte, M.; Buchanan, I.; Mendell, M. Outdoor Ozone and Building-Related Symptoms in the BASE Study. *Indoor air* **2008**, *18* (2), 156–170.
(69) Knudsen, H. N.; Nielsen, P. A.; Clausen, P. A.; Wilkins, C. K.; Wolkoff, P. Sensory Evaluation of Emissions from Selected Building Products Exposed to Ozone: Emission from Selected Building Products Exposed to Ozone. *Indoor Air* **2003**, *13* (3), 223–231. https://doi.org/10.1034/j.1600-0668.2003.00182.x.
(70) Wolkoff, P.; Clausen, P. A.; Larsen, K.; Hammer, M.; Larsen, S. T.; Nielsen, G. D. Acute Airway Effects of Ozone-Initiated d-Limonene Chemistry: Importance of Gaseous Products. *Toxicology Letters* **2008**, *181* (3), 171–176. https://doi.org/10.1016/j.toxlet.2008.07.018.
(71) Rohr, A. C.; Wilkins, C. K.; Clausen, P. A.; Hammer, M.; Nielsen, G. D.; Wolkoff, P.; Spengler, J. D. Upper Airway and Pulmonary Effects of Oxidation Products of (+)-α-Pinene, d-Limonene, and Isoprene in BALB/c Mice. *Inhalation Toxicology* **2002**, *14* (7), 663–684.
(72) Clausen, P. A.; Wilkins, C. K.; Wolkoff, P.; Nielsen, G. D. Chemical and Biological Evaluation of a Reaction Mixture of R-(+)-Limonene/Ozone Formation of Strong Airway Irritants. *Environment International* **2001**, 12.
(73) Destaillats, H.; Chen, W.; Apte, M. G.; Li, N.; Spears, M.; Almosni, J.; Brunner, G.; Zhang, J. (Jensen); Fisk, W. J. Secondary Pollutants from Ozone Reactions with Ventilation Filters and Degradation of Filter Media Additives. *Atmospheric Environment* **2011**, *45* (21), 3561–3568. https://doi.org/10.1016/j.atmosenv.2011.03.066.
(74) Destaillats, H.; Lunden, M. M.; Singer, B. C.; Coleman, B. K.; Hodgson, A. T.; Weschler, C. J.; Nazaroff, W. W. Indoor Secondary Pollutants from Household Product Emissions in the Presence of Ozone: A Bench-Scale Chamber Study. *Environ. Sci. Technol.* **2006**, *40* (14), 4421–4428. https://doi.org/10.1021/es052198z.
(75) Kim, K.-H.; Jahan, S. A.; Lee, J.-T. Exposure to Formaldehyde and Its Potential Human Health Hazards. *Journal of Environmental Science and Health, Part C* **2011**, *29* (4), 277–299. https://doi.org/10.1080/10590501.2011.629972.
(76) Lemus, R.; Abdelghani, A.; Akers, T.; Horner, W. Potential Health Risks from Exposure to Indoor Formaldehyde. *Rev Environ Health* **1998**, *13* (1–2), 91–98.
(77) Rovira, J.; Roig, N.; Nadal, M.; Schuhmacher, M.; Domingo, J. L. Human Health Risks of Formaldehyde Indoor Levels: An Issue of Concern. *Journal of*

Environmental Science and Health, Part A **2016**, *51* (4), 357–363. https://doi.org/10.1080/10934529.2015.1109411.
(78) Weisel, C.; Weschler, C. J.; Mohan, K.; Vallarino, J.; Spengler, J. D. Ozone and Ozone Byproducts in the Cabins of Commercial Aircraft. *Environ. Sci. Technol.* **2013**, *47* (9), 4711–4717. https://doi.org/10.1021/es3046795.
(79) Mølhave, L.; Kjaergaard, S.; Sigsgaard, T.; Lebowitz, M. Interaction between Ozone and Airborne Particulate Matter in Office Air. *Indoor Air* **2005**, *15* (6), 383–392.
(80) Ibald-Mulli, A.; Wichmann, H.-E.; Kreyling, W.; Peters, A. Epidemiological Evidence on Health Effects of Ultrafine Particles. *Journal of Aerosol Medicine* **2002**, *15* (2), 189–201. https://doi.org/10.1089/089426802320282310.
(81) Schraufnagel, D. E. The Health Effects of Ultrafine Particles. *Exp Mol Med* **2020**, *52* (3), 311–317. https://doi.org/10.1038/s12276-020-0403-3.
(82) Peters, A.; Wichmann, H. E.; Tuch, T.; Heinrich, J.; Heyder, J. Respiratory Effects Are Associated with the Number of Ultrafine Particles. *American journal of respiratory and critical care medicine* **1997**, *155* (4), 1376–1383.
(83) Donaldson, K. Ultrafine Particles. *Occupational and Environmental Medicine* **2001**, *58* (3), 211–216. https://doi.org/10.1136/oem.58.3.211.
(84) Levy, J. I.; Carrothers, T. J.; Tuomisto, J. T.; Hammitt, J. K.; Evans, J. S. Assessing the Public Health Benefits of Reduced Ozone Concentrations. *Environmental Health Perspectives* **2001**, *109* (12), 12.
(85) Krupnick, A. J.; Harrington, W.; Ostro, B. Ambient Ozone and Acute Health Effects: Evidence from Daily Data. *Journal of Environmental Economics and Management* **1990**, *18* (1), 1–18. https://doi.org/10.1016/0095-0696(90)90048-4.
(86) Wyon, D. P. The Effects of Indoor Air Quality on Performance and Productivity: **The Effects of IAQ on Performance and Productivity**. *Indoor Air* **2004**, *14*, 92–101. https://doi.org/10.1111/j.1600-0668.2004.00278.x.
(87) Ruan, T.; Rim, D. Indoor Air Pollution in Office Buildings in Mega-Cities: Effects of Filtration Efficiency and Outdoor Air Ventilation Rates. *Sustainable Cities and Society* **2019**, *49*, 101609. https://doi.org/10.1016/j.scs.2019.101609.
(88) Zaatari, M.; Novoselac, A.; Siegel, J. The Relationship between Filter Pressure Drop, Indoor Air Quality, and Energy Consumption in Rooftop HVAC Units. *Building and Environment* **2014**, *73*, 151–161. https://doi.org/10.1016/j.buildenv.2013.12.010.
(89) Sundell, J. On the History of Indoor Air Quality and Health. *Indoor Air* **2004**, *14* (s7), 51–58. https://doi.org/10.1111/j.1600-0668.2004.00273.x.
(90) Burge, P. S. Sick Building Syndrome. *Occupational and Environmental Medicine* **2004**, *61* (2), 185–190. https://doi.org/10.1136/oem.2003.008813.
(91) Redlich, C. A.; Sparer, J.; Cullen, M. R. Sick-Building Syndrome. *The Lancet* **1997**, *349* (9057), 1013–1016.
(92) Norhidayah, A.; Chia-Kuang, L.; Azhar, M. K.; Nurulwahida, S. Indoor Air Quality and Sick Building Syndrome in Three Selected Buildings. *Procedia Engineering* **2013**, *53*, 93–98. https://doi.org/10.1016/j.proeng.2013.02.014.

(93) Landrigan, P. J.; Fuller, R.; Acosta, N. J. R.; Adeyi, O.; Arnold, R.; Basu, N. (Nil); Baldé, A. B.; Bertollini, R.; Bose-O'Reilly, S.; Boufford, J. I.; Breysse, P. N.; Chiles, T.; Mahidol, C.; Coll-Seck, A. M.; Cropper, M. L.; Fobil, J.; Fuster, V.; Greenstone, M.; Haines, A.; Hanrahan, D.; Hunter, D.; Khare, M.; Krupnick, A.; Lanphear, B.; Lohani, B.; Martin, K.; Mathiasen, K. V.; McTeer, M. A.; Murray, C. J. L.; Ndahimananjara, J. D.; Perera, F.; Potočnik, J.; Preker, A. S.; Ramesh, J.; Rockström, J.; Salinas, C.; Samson, L. D.; Sandilya, K.; Sly, P. D.; Smith, K. R.; Steiner, A.; Stewart, R. B.; Suk, W. A.; van Schayck, O. C. P.; Yadama, G. N.; Yumkella, K.; Zhong, M. The Lancet Commission on Pollution and Health. *The Lancet* **2018**, *391* (10119), 462–512. https://doi.org/10.1016/S0140-6736(17)32345-0.

(94) Gall, E. T.; Corsi, R. L.; Siegel, J. A. Barriers and Opportunities for Passive Removal of Indoor Ozone. *Atmospheric Environment* **2011**, *45* (19), 3338–3341. https://doi.org/10.1016/j.atmosenv.2011.03.032.

(95) Liu, D.-L.; Nazaroff, W. W. Modeling Pollutant Penetration across Building Envelopes. *Atmospheric Environment* **2001**, *35* (26), 4451–4462. https://doi.org/10.1016/S1352-2310(01)00218-7.

(96) Lai, D.; Karava, P.; Chen, Q. Study of Outdoor Ozone Penetration into Buildings through Ventilation and Infiltration. *Building and Environment* **2015**, *93*, 112–118. https://doi.org/10.1016/j.buildenv.2015.06.015.

(97) Stephens, B.; Gall, E. T.; Siegel, J. A. Measuring the Penetration of Ambient Ozone into Residential Buildings. *Environ. Sci. Technol.* **2012**, 8.

(98) Awbi, H. B. Ventilation for Good Indoor Air Quality and Energy Efficiency. *Energy Procedia* **2017**, *112*, 277–286. https://doi.org/10.1016/j.egypro.2017.03.1098.

(99) Melikov, A. K. Personalized Ventilation. *Indoor Air* **2004**, *14* (s7), 157–167. https://doi.org/10.1111/j.1600-0668.2004.00284.x.

(100) Zhang, H.; Yang, D.; Tam, V. W. Y.; Tao, Y.; Zhang, G.; Setunge, S.; Shi, L. A Critical Review of Combined Natural Ventilation Techniques in Sustainable Buildings. *Renewable and Sustainable Energy Reviews* **2021**, *141*, 110795. https://doi.org/10.1016/j.rser.2021.110795.

(101) Walker, I. S.; Sherman, M. H. Effect of Ventilation Strategies on Residential Ozone Levels. *Building and Environment* **2013**, *59*, 456–465. https://doi.org/10.1016/j.buildenv.2012.09.013.

(102) Shen, J.; Gao, Z. Ozone Removal on Building Material Surface: A Literature Review. *Building and Environment* **2018**, *134*, 205–217. https://doi.org/10.1016/j.buildenv.2018.02.046.

(103) Cano-Ruiz, J. A.; Kong, D.; Balas, R. B.; Nazaroff, W. W. Removal of Reactive Gases at Indoor Surfaces: Combining Mass Transport and Surface Kinetics. *Atmospheric Environment. Part A. General Topics* **1993**, *27* (13), 2039–2050. https://doi.org/10.1016/0960-1686(93)90276-5.

(104) Chamberlain, A. C. Transport of Gases To and From Grass and Grass-Like Surfaces. *Proceedings of the Royal Society of London. Series A, Mathematical and Physical Sciences* **1966**, *290* (1421), 236–265.
(105) Hoang, C. P.; Kinney, K. A.; Corsi, R. L. Ozone Removal by Green Building Materials. *Building and Environment* **2009**, *44* (8), 1627–1633. https://doi.org/10.1016/j.buildenv.2008.10.007.
(106) Lin, C.-C.; Hsu, S.-C. Deposition Velocities and Impact of Physical Properties on Ozone Removal for Building Materials. *Atmospheric Environment* **2015**, *101*, 194–199. https://doi.org/10.1016/j.atmosenv.2014.11.029.
(107) Kruza, M.; Lewis, A. C.; Morrison, G. C.; Carslaw, N. Impact of Surface Ozone Interactions on Indoor Air Chemistry: A Modeling Study. *Indoor Air* **2017**, *27* (5), 1001–1011. https://doi.org/10.1111/ina.12381.
(108) Rim, D.; Gall, E. T.; Maddalena, R. L.; Nazaroff, W. W. Ozone Reaction with Interior Building Materials: Influence of Diurnal Ozone Variation, Temperature and Humidity. *Atmospheric Environment* **2016**, *125*, 15–23. https://doi.org/10.1016/j.atmosenv.2015.10.093.
(109) Wells, J. R.; Morrison, G. C.; Coleman, B. K.; Spicer, C.; Dean, S. W. Kinetics and Reaction Products of Ozone and Surface-Bound Squalene. *J. ASTM Int.* **2008**, *5* (7), 101629. https://doi.org/10.1520/JAI101629.
(110) Chin, K.; Laguerre, A.; Ramasubramanian, P.; Pleshakov, D.; Stephens, B.; Gall, E. T. Emerging Investigator Series: Primary Emissions, Ozone Reactivity, and Byproduct Emissions from Building Insulation Materials. *Environ. Sci.: Processes Impacts* **2019**, *21* (8), 1255–1267. https://doi.org/10.1039/C9EM00024K.
(111) Gall, E.; Darling, E.; Siegel, J. A.; Morrison, G. C.; Corsi, R. L. Evaluation of Three Common Green Building Materials for Ozone Removal, and Primary and Secondary Emissions of Aldehydes. *Atmospheric Environment* **2013**, *77*, 910–918. https://doi.org/10.1016/j.atmosenv.2013.06.014.
(112) Fischer, A.; Ljungström, E.; Langer, S. Ozone Removal by Occupants in a Classroom. *Atmospheric Environment* **2013**, 7.
(113) Cheng, Y.-H.; Lin, C.-C.; Hsu, S.-C. Comparison of Conventional and Green Building Materials in Respect of VOC Emissions and Ozone Impact on Secondary Carbonyl Emissions. *Building and Environment* **2015**, *87*, 274–282. https://doi.org/10.1016/j.buildenv.2014.12.025.
(114) Wang, H.; Morrison, G. C. Ozone-Initiated Secondary Emission Rates of Aldehydes from Indoor Surfaces in Four Homes. *Environ. Sci. Technol.* **2006**, *40* (17), 5263–5268. https://doi.org/10.1021/es060080s.
(115) Wang, H.; Morrison, G. Ozone-surface Reactions in Five Homes: Surface Reaction Probabilities, Aldehyde Yields, and Trends. *Indoor air* **2010**, *20* (3), 224–234.
(116) Weschler, C. J.; Shields, H. C. The Influence of Ventilation on Reactions Among Indoor Pollutants: Modeling and Experimental Observations: The Influence of Ventilation on Reactions Among Indoor Pollutants: Modeling and Experimental Observations. *Indoor Air* **2000**, *10* (2), 92–100. https://doi.org/10.1034/j.1600-0668.2000.010002092.x.

(117) Wolkoff, P.; Clausen, P. A.; Wilkins, C. K.; Nielsen, G. D. Formation of Strong Airway Irritants in Terpene/Ozone Mixtures. *Indoor Air* **2000**, *10* (2), 82–91. https://doi.org/10.1034/j.1600-0668.2000.010002082.x.
(118) Sarwar, G.; Corsi, R. The Effects of Ozone/Limonene Reactions on Indoor Secondary Organic Aerosols. *Atmospheric Environment* **2007**, 15.
(119) Singer, B. C.; Coleman, B. K.; Destaillats, H.; Hodgson, A. T.; Lunden, M. M.; Weschler, C. J.; Nazaroff, W. W. Indoor Secondary Pollutants from Cleaning Product and Air Freshener Use in the Presence of Ozone. *Atmospheric Environment* **2006**, *40* (35), 6696–6710. https://doi.org/10.1016/j.atmosenv.2006.06.005.
(120) Nazaroff, W. W.; Weschler, C. J. Cleaning Products and Air Fresheners: Exposure to Primary and Secondary Air Pollutants. *Atmospheric Environment* **2004**, *38* (18), 2841–2865. https://doi.org/10.1016/j.atmosenv.2004.02.040.
(121) Aschmann, S. M.; Arey, J.; Atkinson, R. OH Radical Formation from the Gas-Phase Reactions of O3 with a Series of Terpenes. *Atmospheric Environment* **2002**, *36* (27), 4347–4355. https://doi.org/10.1016/S1352-2310(02)00355-2.
(122) Salvador, C. M.; Bekö, G.; Weschler, C. J.; Morrison, G.; Le Breton, M.; Hallquist, M.; Ekberg, L.; Langer, S. Indoor Ozone/Human Chemistry and Ventilation Strategies. *Indoor Air* **2019**, *29* (6), 913–925. https://doi.org/10.1111/ina.12594.
(123) Weschler, C. J.; Shields, H. C. Production of the Hydroxyl Radical in Indoor Air. *Environ. Sci. Technol.* **1996**, *30* (11), 3250–3258. https://doi.org/10.1021/es960032f.
(124) Sarwar, G.; Corsi, R.; Kimura, Y.; Allen, D.; Weschler, C. J. Hydroxyl Radicals in Indoor Environments. *Atmospheric Environment* **2002**, *36* (24), 3973–3988. https://doi.org/10.1016/S1352-2310(02)00278-9.
(125) Forester, C. D.; Wells, J. R. Hydroxyl Radical Yields from Reactions of Terpene Mixtures with Ozone: Hydroxyl Radical Yields from Reactions of Terpene Mixtures with Ozone. *Indoor Air* **2011**, *21* (5), 400–409. https://doi.org/10.1111/j.1600-0668.2011.00718.x.
(126) Gligorovski, S.; Wortham, H.; Kleffmann, J. The Hydroxyl Radical (OH) in Indoor Air: Sources and Implications. *Atmospheric Environment* **2014**, *99*, 568–570. https://doi.org/10.1016/j.atmosenv.2014.10.031.
(127) Gligorovski, S.; Weschler, C. J. The Oxidative Capacity of Indoor Atmospheres. *Environ. Sci. Technol.* **2013**, *47* (24), 13905–13906. https://doi.org/10.1021/es404928t.
(128) Wilkins, C. K.; Clausen, P. A.; Wolkoff, P.; Larsen, S. T.; Hammer, M.; Larsen, K.; Hansen, V.; Nielsen, G. D. Formation of Strong Airway Irritants in Mixtures of Isoprene/Ozone and Isoprene/Ozone/Nitrogen Dioxide. *Environmental Health Perspectives* **2001**, *109* (9), 5.
(129) Nielsen, G. D.; Wolkoff, P. Cancer Effects of Formaldehyde: A Proposal for an Indoor Air Guideline Value. *Arch Toxicol* **2010**, *84* (6), 423–446. https://doi.org/10.1007/s00204-010-0549-1.

(130) McLaughlin, J. K. Formaldehyde and Cancer: A Critical Review. 7.
(131) Calogirou, A.; Larsen, B.; Kotzias, D. Gas-Phase Terpene Oxidation Products: A Review. *Atmospheric Environment* **1999**, *33* (9), 1423–1439.
(132) Glasius, M.; Lahaniati, M.; Calogirou, A.; Di Bella, D.; Jensen, N. R.; Hjorth, J.; Kotzias, D.; Larsen, B. R. Carboxylic Acids in Secondary Aerosols from Oxidation of Cyclic Monoterpenes by Ozone. *Environ. Sci. Technol.* **2000**, *34* (6), 1001–1010. https://doi.org/10.1021/es990445r.
(133) Baltensperger, U.; Dommen, J.; Alfarra, M. R.; Duplissy, J.; Gaeggeler, K.; Metzger, A.; Facchini, M. C.; Decesari, S.; Finessi, E.; Reinnig, C.; Schott, M.; Warnke, J.; Hoffmann, T.; Klatzer, B.; Puxbaum, H.; Geiser, M.; Savi, M.; Lang, D.; Kalberer, M.; Geiser, T. Combined Determination of the Chemical Composition and of Health Effects of Secondary Organic Aerosols: The POLYSOA Project. *Journal of Aerosol Medicine and Pulmonary Drug Delivery* **2008**, *21* (1), 145–154. https://doi.org/10.1089/jamp.2007.0655.
(134) Hallquist, M.; Wenger, J. C.; Baltensperger, U.; Rudich, Y.; Simpson, D.; Claeys, M.; Dommen, J.; Donahue, N. M.; George, C.; Goldstein, A. H.; Hamilton, J. F.; Herrmann, H.; Hoffmann, T.; Iinuma, Y.; Jang, M.; Jenkin, M. E.; Jimenez, J. L.; Kiendler-Scharr, A.; Maenhaut, W.; McFiggans, G.; Mentel, T. F.; Monod, A.; Prevot, A. S. H.; Seinfeld, J. H.; Surratt, J. D.; Szmigielski, R.; Wildt, J. The Formation, Properties and Impact of Secondary Organic Aerosol: Current and Emerging Issues. *Atmos. Chem. Phys.* **2009**, 82.
(135) Lin, Y.-H.; Arashiro, M.; Martin, E.; Chen, Y.; Zhang, Z.; Sexton, K. G.; Gold, A.; Jaspers, I.; Fry, R. C.; Surratt, J. D. Isoprene-Derived Secondary Organic Aerosol Induces the Expression of Oxidative Stress Response Genes in Human Lung Cells. *Environ. Sci. Technol. Lett.* **2016**, *3* (6), 250–254. https://doi.org/10.1021/acs.estlett.6b00151.
(136) Andreae, M. O.; Crutzen, P. J. Atmospheric Aerosols: Biogeochemical Sources and Role in Atmospheric Chemistry. *Science* **1997**, *276* (5315), 1052–1058.
(137) Haywood, J.; Boucher, O. Estimates of the Direct and Indirect Radiative Forcing Due to Tropospheric Aerosols: A Review. *Reviews of geophysics* **2000**, *38* (4), 513–543.
(138) Oberdörster, G. Pulmonary Effects of Inhaled Ultrafine Particles. *International archives of occupational and environmental health* **2000**, *74* (1), 1–8.
(139) Sarwar, G.; Olson, D. A.; Corsi, R. L.; Weschler, C. J. Indoor Fine Particles: The Role of Terpene Emissions from Consumer Products. *Journal of the Air & Waste Management Association* **2004**, *54* (3), 367–377. https://doi.org/10.1080/10473289.2004.10470910.
(140) Sarwar, G.; Corsi, R.; Allen, D.; Weschler, C. The Significance of Secondary Organic Aerosol Formation and Growth in Buildings: Experimental and Computational Evidence. *Atmospheric Environment* **2003**, *37* (9–10), 1365–1381. https://doi.org/10.1016/S1352-2310(02)01013-0.
(141) Suárez-Cáceres, G. P.; Fernández-Cañero, R.; Fernández-Espinosa, A. J.; Rossini-Oliva, S.; Franco-Salas, A.; Pérez-Urrestarazu, L. Volatile Organic Compounds

Removal by Means of a Felt-Based Living Wall to Improve Indoor Air Quality. *Atmospheric Pollution Research* **2021**, *12* (3), 224–229. https://doi.org/10.1016/j.apr.2020.11.009.

(142) Kunkel, D. A.; Gall, E. T.; Siegel, J. A.; Novoselac, A.; Morrison, G. C.; Corsi, R. L. Passive Reduction of Human Exposure to Indoor Ozone. *Building and Environment* **2010**, *45* (2), 445–452. https://doi.org/10.1016/j.buildenv.2009.06.024.

(143) Sekine, Y. Removal of Formaldehyde from Indoor Air by Passive Type Air-Cleaning Materials. *Atmospheric Environment* **2001**, *35* (11), 2001–2007. https://doi.org/10.1016/S1352-2310(00)00465-9.

(144) Cros, C. J.; Morrison, G. C.; Siegel, J. A.; Corsi, R. L. Long-Term Performance of Passive Materials for Removal of Ozone from Indoor Air: Long-Term Performance of Passive Materials. *Indoor Air* **2012**, *22* (1), 43–53. https://doi.org/10.1111/j.1600-0668.2011.00734.x.

(145) Yang, J.; Yu, Q.; Gong, P. Quantifying Air Pollution Removal by Green Roofs in Chicago. *Atmospheric Environment* **2008**, *42* (31), 7266–7273. https://doi.org/10.1016/j.atmosenv.2008.07.003.

(146) Baraldi, R.; Chieco, C.; Neri, L.; Facini, O.; Rapparini, F.; Morrone, L.; Rotondi, A.; Carriero, G. An Integrated Study on Air Mitigation Potential of Urban Vegetation: From a Multi-Trait Approach to Modeling. *Urban Forestry & Urban Greening* **2019**, *41*, 127–138. https://doi.org/10.1016/j.ufug.2019.03.020.

(147) Bottalico, F.; Chirici, G.; Giannetti, F.; De Marco, A.; Nocentini, S.; Paoletti, E.; Salbitano, F.; Sanesi, G.; Serenelli, C.; Travaglini, D. Air Pollution Removal by Green Infrastructures and Urban Forests in the City of Florence. *Agriculture and Agricultural Science Procedia* **2016**, *8*, 243–251. https://doi.org/10.1016/j.aaspro.2016.02.099.

(148) McPherson, G. E.; Nowak, D. J.; Rowntree, R. A. *Chicago's Urban Forest Ecosystem: Results of the Chicago Urban Forest Climate Project*; NE-GTR-186; U.S. Department of Agriculture, Forest Service, Northeastern Forest Experimental Station: Radnor, PA, 1994; p NE-GTR-186. https://doi.org/10.2737/NE-GTR-186.

(149) Wargocki, P.; Kuehn, T.; Muller, C.; Conrad, E. ASHRAE Position Document on Filtration and Air Cleaning. *ASHRAE, Atlanta* **2018**.

(150) Bennett, D. H.; Fisk, W.; Apte, M. G.; Wu, X.; Trout, A.; Faulkner, D.; Sullivan, D. Ventilation, Temperature, and HVAC Characteristics in Small and Medium Commercial Buildings in California: Small and Medium Commercial Buildings in California. *Indoor Air* **2012**, *22* (4), 309–320. https://doi.org/10.1111/j.1600-0668.2012.00767.x.

(151) Walker, I. S.; Dickerhoff, D. J.; Faulkner, D.; Turner, W. J. N. System Effects of High Efficiency Filters in Homes. 10.

(152) Lam, K. S.; Chan, F. S.; Fung, W. Y.; Lui, B. S. S.; Lau, L. W. L. Achieving "excellent" Indoor Air Quality in Commercial Offices Equipped with Air-Handling Unit - Respirable Suspended Particulate. *Indoor Air* **2006**, *0* (0), 060207062917008. https://doi.org/10.1111/j.1600-0668.2005.00409.x.

(153) Fisk, W. J.; Spears, M.; Sullivan, D. P.; Mendell, M. Ozone Removal by Filters Containing Activated Carbon: A Pilot Study. **2009**, 7.
(154) Shields, H. C.; Weschlerl, C. J.; Naik, D. Ozone Removal By Charcoal Filters After Continuous Extensive Use (5 To 8 Years). **1999**, 6.
(155) Lee, P.; Davidson, J. Evaluation of Activated Carbon Filters for Removal of Ozone at the Ppb Level. *American Industrial Hygiene Association Journal* **1999**, *60* (5), 589–600.
(156) Aldred, J. R.; Darling, E.; Morrison, G.; Siegel, J.; Corsi, R. L. Benefit-Cost Analysis of Commercially Available Activated Carbon Filters for Indoor Ozone Removal in Single-Family Homes. *Indoor Air* **2016**, *26* (3), 501–512. https://doi.org/10.1111/ina.12220.
(157) Lin, C.-C.; Chen, H.-Y. Impact of HVAC Filter on Indoor Air Quality in Terms of Ozone Removal and Carbonyls Generation. *Atmospheric Environment* **2014**, *89*, 29–34. https://doi.org/10.1016/j.atmosenv.2014.02.020.
(158) Carslaw, N.; Ashmore, M.; Terry, A. C.; Carslaw, D. C. Crucial Role for Outdoor Chemistry in Ultrafine Particle Formation in Modern Office Buildings. *Environ. Sci. Technol.* **2015**, 8.
(159) Shaughnessy, R. J.; Sextro, R. G. What Is an Effective Portable Air Cleaning Device? A Review. *Journal of Occupational and Environmental Hygiene* **2006**, *3* (4), 169–181. https://doi.org/10.1080/15459620600580129.
(160) Siegel, J. A.; Waring, M. S.; Yu, X.; Corsi, R. L. Indoor Air Quality Implications of Portable Ion Generators. 12. **2006**
(161) Sidheswaran, M.; Chen, W.; Miller, R.; Cohn, S.; Kumagai, K.; Destaillats, H. Formaldehyde Emissions from Ventilation Filter Under Different Relative Humidity Conditions. **2013**, 27.
(162) Laguerre, A.; George, L. A.; Gall, E. T. High-Efficiency Air Cleaning Reduces Indoor Traffic-Related Air Pollution and Alters Indoor Air Chemistry in a Near-Roadway School. *Environ. Sci. Technol.* **2020**, *54* (19), 11798–11808. https://doi.org/10.1021/acs.est.0c02792.
(163) Stinson, B.; Laguerre, A.; Gall, E. T. Per-Person and Whole-Building VOC Emission Factors in an Occupied School with Gas-Phase Air Cleaning. *Environ. Sci. Technol.* **2022**, *56* (6), 3354–3364. https://doi.org/10.1021/acs.est.1c06767.
(164) Jo, W.-K.; Yang, C.-H. Granular-Activated Carbon Adsorption Followed by Annular-Type Photocatalytic System for Control of Indoor Aromatic Compounds. *Separation and Purification Technology* **2009**, *66* (3), 438–442. https://doi.org/10.1016/j.seppur.2009.02.014.
(165) Chen, W.; Zhang, J. S.; Zhang, Z. Performance of Air Cleaners for Removing Multiple Volatile Organic Compounds in Indoor Air. *ASHRAE Transactions* 14.
(166) Zhao, J.; Yang, X. Photocatalytic Oxidation for Indoor Air Purification: A Literature Review. *Building and Environment* **2003**, *38* (5), 645–654. https://doi.org/10.1016/S0360-1323(02)00212-3.
(167) Dalrymple, O. K.; Stefanakos, E.; Trotz, M. A.; Goswami, D. Y. A Review of the Mechanisms and Modeling of Photocatalytic Disinfection. *Applied Catalysis B:*

Environmental **2010**, *98* (1–2), 27–38. https://doi.org/10.1016/j.apcatb.2010.05.001.
(168) Zhang, Y.; Mo, J.; Li, Y.; Sundell, J.; Wargocki, P.; Zhang, J.; Little, J. C.; Corsi, R.; Deng, Q.; Leung, M. H. K.; Fang, L.; Chen, W.; Li, J.; Sun, Y. Can Commonly-Used Fan-Driven Air Cleaning Technologies Improve Indoor Air Quality? A Literature Review. *Atmospheric Environment* **2011**, *45* (26), 4329–4343. https://doi.org/10.1016/j.atmosenv.2011.05.041.
(169) Hodgson, A. T.; Destaillats, H.; Sullivan, D. P.; Fisk, W. J. Performance of Ultraviolet Photocatalytic Oxidation for Indoor Air Cleaning Applications. *Indoor Air* **2007**, *17* (4), 305–316. https://doi.org/10.1111/j.1600-0668.2007.00479.x.
(170) Bauman, F.; Zhang, H.; Arens, E. A.; Benton, C. Localized Comfort Control with a Desktop Task Conditioning System: Laboratory and Field Measurements. *ASHRAE Transactions* **1993**, *99*, 733–749.
(171) Tsuzuki, K.; Arens, E.; Bauman, F.; Wyon, D. Individual Thermal Comfort Control with Desk-Mounted and Floor-Mounted Task/Ambient Conditioning (TAC) Systems. **1999**.
(172) Kaczmarczyk, J.; Zeng, Q.; Melikov, A.; Fanger, P. Individual Control and People's Preferences in an Experiment with a Personalized Ventilation System (PVS). **2002**.
(173) Cermak, R.; Melikov, A.; Forejt, L.; Kovar, O. Performance of Personalized Ventilation in Conjunction with Mixing and Displacement Ventilation. *HVAC&R Res.* **2006**, *12* (2), 295–311. https://doi.org/10.1080/10789669.2006.10391180.
(174) Cermak, R.; Melikov, A. Protection of Occupants from Exhaled Infectious Agents and Floor Material Emissions in Rooms with Personalized and Underfloor Ventilation. *HVAC&R Res.* **2007**, *13* (1), 23–38. https://doi.org/10.1080/10789669.2007.10390942.
(175) Nielsen, P.; Hyldgaard, C. E.; Melikov, A.; Andersen, H.; Soennichsen, M. Personal Exposure Between People in a Room Ventilated by Textile Terminals—with and without Personalized Ventilation. *HVAC&R Res.* **2007**, *13* (4), 635–643. https://doi.org/10.1080/10789669.2007.10390976.
(176) Bolashikov, Z.; Melikov, A.; Spilak, M. Experimental Investigation on Reduced Exposure to Pollutants Indoors by Applying Wearable Personalized Ventilation. **2013**, *19* (4), 16.
(177) Bolashikov, Z. D.; Melikov, A.; Krenek, M. Control of the Free Convective Flow around the Human Body for Enhanced Inhaled Air Quality: Application to a Seat-Incorporated Personalized Ventilation Unit. *Hvac&r Research* **2010**, *16*, 161–188. https://doi.org/10.1080/10789669.2010.10390899.
(178) Bolashikov, Z.; Nikolaev, L.; Melikov, A. K.; Kaczmarczyk, J.; Fanger, P. O. New Air Terminal Devices with High Efficiency for Personalized Ventilation Application; NUS Press, 2003; pp 850–855.
(179) Faulkner, D.; Fisk, W.; Sullivan, D.; Wyon, D. Ventilation Efficiencies of Desk-Mounted Task/Ambient Conditioning Systems. *Indoor air* **2000**, *9*, 273–281. https://doi.org/10.1111/j.1600-0668.1999.00007.x.

(180) Faulkner, D.; Fisk, W. J.; Sullivan, D. P.; Lee, S. M. *Ventilation Efficiencies of a Desk-Edge-Mounted Task Ventilation System*; LBNL--49939, 795368; **2002**; p LBNL--49939, 795368. https://doi.org/10.2172/795368.
(181) Faulkner, D.; Fisk, W.; Sullivan, D.; Lee, S. Ventilation Efficiencies and Thermal Comfort Results of a Desk-Edge-Mounted Task Ventilation System. *Indoor Air (Supplement 8)* **2003**, *14* (LBNL-53798).
(182) Kaczmarczyk, J.; Melikov, A.; Bolashikov, Z.; Nikolaev, L.; Fanger, P. O. Human Response to Five Designs of Personalized Ventilation. *Hvac&R Research* **2006**, *12* (2), 367–384.
(183) Liu; Zhu; Kim; Srebric. A Review of CFD Analysis Methods for Personalized Ventilation (PV) in Indoor Built Environments. *Sustainability* **2019**, *11* (15), 4166. https://doi.org/10.3390/su11154166.
(184) Makhoul, A.; Ghali, K.; Ghaddar, N. Desk Fans for the Control of the Convection Flow around Occupants Using Ceiling Mounted Personalized Ventilation. *Building and Environment* **2013**, *59*, 336–348. https://doi.org/10.1016/j.buildenv.2012.08.031.
(185) Makhoul, A.; Ghali, K.; Ghaddar, N. Low-Mixing Coaxial Nozzle for Effective Personalized Ventilation. *Indoor and Built Environment* **2015**, *24* (2), 225–243. https://doi.org/10.1177/1420326X13508967.
(186) Schiavon, S.; Melikov, A. K.; Sekhar, C. Energy Analysis of the Personalized Ventilation System in Hot and Humid Climates. *Energy and Buildings* **2010**, *42* (5), 699–707. https://doi.org/10.1016/j.enbuild.2009.11.009.
(187) Xu, C.; Nielsen, P. V.; Liu, L.; Jensen, R. L.; Gong, G. Impacts of Airflow Interactions with Thermal Boundary Layer on Performance of Personalized Ventilation. *Building and Environment* **2018**, *135*, 31–41. https://doi.org/10.1016/j.buildenv.2018.02.048.
(188) Kalmár, F.; Kalmár, T. Alternative Personalized Ventilation. *Energy and Buildings* **2013**, *65*, 37–44. https://doi.org/10.1016/j.enbuild.2013.05.010.
(189) Khalifa, H. E.; Janos, M. I.; Dannenhoffer, J. F. Experimental Investigation of Reduced-Mixing Personal Ventilation Jets. *Building and Environment* **2009**, *44* (8), 1551–1558. https://doi.org/10.1016/j.buildenv.2008.11.006.
(190) Halvoňová, B.; Melikov, A. K. Performance of "Ductless" Personalized Ventilation in Conjunction with Displacement Ventilation: Impact of Disturbances Due to Walking Person(s). *Building and Environment* **2010**, *45* (2), 427–436. https://doi.org/10.1016/j.buildenv.2009.06.023.
(191) Gao, N.; Niu, J. CFD Study on Micro-Environment around Human Body and Personalized Ventilation. *Building and Environment* **2004**, *39* (7), 795–805. https://doi.org/10.1016/j.buildenv.2004.01.026.
(192) Niu, J.; Gao, N.; Phoebe, M.; Huigang, Z. Experimental Study on a Chair-Based Personalized Ventilation System. *Building and Environment* **2007**, *42* (2), 913–925. https://doi.org/10.1016/j.buildenv.2005.10.011.
(193) Nagano, H.; Bolashikov, Z. D.; Melikov, A. K.; Kato, S.; Meyer, K. E. Control of the Free Convection Flow within the Breathing Zone by Confluent Jets for

Improved Performance of Personalized Ventilation: Part 1 – Thermal Influence. 4. **2009**
(194) Muhič, S.; Butala, V. Effectiveness of Personal Ventilation System Using Relative Decrease of Tracer Gas in the First Minute Parameter. *Energy and Buildings* **2006**, *38* (5), 534–542. https://doi.org/10.1016/j.enbuild.2005.09.001.
(195) Pantelic, J.; Tham, K. W.; Licina, D. Effectiveness of a Personalized Ventilation System in Reducing Personal Exposure against Directly Released Simulated Cough Droplets. *Indoor Air* **2015**, *25* (6), 683–693. https://doi.org/10.1111/ina.12187.
(196) Russo, J.; Khalifa, H. E. CFD Analysis of Personal Ventilation with Volumetric Chemical Reactions. *HVAC&R Res.* **2010**, *16* (6), 799–812. https://doi.org/10.1080/10789669.2010.10390935.
(197) Russo, J.; Khalifa, H. E. Surface Reactions on the Human Body: Using Personal Ventilation to Remove Squalene Oxidation Products from the Breathing Zone with CFD; **2011**; pp 1719–1724.
(198) Hedge, A.; Mitchell, G. E.; McCarthy, J. F.; Ludwig, J. Effects of a Furniture-integrated Breathing-zone Filtration System on Indoor Air Quality, Sick Building Syndrome, and Productivity. *Indoor Air* **1993**, *3* (4), 328–336.
(199) Gore, R.; Boyle, R.; Gore, C.; Custovic, A.; Hanna, H.; Svensson, P.; Warner, J. Effect of a Novel Temperature-controlled Laminar Airflow Device on Personal Breathing Zone Aeroallergen Exposure. *Indoor air* **2015**, *25* (1), 36–44.
(200) Spilak, M. P.; Sigsgaard, T.; Takai, H.; Zhang, G. A Comparison between Temperature-Controlled Laminar Airflow Device and a Room Air-Cleaner in Reducing Exposure to Particles While Asleep. *PLoS ONE* **2016**, *11* (11), e0166882. https://doi.org/10.1371/journal.pone.0166882.
(201) Clifton, O. E.; Fiore, A. M.; Massman, W. J.; Baublitz, C. B.; Coyle, M.; Emberson, L.; Fares, S.; Farmer, D. K.; Gentine, P.; Gerosa, G.; Guenther, A. B.; Helmig, D.; Lombardozzi, D. L.; Munger, J. W.; Patton, E. G.; Pusede, S. E.; Schwede, D. B.; Silva, S. J.; Sörgel, M.; Steiner, A. L.; Tai, A. P. K. Dry Deposition of Ozone Over Land: Processes, Measurement, and Modeling. *Rev. Geophys.* **2020**, *58* (1). https://doi.org/10.1029/2019RG000670.
(202) Kerstiens, G.; Lendzian, K. J. Interactions between Ozone and Plant Cuticles. I. Ozone Deposition and Permeability. *New Phytol* **1989**, *112* (1), 13–19. https://doi.org/10.1111/j.1469-8137.1989.tb00303.x.
(203) Weissert, L. F.; Salmond, J. A.; Schwendenmann, L. A Review of the Current Progress in Quantifying the Potential of Urban Forests to Mitigate Urban CO2 Emissions. *Urban Climate* **2014**, *8*, 100–125. https://doi.org/10.1016/j.uclim.2014.01.002.
(204) Nowak, D. J.; Crane, D. E. Carbon Storage and Sequestration by Urban Trees in the USA. *Environmental Pollution* **2002**, *116* (3), 381–389. https://doi.org/10.1016/S0269-7491(01)00214-7.

(205) Brack, C. L. Pollution Mitigation and Carbon Sequestration by an Urban Forest. *Environmental Pollution* **2002**, *116*, S195–S200. https://doi.org/10.1016/S0269-7491(01)00251-2.
(206) Getter, K. L.; Rowe, D. B.; Robertson, G. P.; Cregg, B. M.; Andresen, J. A. Carbon Sequestration Potential of Extensive Green Roofs. *Environ. Sci. Technol.* **2009**, *43* (19), 7564–7570. https://doi.org/10.1021/es901539x.
(207) Heusinger, J.; Weber, S. Extensive Green Roof CO2 Exchange and Its Seasonal Variation Quantified by Eddy Covariance Measurements. *Science of The Total Environment* **2017**, *607–608*, 623–632. https://doi.org/10.1016/j.scitotenv.2017.07.052.
(208) Konopka, J.; Heusinger, J.; Weber, S. Extensive Urban Green Roof Shows Consistent Annual Net Uptake of Carbon as Documented by 5 Years of Eddy-Covariance Flux Measurements. *J Geophys Res Biogeosci* **2021**, *126* (2). https://doi.org/10.1029/2020JG005879.
(209) Pataki, D. E.; Carreiro, M. M.; Cherrier, J.; Grulke, N. E.; Jennings, V.; Pincetl, S.; Pouyat, R. V.; Whitlow, T. H.; Zipperer, W. C. Coupling Biogeochemical Cycles in Urban Environments: Ecosystem Services, Green Solutions, and Misconceptions. *Frontiers in Ecology and the Environment* **2011**, *9* (1), 27–36. https://doi.org/10.1890/090220.
(210) Velasco, E.; Roth, M.; Tan, S. H.; Quak, M.; Nabarro, S. D. A.; Norford, L. The Role of Vegetation in the CO2 Flux from a Tropical Urban Neighbourhood. *Atmos. Chem. Phys.* **2013**, *13* (20), 10185–10202. https://doi.org/10.5194/acp-13-10185-2013.
(211) Velasco, E.; Roth, M.; Norford, L.; Molina, L. T. Does Urban Vegetation Enhance Carbon Sequestration? *Landscape and Urban Planning* **2016**, *148*, 99–107. https://doi.org/10.1016/j.landurbplan.2015.12.003.
(212) Jo, H. Impacts of Urban Greenspace on Offsetting Carbon Emissions for Middle Korea. *Journal of Environmental Management* **2002**, *64* (2), 115–126. https://doi.org/10.1006/jema.2001.0491.
(213) Agra, H.; Klein, T.; Vasl, A.; Shalom, H.; Kadas, G.; Blaustein, L. Sedum-Dominated Green-Roofs in a Semi-Arid Region Increase CO2 Concentrations during the Dry Season. *Science of The Total Environment* **2017**, *584–585*, 1147–1151. https://doi.org/10.1016/j.scitotenv.2017.01.176.
(214) Li, J.; Wai, O. W. H.; Li, Y. S.; Zhan, J.; Ho, Y. A.; Li, J.; Lam, E. Effect of Green Roof on Ambient CO2 Concentration. *Building and Environment* **2010**, *45* (12), 2644–2651. https://doi.org/10.1016/j.buildenv.2010.05.025.
(215) Ramasubramanian, P.; Starry, O.; Rosenstiel, T.; Gall, E. T. Pilot Study on the Impact of Green Roofs on Ozone Levels near Building Ventilation Air Supply. *Building and Environment* **2019**, *151*, 43–53. https://doi.org/10.1016/j.buildenv.2019.01.023.
(216) Karner, A. A.; Eisinger, D. S.; Niemeier, D. A. Near-Roadway Air Quality: Synthesizing the Findings from Real-World Data. *Environmental Science & Technology* **2010**, *44* (14), 5334–5344. https://doi.org/10.1021/es100008x.

(217) Bans, A. *A Seasonal Study of Ecoroof Metal and Nutrient Dynamics and Associated Drivers in an Ecoroof on a Commercial Building in North Portland Oregon*; 2020. https://doi.org/10.15760/etd.7449.
(218) Keronen, P.; Reissell, A.; Rannik, Ü.; Pohja, T.; Siivola, E.; Hiltunen, V.; Hari, P.; Kulmala, M.; Vesala, T. Ozone FLux Measurements over a Scots Pine Forest Using Eddy Covariance Method: Performance Evaluation and Comparison with FLux-Profile Method. *Boreal environment research* **2003**, *8* (4), 425–444.
(219) Bryan, A. M.; Bertman, S. B.; Carroll, M. A.; Dusanter, S.; Edwards, G. D.; Forkel, R.; Griffith, S.; Guenther, A. B.; Hansen, R. F.; Helmig, D.; Jobson, B. T.; Keutsch, F. N.; Lefer, B. L.; Pressley, S. N.; Shepson, P. B.; Stevens, P. S.; Steiner, A. L. In-Canopy Gas-Phase Chemistry during CABINEX 2009: Sensitivity of a 1-D Canopy Model to Vertical Mixing and Isoprene Chemistry. *Atmospheric Chemistry and Physics* **2012**, *12* (18), 8829–8849. https://doi.org/10.5194/acp-12-8829-2012.
(220) Vesala, T.; Järvi, L.; Launiainen, S.; Sogachev, A.; Rannik, Ü.; Mammarella, I.; Ivola, E. S.; Keronen, P.; Rinne, J.; Riikonen, A.; Nikinmaa, E. Surface–Atmosphere Interactions over Complex Urban Terrain in Helsinki, Finland. *Tellus B: Chemical and Physical Meteorology* **2008**, *60* (2), 188–199. https://doi.org/10.1111/j.1600-0889.2007.00312.x.
(221) Grimmond, C. S. B. Flux and Turbulence Measurements at a Densely Built-up Site in Marseille: Heat, Mass (Water and Carbon Dioxide), and Momentum. *J. Geophys. Res.* **2004**, *109* (D24), D24101. https://doi.org/10.1029/2004JD004936.
(222) Crawford, B.; Grimmond, C. S. B.; Christen, A. Five Years of Carbon Dioxide Fluxes Measurements in a Highly Vegetated Suburban Area. *Atmospheric Environment* **2011**, *45* (4), 896–905. https://doi.org/10.1016/j.atmosenv.2010.11.017.
(223) Coutts, A. M.; Beringer, J.; Tapper, N. J. Characteristics Influencing the Variability of Urban CO2 Fluxes in Melbourne, Australia. *Atmospheric Environment* **2007**, *41* (1), 51–62. https://doi.org/10.1016/j.atmosenv.2006.08.030.
(224) Bergeron, O.; Strachan, I. B. CO2 Sources and Sinks in Urban and Suburban Areas of a Northern Mid-Latitude City. *Atmospheric Environment* **2011**, *45* (8), 1564–1573. https://doi.org/10.1016/j.atmosenv.2010.12.043.
(225) Järvi, L.; Nordbo, A.; Junninen, H.; Riikonen, A.; Moilanen, J.; Nikinmaa, E.; Vesala, T. Seasonal and Annual Variation of Carbon Dioxide Surface Fluxes in Helsinki, Finland, in 2006–2010. *Atmos. Chem. Phys.* **2012**, *12* (18), 8475–8489. https://doi.org/10.5194/acp-12-8475-2012.
(226) Grimmond, C. S. B.; King, T. S.; Cropley, F. D.; Nowak, D. J.; Souch, C. Local-Scale Fluxes of Carbon Dioxide in Urban Environments: Methodological Challenges and Results from Chicago. *Environmental Pollution* **2002**, *116*, S243–S254. https://doi.org/10.1016/S0269-7491(01)00256-1.
(227) Kormann, R.; Meixner, F. X. An Analytical Footprint Model For Non-Neutral Stratification. *Boundary-Layer Meteorology* **2001**, *99* (2), 207–224. https://doi.org/10.1023/A:1018991015119.

(228) Grimmond, C.; Souch, C. Surface Description for Urban Climate Studies: A GIS Based Methodology. *Geocarto International* **1994**, *9* (1), 47–59.
(229) Leclerc, M.; Meskhidze, N.; Finn, D. Footprint Predictions Comparison with a Tracer Flux Experiment over a Homogeneous Canopy of Intermediate Roughness. *Agricultural and Forest Meteorology* **2003**, *117*, 17–34.
(230) Webb, E. K. Effects of Heat and Water Vapour Transfer. 4.**1982**
(231) Webb, E. K.; Pearman, G. I.; Leuning, R. Correction of Flux Measurements for Density Effects Due to Heat and Water Vapour Transfer. *Quarterly Journal of the Royal Meteorological Society* **1980**, *106* (447), 85–100.
(232) Moncrieff, J. B.; Massheder, J. M.; de Bruin, H.; Elbers, J.; Friborg, T.; Heusinkveld, B.; Kabat, P.; Scott, S.; Soegaard, H.; Verhoef, A. A System to Measure Surface Fluxes of Momentum, Sensible Heat, Water Vapour and Carbon Dioxide. *Journal of Hydrology* **1997**, *188–189*, 589–611. https://doi.org/10.1016/S0022-1694(96)03194-0.
(233) Vickers, D.; Mahrt, L. Quality Control and Flux Sampling Problems for Tower and Aircraft Data. *Journal Of Atmospheric And Oceanic Technology* **1997**, *14*, 15.
(234) Foken, T.; Gockede, M.; Mauder, M.; Mahrt, L.; Amiro, B.; Munger, W. Post-Field Data Quality Control. *Handbook Of Micrometeorology* 28. 2004
(235) Heusinger, J.; Weber, S. Surface Energy Balance of an Extensive Green Roof as Quantified by Full Year Eddy-Covariance Measurements. *Science of The Total Environment* **2017**, *577*, 220–230. https://doi.org/10.1016/j.scitotenv.2016.10.168.
(236) Kormann, R.; Meixner, F. X. An Analytical Footprint Model For Non-Neutral Stratification. *Boundary-Layer Meteorology* **2001**, *99* (2), 207–224. https://doi.org/10.1023/A:1018991015119.
(237) Sargent, M.; Barrera, Y.; Nehrkorn, T.; Hutyra, L. R.; Gately, C. K.; Jones, T.; McKain, K.; Sweeney, C.; Hegarty, J.; Hardiman, B.; Wang, J. A.; Wofsy, S. C. Anthropogenic and Biogenic CO_2 Fluxes in the Boston Urban Region. *Proc Natl Acad Sci USA* **2018**, *115* (29), 7491–7496. https://doi.org/10.1073/pnas.1803715115.
(238) Miller, J. B.; Lehman, S. J.; Verhulst, K. R.; Miller, C. E.; Duren, R. M.; Yadav, V.; Newman, S.; Sloop, C. D. Large and Seasonally Varying Biospheric CO_2 Fluxes in the Los Angeles Megacity Revealed by Atmospheric Radiocarbon. *Proc Natl Acad Sci USA* **2020**, *117* (43), 26681–26687. https://doi.org/10.1073/pnas.2005253117.
(239) Järvi, L.; Nordbo, A.; Junninen, H.; Riikonen, A.; Moilanen, J.; Nikinmaa, E.; Vesala, T. Seasonal and Annual Variation of Carbon Dioxide Surface Fluxes in Helsinki, Finland, in 2006–2010. *Atmos. Chem. Phys.* **2012**, *12* (18), 8475–8489. https://doi.org/10.5194/acp-12-8475-2012.
(240) Pawlak, W.; Fortuniak, K.; Siedlecki, M. Carbon Dioxide Flux in the Centre of Łódź, Poland—Analysis of a 2-year Eddy Covariance Measurement Data Set. *International Journal of Climatology* **2011**, *31* (2), 232–243.
(241) Velasco, E.; Pressley, S.; Grivicke, R.; Allwine, E.; Coons, T.; Foster, W.; Jobson, B. T.; Westberg, H.; Ramos, R.; Hernandez, F.; Molina, L. T.; Lamb, B. Eddy

Covariance FLux Measurements of Pollutant Gases in Urban Mexico City. *Atmos. Chem. Phys.* **2009**, 18.
(242) Idso, S. B.; Idso, C. D.; Balling, R. C. Seasonal and Diurnal Variations of Near-Surface Atmospheric CO2 Concentration within a Residential Sector of the Urban CO2 Dome of Phoenix, AZ, USA. *Atmospheric Environment* **2002**, *36* (10), 1655–1660. https://doi.org/10.1016/S1352-2310(02)00159-0.
(243) Lietzke, B.; Vogt, R. Variability of CO2 Concentrations and Fluxes in and above an Urban Street Canyon. *Atmospheric Environment* **2013**, *74*, 60–72. https://doi.org/10.1016/j.atmosenv.2013.03.030.
(244) Ward, H. C.; Kotthaus, S.; Grimmond, C. S. B.; Bjorkegren, A.; Wilkinson, M.; Morrison, W. T. J.; Evans, J. G.; Morison, J. I. L.; Iamarino, M. Effects of Urban Density on Carbon Dioxide Exchanges: Observations of Dense Urban, Suburban and Woodland Areas of Southern England. *Environmental Pollution* **2015**, *198*, 186–200. https://doi.org/10.1016/j.envpol.2014.12.031.
(245) Hirano, T.; Sugawara, H.; Murayama, S.; Kondo, H. Diurnal Variation of CO_2 Flux in an Urban Area of Tokyo. *SOLA* **2015**, *11* (0), 100–103. https://doi.org/10.2151/sola.2015-024.
(246) Zhang, L.; Lemeur, R. Evaluation of Daily Evapotranspiration Estimates from Instantaneous Measurements. *Agricultural and Forest Meteorology* **1995**, *74* (1–2), 139–154. https://doi.org/10.1016/0168-1923(94)02181-I.
(247) Chang, H.; Makido, Y.; Foster, E. Effects of Land Use Change, Wetland Fragmentation, and Best Management Practices on Total Suspended Solids Concentrations in an Urbanizing Oregon Watershed, USA. *Journal of Environmental Management* **2021**, *282*, 111962. https://doi.org/10.1016/j.jenvman.2021.111962.
(248) Kairu, E. A Review of Methods for Estimating Evapotranspiration. *GeoJournal* **1991**, *25* (4), 371–376.
(249) Dickinson, R. E.; Henderson-Sellers, A.; Rosenzweig, C.; Sellers, P. J. Evapotranspiration Models with Canopy Resistance for Use in Climate Models, a Review. *Agricultural and Forest Meteorology* **1991**, *54* (2–4), 373–388. https://doi.org/10.1016/0168-1923(91)90014-H.
(250) Whittinghill, L. J.; Rowe, D. B.; Schutzki, R.; Cregg, B. M. Quantifying Carbon Sequestration of Various Green Roof and Ornamental Landscape Systems. *Landscape and Urban Planning* **2014**, *123*, 41–48. https://doi.org/10.1016/j.landurbplan.2013.11.015.
(251) Akbari, H.; Pomerantz, M.; Taha, H. Cool Surfaces and Shade Trees to Reduce Energy Use and Improve Air Quality in Urban Areas. *Solar Energy* **2001**, *70* (3), 295–310. https://doi.org/10.1016/S0038-092X(00)00089-X.
(252) Qiu, G.; Li, H.; Zhang, Q.; Chen, W.; Liang, X.; Li, X. Effects of Evapotranspiration on Mitigation of Urban Temperature by Vegetation and Urban Agriculture. *Journal of Integrative Agriculture* **2013**, *12* (8), 1307–1315. https://doi.org/10.1016/S2095-3119(13)60543-2.

(253) Taha, H. Urban Climates and Heat Islands: Albedo, Evapotranspiration, and Anthropogenic Heat. *Energy and Buildings* **1997**, *25* (2), 99–103. https://doi.org/10.1016/S0378-7788(96)00999-1.
(254) Qiu, G. Y.; Zou, Z.; Li, X.; Li, H.; Guo, Q.; Yan, C.; Tan, S. Experimental Studies on the Effects of Green Space and Evapotranspiration on Urban Heat Island in a Subtropical Megacity in China. *Habitat International* **2017**, *68*, 30–42. https://doi.org/10.1016/j.habitatint.2017.07.009.
(255) Wu, Z. Y.; Zhang, L.; Wang, X. M.; Munger, J. W. A Modified Micrometeorological Gradient Method for Estimating O_3 Dry Deposition over a Forest Canopy. *Atmospheric Chemistry and Physics Discussions* **2015**, *15* (1), 779–806. https://doi.org/10.5194/acpd-15-779-2015.
(256) Baldocchi, D. A Multi-Layer Model for Estimating Sulfur Dioxide Deposition to a Deciduous Oak Forest Canopy. *Atmospheric Environment* **1988**, *22* (5), 869–884. https://doi.org/10.1016/0004-6981(88)90264-8.
(257) Raupach, M. R.; Legg, B. J. The Uses and Limitations of Flux-Gradient Relationships in Micrometeorology. In *Developments in Agricultural and Managed Forest Ecology*; SHARMA, M. L., Ed.; Elsevier, **1984**; Vol. 13, pp 119–131. https://doi.org/10.1016/B978-0-444-42250-7.50011-2.
(258) Harman, I. N.; Finnigan, J. J. A Simple Unified Theory for Flow in the Canopy and Roughness Sublayer. *Boundary-Layer Meteorol* **2007**, *123* (2), 339–363. https://doi.org/10.1007/s10546-006-9145-6.
(259) Huang, J.; Katul, G.; Albertson, J. The Role of Coherent Turbulent Structures in Explaining Scalar Dissimilarity within the Canopy Sublayer. *Environ Fluid Mech* **2013**, *13* (6), 571–599. https://doi.org/10.1007/s10652-013-9280-9.
(260) Harman, I. N.; Finnigan, J. J. Scalar Concentration Profiles in the Canopy and Roughness Sublayer. *Boundary-Layer Meteorol* **2008**, *129* (3), 323–351. https://doi.org/10.1007/s10546-008-9328-4.
(261) Raupach, M. R.; Finnigan, J. J.; Brunet, Y. Coherent Eddies and Turbulence in Vegetation Canopies: The Mixing-Layer Analogy. In *Boundary-layer meteorology 25th anniversary volume, 1970–1995*; Springer, **1996**; pp 351–382.
(262) Ulrich, R. S. View Through a Window May Influence Recovery from Surgery. *Science* **1984**, *224* (4647), 420–421. https://doi.org/10.1126/science.6143402.
(263) Takano, T.; Nakamura, K.; Watanabe, M. Urban Residential Environments and Senior Citizens' Longevity in Megacity Areas: The Importance of Walkable Green Spaces. *Journal of Epidemiology & Community Health* **2002**, *56* (12), 913–918.
(264) Korpela, K. M.; Ylen, M. Perceived Health Is Associated with Visiting Natural Favourite Places in the Vicinity. *Health & Place* **2007**, *13* (1), 138–151.
(265) Bell, J. F.; Wilson, J. S.; Liu, G. C. Neighborhood Greenness and 2-Year Changes in Body Mass Index of Children and Youth. *American journal of preventive medicine* **2008**, *35* (6), 547–553.
(266) Kuo, F. E.; Sullivan, W. C. Environment and Crime in the Inner City: Does Vegetation Reduce Crime? *Environment and Behavior* **2001**, *33* (3), 343–367. https://doi.org/10.1177/0013916501333002.

(267) Bezyk, Y.; Sówka, I.; Górka, M. Assessment of Urban CO2 Budget: Anthropogenic and Biogenic Inputs. *Urban Climate* **2021**, *39*, 100949. https://doi.org/10.1016/j.uclim.2021.100949.
(268) Pataki, D. E. Seasonal Cycle of Carbon Dioxide and Its Isotopic Composition in an Urban Atmosphere: Anthropogenic and Biogenic Effects. *J. Geophys. Res.* **2003**, *108* (D23), 4735. https://doi.org/10.1029/2003JD003865.
(269) Logan, J. A. Ozone in Rural Areas of the United States. *J. Geophys. Res.* **1989**, *94* (D6), 8511–8532. https://doi.org/10.1029/JD094iD06p08511.
(270) Utiyama, M.; Fukuyama, T.; Yamada Maruo, Y.; Ichino, T.; Izumi, K.; Hara, H.; Takano, K.; Suzuki, H.; Aoki, M. Formation and Deposition of Ozone in a Red Pine Forest. *Water, Air, & Soil Pollution* **2004**, *151* (1–4), 53–70. https://doi.org/10.1023/B:WATE.0000009891.12108.b9.
(271) Stowell, J. D.; Kim, Y.; Gao, Y.; Fu, J. S.; Chang, H. H.; Liu, Y. The Impact of Climate Change and Emissions Control on Future Ozone Levels: Implications for Human Health. *Environment International* **2017**, *108*, 41–50. https://doi.org/10.1016/j.envint.2017.08.001.
(272) Weschler, C. J. Ozone's Impact on Public Health: Contributions from Indoor Exposures to Ozone and Products of Ozone-Initiated Chemistry. *Environmental Health Perspectives* **2006**, *114* (10), 1489–1496. https://doi.org/10.1289/ehp.9256.
(273) Wesely, M. L. Parameterization of Surface Resistances To Gaseous Dry Deposition In Regional-Scale Numerical Models. 12.
(274) Nowak, D. J.; Crane, D. E.; Stevens, J. C. Air Pollution Removal by Urban Trees and Shrubs in the United States. *Urban Forestry & Urban Greening* **2006**, *4* (3–4), 115–123. https://doi.org/10.1016/j.ufug.2006.01.007.
(275) Nowak, D. J.; Hirabayashi, S.; Bodine, A.; Greenfield, E. Tree and Forest Effects on Air Quality and Human Health in the United States. *Environmental Pollution* **2014**, *193*, 119–129. https://doi.org/10.1016/j.envpol.2014.05.028.
(276) Selmi, W.; Weber, C.; Rivière, E.; Blond, N.; Mehdi, L.; Nowak, D. Air Pollution Removal by Trees in Public Green Spaces in Strasbourg City, France. *Urban Forestry & Urban Greening* **2016**, *17*, 192–201. https://doi.org/10.1016/j.ufug.2016.04.010.
(277) Sicard, P.; Agathokleous, E.; Araminiene, V.; Carrari, E.; Hoshika, Y.; De Marco, A.; Paoletti, E. Should We See Urban Trees as Effective Solutions to Reduce Increasing Ozone Levels in Cities? *Environmental Pollution* **2018**, *243*, 163–176. https://doi.org/10.1016/j.envpol.2018.08.049.
(278) Nowak, D. J.; Dwyer, J. F. Understanding the Benefits and Costs of Urban Forest Ecosystems. In *Urban and community forestry in the northeast*; Springer, **2007**; pp 25–46.
(279) Bottalico, F.; Travaglini, D.; Chirici, G.; Garfì, V.; Giannetti, F.; De Marco, A.; Fares, S.; Marchetti, M.; Nocentini, S.; Paoletti, E.; Salbitano, F.; Sanesi, G. A Spatially-Explicit Method to Assess the Dry Deposition of Air Pollution by Urban Forests in the City of Florence, Italy. *Urban Forestry & Urban Greening* **2017**, *27*, 221–234. https://doi.org/10.1016/j.ufug.2017.08.013.

(280) Bottalico, F.; Chirici, G.; Giannetti, F.; De Marco, A.; Nocentini, S.; Paoletti, E.; Salbitano, F.; Sanesi, G.; Serenelli, C.; Travaglini, D. Air Pollution Removal by Green Infrastructures and Urban Forests in the City of Florence. *Agriculture and Agricultural Science Procedia* **2016**, *8*, 243–251. https://doi.org/10.1016/j.aaspro.2016.02.099.
(281) Bytnerowicz, A.; Fenn, M.; Miller, P.; Arbaugh, M. Wet and Dry Pollutant Deposition to the Mixed Conifer Forest. In *Oxidant air pollution impacts in the montane forests of southern California*; Springer, 1999; pp 235–269.
(282) Aoki, T.; Tanabe, S. Generation of Sub-Micron Particles and Secondary Pollutants from Building Materials by Ozone Reaction. *Atmospheric Environment* **2007**, *41* (15), 3139–3150. https://doi.org/10.1016/j.atmosenv.2006.07.053.
(283) Hoang, C. P.; Kinney, K. A.; Corsi, R. L. Ozone Removal by Green Building Materials. *Building and Environment* **2009**, *44* (8), 1627–1633. https://doi.org/10.1016/j.buildenv.2008.10.007.
(284) Lamble, S. P.; Corsi, R. L.; Morrison, G. C. Ozone Deposition Velocities, Reaction Probabilities and Product Yields for Green Building Materials. *Atmospheric Environment* **2011**, *45* (38), 6965–6972. https://doi.org/10.1016/j.atmosenv.2011.09.025.
(285) Nicolas, M.; Ramalho, O.; Maupetit, F. Reactions between Ozone and Building Products: Impact on Primary and Secondary Emissions. *Atmospheric Environment* **2007**, *41* (15), 3129–3138. https://doi.org/10.1016/j.atmosenv.2006.06.062.
(286) Hewitt, N.; Terry, G. Understanding Ozone Plant Chemistry. *Environmental Science & Technology* **1992**, *26* (10), 1890–1891. https://doi.org/10.1021/es00034a004.
(287) Ramasubramanian, P.; Luhung, I.; Lim, S. B. Y.; Schuster, S. C.; Starry, O.; Gall, E. T. Impact of Green and White Roofs on Air Handler Filters and Indoor Ventilation Air. *Building and Environment* **2021**, *197*, 107860. https://doi.org/10.1016/j.buildenv.2021.107860.
(288) Lin, C.-C.; Chen, H.-Y. Impact of HVAC Filter on Indoor Air Quality in Terms of Ozone Removal and Carbonyls Generation. *Atmospheric Environment* **2014**, *89*, 29–34. https://doi.org/10.1016/j.atmosenv.2014.02.020.
(289) Destaillats, H.; Chen, W.; Apte, M. G.; Li, N.; Spears, M.; Almosni, J.; Brunner, G.; Zhang, J. (Jensen); Fisk, W. J. Secondary Pollutants from Ozone Reactions with Ventilation Filters and Degradation of Filter Media Additives. *Atmospheric Environment* **2011**, *45* (21), 3561–3568. https://doi.org/10.1016/j.atmosenv.2011.03.066.
(290) Simmons, A.; Colbeck, I. Resistance of Various Building Materials to Ozone Deposition. *Environmental Technology* **1990**, *11* (10), 973–978. https://doi.org/10.1080/09593339009384949.
(291) Almand-Hunter, B. B.; Walker, J. T.; Masson, N. P.; Hafford, L.; Hannigan, M. P. Development and Validation of Inexpensive, Automated, Dynamic Flux Chambers. *Atmos. Meas. Tech.* **2015**, *8* (1), 267–280. https://doi.org/10.5194/amt-8-267-2015.

(292) Gall, E. T.; Siegel, J. A.; Corsi, R. L. Modeling Ozone Removal to Indoor Materials, Including the Effects of Porosity, Pore Diameter, and Thickness. *Environ. Sci. Technol.* **2015**, *49* (7), 4398–4406. https://doi.org/10.1021/acs.est.5b00023.
(293) Pape, L.; Ammann, C.; Nyfeler-Brunner, A.; Spirig, C.; Hens, K.; Meixner, F. X. An Automated Dynamic Chamber System for Surface Exchange Measurement of Non-Reactive and Reactive Trace Gases of Grassland Ecosystems. **2009**, 25.
(294) Baldocchi, D. D.; Hicks, B. B.; Camara, P. A Canopy Stomatal Resistance Model for Gaseous Deposition to Vegetated Surfaces. *Atmospheric Environment* **1987**, *21* (1), 91–101. https://doi.org/10.1016/0004-6981(87)90274-5.
(295) Meyers, T. P.; Baldocchi, D. D. A Comparison of Models for Deriving Dry Deposition Fluxes of O_3 and SO_2 to a Forest Canopy. *Tellus B* **1988**, *40B* (4), 270–284. https://doi.org/10.1111/j.1600-0889.1988.tb00297.x.
(296) Foken, T. 50 Years of the Monin–Obukhov Similarity Theory. *Boundary-Layer Meteorol* **2006**, *119* (3), 431–447. https://doi.org/10.1007/s10546-006-9048-6.
(297) Wesely, M. L.; Hicks, B. B. Some Factors That Affect the Deposition Rates of Sulfur Dioxide and Similar Gases on Vegetation. *Journal of the Air Pollution Control Association* **1977**, *27* (11), 1110–1116. https://doi.org/10.1080/00022470.1977.10470534.
(298) Clifton, O. E. Constraints on Ozone Removal by Land and Implications for 21st Century Ozone Pollution. **2018**, 190.
(299) Seinfeld, J. H.; Pandis, S. N. From Air Pollution to Climate Change. 1248.
(300) Tagesson, T. *Turbulent Transport in the Atmospheric Surface Layer*; Swedish Nuclear Fuel and Waste Management Co., **2012**; p 27.
(301) Wesely, M. L. Parameterization of Surface Resistances to Gaseous Dry Deposition In Regional-Scale Numerical Models. 12. **1989**
(302) McMahon, T. A.; Denison, P. J. Empirical Atmospheric Deposition Parameters—A Survey. *Atmospheric Environment (1967)* **1979**, *13* (5), 571–585. https://doi.org/10.1016/0004-6981(79)90186-0.
(303) Padro, J. Summary of Ozone Dry Deposition Velocity Measurements and Model Estimates over Vineyard, Cotton, Grass and Deciduous Forest in Summer. *Atmospheric Environment* **1996**, *30* (13), 2363–2369. https://doi.org/10.1016/1352-2310(95)00352-5.
(304) Starry, O.; Lea-Cox, J. D.; Kim, J.; van Iersel, M. W. Photosynthesis and Water Use by Two Sedum Species in Green Roof Substrate. *Environmental and Experimental Botany* **2014**, *107*, 105–112. https://doi.org/10.1016/j.envexpbot.2014.05.014.
(305) Usher, C. R.; Michel, A. E.; Grassian, V. H. Reactions on Mineral Dust. *Chem. Rev.* **2003**, *103* (12), 4883–4940. https://doi.org/10.1021/cr020657y.
(306) Erisman, J. W.; Van Pul, A.; Wyers, P. Parametrization of Surface Resistance for the Quantification of Atmospheric Deposition of Acidifying Pollutants and Ozone. *Atmospheric Environment* **1994**, *28* (16), 2595–2607. https://doi.org/10.1016/1352-2310(94)90433-2.

(307) Loubet, B.; Cellier, P.; Fléchard, C.; Zurfluh, O.; Irvine, M.; Lamaud, E.; Stella, P.; Roche, R.; Durand, B.; Flura, D.; Masson, S.; Laville, P.; Garrigou, D.; Personne, E.; Chelle, M.; Castell, J.-F. Investigating Discrepancies in Heat, CO2 Fluxes and O3 Deposition Velocity over Maize as Measured by the Eddy-Covariance and the Aerodynamic Gradient Methods. *Agricultural and Forest Meteorology* **2013**, *169*, 35–50. https://doi.org/10.1016/j.agrformet.2012.09.010.
(308) Schuber, M.; Kluge, M. In Situ Studies on Crassulacean Acid Metabolism in Sedum Acre L. and Sedum Mite Gil. *Oecologia* **1981**, *50* (1), 82–87. https://doi.org/10.1007/BF00378797.
(309) Silvola, J. Photosynthesis Measurements on a CAM Plant, Sedum Telephium (Crassulaceae). 7.
(310) Abbass, O. A.; Sailor, D. J.; Gall, E. T. Ozone Removal Efficiency and Surface Analysis of Green and White Roof HVAC Filters. *Building and Environment* **2018**, *136*, 118–127. https://doi.org/10.1016/j.buildenv.2018.03.042.
(311) Schleibinger, H.; Ruden, H. Air Filters from HVAC Systems as Possible Source of Volatile Organic Compounds (VOC) - Laboratory and Field Assays. *Atmospheric Environment* **1999**, 7.
(312) Ahearn, D. G. Fungal Colonization of Air Filters and Insulation in a Multi-Story Office Building: Production of Volatile Organics. *Current Microbiology* **1997**, *35* (5), 305–308. https://doi.org/10.1007/s002849900259.
(313) Batterman, S. A.; Burge, H. HVAC Systems As Emission Sources Affecting Indoor Air Quality: A Critical Review. *HVAC&R Research* **1995**, *1* (1), 61–78. https://doi.org/10.1080/10789669.1995.10391309.
(314) Evans, R. C.; Tingey, D. T.; Gumpertz, M. L.; Burns, W. F. Estimates of Isoprene and Monoterpene Emission Rates in Plants. *Botanical Gazette* **1982**, *143* (3), 304–310. https://doi.org/10.1086/botanicalgazette.143.3.2474826.
(315) Singh, B.; Sharma, R. A. Plant Terpenes: Defense Responses, Phylogenetic Analysis, Regulation and Clinical Applications. *3 Biotech* **2015**, *5* (2), 129–151. https://doi.org/10.1007/s13205-014-0220-2.
(316) Destaillats, H. Secondary Pollutants from Ozone Reactions with Ventilation Filters and Degradation of Filter Media Additives. *Atmospheric Environment* **2011**, 8.
(317) Potard, K.; Monard, C.; Le Garrec, J.-L.; Caudal, J.-P.; Le Bris, N.; Binet, F. Organic Amendment Practices as Possible Drivers of Biogenic Volatile Organic Compounds Emitted by Soils in Agrosystems. *Agriculture, Ecosystems & Environment* **2017**, *250*, 25–36. https://doi.org/10.1016/j.agee.2017.09.007.
(318) Maleknia, S. D.; Bell, T. L.; Adams, M. A. PTR-MS Analysis of Reference and Plant-Emitted Volatile Organic Compounds. *International Journal of Mass Spectrometry* **2007**, *262* (3), 203–210. https://doi.org/10.1016/j.ijms.2006.11.010.
(319) Abis, L.; Loubet, B.; Ciuraru, R.; Lafouge, F.; Dequiedt, S.; Houot, S.; Maron, P. A.; Bourgeteau-Sadet, S. Profiles of Volatile Organic Compound Emissions from Soils Amended with Organic Waste Products. *Science of The Total Environment* **2018**, *636*, 1333–1343. https://doi.org/10.1016/j.scitotenv.2018.04.232. **2018**

(320) Nemecek-Marshall, M.; MacDonald, R. C.; Franzen, J. J.; Wojciechowski, C. L.; Fall, R. Methanol Emission from Leaves (Enzymatic Detection of Gas-Phase Methanol and Relation of Methanol Fluxes to Stomatal Conductance and Leaf Development). *Plant Physiol.* **1995**, *108* (4), 1359–1368. https://doi.org/10.1104/pp.108.4.1359.
(321) Greenberg, J. P.; Asensio, D.; Turnipseed, A.; Guenther, A. B.; Karl, T.; Gochis, D. Contribution of Leaf and Needle Litter to Whole Ecosystem BVOC Fluxes. *Atmospheric Environment* **2012**, 10.
(322) Kim, S.; Karl, T.; Guenther, A.; Tyndall, G.; Orlando, J.; Harley, P.; Rasmussen, R.; Apel, E. Emissions and Ambient Distributions of Biogenic Volatile Organic Compounds (BVOC) in a Ponderosa Pine Ecosystem: Interpretation of PTR-MS Mass Spectra. *Atmos. Chem. Phys.* **2010**, *10* (4), 1759–1771. https://doi.org/10.5194/acp-10-1759-2010.
(323) Laothawornkitkul, J.; Taylor, J. E.; Paul, N. D.; Hewitt, C. N. Biogenic Volatile Organic Compounds in the Earth System. *New Phytologist* **2009**, *183* (1), 27–51. https://doi.org/10.1111/j.1469-8137.2009.02859.x.
(324) Bourtsoukidis, E.; Bonn, B.; Noe, S. M. On-Line Field Measurements of BVOC Emissions from Norway Spruce (Picea Abies) at the Hemiboreal SMEAR-Estonia Site under Autumn Conditions. *19*, 15. **2013**
(325) Bamberger, I.; Hörtnagl, L.; Schnitzhofer, R.; Graus, M.; Ruuskanen, T. M.; Müller, M.; Dunkl, J.; Wohlfahrt, G.; Hansel, A. BVOC Fluxes above Mountain Grassland. *Biogeosciences* **2010**, *7* (5), 1413–1424. https://doi.org/10.5194/bg-7-1413-2010.
(326) Sanhueza, E.; Andreae, M. O. Emission of Formic and Acetic Acids from Tropical Savanna Soils. *Geophys. Res. Lett.* **1991**, *18* (9), 1707–1710. https://doi.org/10.1029/91GL01565.
(327) Coleman, B. K.; Destaillats, H.; Hodgson, A. T.; Nazaroff, W. W. Ozone Consumption and Volatile Byproduct Formation from Surface Reactions with Aircraft Cabin Materials and Clothing Fabrics. *Atmospheric Environment* **2008**, *42* (4), 642–654. https://doi.org/10.1016/j.atmosenv.2007.10.001.
(328) Friedman, M. The Use of Ranks to Avoid the Assumption of Normality Implicit in the Analysis of Variance. *null* **1937**, *32* (200), 675–701. https://doi.org/10.1080/01621459.1937.10503522.
(329) Gabdrashova, R.; Nurzhan, S.; Naseri, M.; Bekezhankyzy, Z.; Gimnkhan, A.; Malekipirbazari, M.; Tabesh, M.; Khanbabaie, R.; Crape, B.; Buonanno, G.; Hopke, P. K.; Amouei Torkmahalleh, A.; Amouei Torkmahalleh, M. The Impact on Heart Rate and Blood Pressure Following Exposure to Ultrafine Particles from Cooking Using an Electric Stove. *Science of The Total Environment* **2021**, *750*, 141334. https://doi.org/10.1016/j.scitotenv.2020.141334.
(330) Vaida Valuntait; Šerevicien, V.; Girgždien, D.; Paliulis. Relative Humidity and Temperature Impact to Ozone And Nitrogen Oxides Removal Rate in The Experimental Chamber. *Journal of Environmental Engineering and Landscape Management*. **2012**

(331) Cosgrove, D. J. Growth of the Plant Cell Wall. *Nat Rev Mol Cell Biol* **2005**, *6* (11), 850–861. https://doi.org/10.1038/nrm1746.
(332) Mellerowicz, E.; Sundberg, B. Wood Cell Walls: Biosynthesis, Developmental Dynamics and Their Implications for Wood Properties. *Current Opinion in Plant Biology* **2008**, *11* (3), 293–300. https://doi.org/10.1016/j.pbi.2008.03.003.
(333) Risholm-Sundman, M.; Lundgren, M.; Vestin, E.; Herder, P. Emissions of Acetic Acid and Other Volatile Organic Compounds from Different Species of Solid Wood. *Holz als Roh-und Werkstoff* **1998**, *56* (2), 125–129. https://doi.org/10.1007/s001070050282.
(334) Gray, C. M.; Monson, R. K.; Fierer, N. Emissions of Volatile Organic Compounds during the Decomposition of Plant Litter. *J. Geophys. Res.* **2010**, *115* (G3), G03015. https://doi.org/10.1029/2010JG001291.
(335) Warneke, C.; Karl, T.; Judmaier, H.; Hansel, A.; Jordan, A.; Lindinger, W.; Crutzen, P. J. Acetone, Methanol, and Other Partially Oxidized Volatile Organic Emissions from Dead Plant Matter by Abiological Processes: Significance for Atmospheric HO_x Chemistry. *Global Biogeochem. Cycles* **1999**, *13* (1), 9–17. https://doi.org/10.1029/98GB02428.
(336) Rantala, P.; Järvi, L.; Taipale, R.; Laurila, T. K.; Patokoski, J.; Kajos, M. K.; Kurppa, M.; Haapanala, S.; Siivola, E.; Petäjä, T.; Ruuskanen, T. M.; Rinne, J. Anthropogenic and Biogenic Influence on VOC Fluxes at an Urban Background Site in Helsinki, Finland. *Atmos. Chem. Phys.* **2016**, *16* (12), 7981–8007. https://doi.org/10.5194/acp-16-7981-2016.
(337) Lange, B. M.; Ahkami, A. Metabolic Engineering of Plant Monoterpenes, Sesquiterpenes and Diterpenes-Current Status and Future Opportunities. *Plant Biotechnol J* **2013**, *11* (2), 169–196. https://doi.org/10.1111/pbi.12022.
(338) Sharkey, T. D.; Yeh, S. Isoprene Emission from Plants. *Annu. Rev. Plant. Physiol. Plant. Mol. Biol.* **2001**, *52* (1), 407–436. https://doi.org/10.1146/annurev.arplant.52.1.407.
(339) Wang, C.; Collins, D. B.; Arata, C.; Goldstein, A. H.; Mattila, J. M.; Farmer, D. K.; Ampollini, L.; DeCarlo, P. F.; Novoselac, A.; Vance, M. E.; Nazaroff, W. W.; Abbatt, J. P. D. Surface Reservoirs Dominate Dynamic Gas-Surface Partitioning of Many Indoor Air Constituents. *Sci. Adv.* **2020**, *6* (8), eaay8973. https://doi.org/10.1126/sciadv.aay8973.
(340) Thanomsub, B.; Anupunpisit, V.; Chanphetch, S.; Watcharachaipong, T.; Poonkhum, R.; Srisukonth, C. Effects of Ozone Treatment on Cell Growth and Ultrastructural Changes in Bacteria. *J. Gen. Appl. Microbiol.* **2002**, *48* (4), 193–199. https://doi.org/10.2323/jgam.48.193.
(341) Guzel-Seydim, Z. B.; Greene, A. K.; Seydim, A. C. Use of Ozone in the Food Industry. *LWT - Food Science and Technology* **2004**, *37* (4), 453–460. https://doi.org/10.1016/j.lwt.2003.10.014.
(342) Schulz, S.; Dickschat, J. S. Bacterial Volatiles: The Smell of Small Organisms. *Nat. Prod. Rep.* **2007**, *24* (4), 814. https://doi.org/10.1039/b507392h.

(343) Li, M.; Nian, R.; Xian, M.; Zhang, H. Metabolic Engineering for the Production of Isoprene and Isopentenol by Escherichia Coli. *Appl Microbiol Biotechnol* **2018**, *102* (18), 7725–7738. https://doi.org/10.1007/s00253-018-9200-5.
(344) Sethia, P.; Ahuja, M.; Rangaswamy, V. Metabolic Engineering of Microorganisms to Produce Isoprene. *11* (419), 9. **2019**
(345) Schnitzler, J.-P.; Louis, S.; Behnke, K.; Loivamäki, M. Poplar Volatiles - Biosynthesis, Regulation and (Eco)Physiology of Isoprene and Stress-Induced Isoprenoids: Plant Volatiles of Poplar. *Plant Biology* **2009**, *12* (2), 302–316. https://doi.org/10.1111/j.1438-8677.2009.00284.x.
(346) Vickers, C. E.; Possell, M.; Cojocariu, C. I.; Velikova, V. B.; Laothawornkitkul, J.; Ryan, A.; Mullineaux, P. M.; Nicholas Hewitt, C. Isoprene Synthesis Protects Transgenic Tobacco Plants from Oxidative Stress. *Plant, Cell & Environment* **2009**, *32* (5), 520–531. https://doi.org/10.1111/j.1365-3040.2009.01946.x.
(347) Velikova, V.; Fares, S.; Loreto, F. Isoprene and Nitric Oxide Reduce Damages in Leaves Exposed to Oxidative Stress. *Plant, Cell & Environment* **2008**, *31* (12), 1882–1894. https://doi.org/10.1111/j.1365-3040.2008.01893.x.
(348) Ander, P.; Eriksson, K.-E. Methanol Formation during Lignin Degradation by Phanerochaete Chrysosporium. *Applied Microbiology and Biotechnology* **1985**, *21* (1), 96–102. https://doi.org/10.1007/BF00252369.
(349) Zhang, Junfeng.; Wilson, W. E.; Lioy, P. J. Indoor Air Chemistry: Formation of Organic Acids and Aldehydes. *Environ. Sci. Technol.* **1994**, *28* (11), 1975–1982. https://doi.org/10.1021/es00060a031.
(350) Nawrocki, J.; Świetlik, J.; Raczyk-Stanisławiak, U.; Dąbrowska, A.; Biłozor, S.; Ilecki, W. Influence of Ozonation Conditions on Aldehyde and Carboxylic Acid Formation. *Ozone: Science & Engineering* **2003**, *25* (1), 53–62. https://doi.org/10.1080/713610650.
(351) US Environmental Protection Agency. Health Assessment Document for Acetaldehyde. **1987**.
(352) Thompson, M. Administered by Inhalation to F344/N Rats and B6C3F1 Mice. *Toxicity Report Series* **1992**, No. 19, 62.
(353) Bergmans, L.; Moisiadis, P.; Van Meerbeek, B.; Quirynen, M.; Lambrechts, P. Microscopic Observation of Bacteria: Review Highlighting the Use of Environmental SEM. *Int Endod J* **2005**, *38* (11), 775–788. https://doi.org/10.1111/j.1365-2591.2005.00999.x.
(354) Solomon, S. J.; Schade, G. W.; Kuttippurath, J.; Ladstätter-Weissenmayer, A.; Burrows, J. P. VOC Concentrations in an Indoor Workplace Environment of a University Building. *Indoor and Built Environment* **2008**, *17* (3), 260–268. https://doi.org/10.1177/1420326X08090822.
(355) Zhang, J.; Wilson, W.; Lioy, P. Sources of Organic Acids in Indoor Air: A Field Study. *Journal of exposure analysis and environmental epidemiology* **1994**, *4* (1), 25—47.

(356) Li, T.; Siegel, J. A. Assessing the Impact of Filtration Systems in Indoor Environments with Effectiveness. *Building and Environment* **2021**, *187*, 107389. https://doi.org/10.1016/j.buildenv.2020.107389.
(357) Nicas, M. Estimating Exposure Intensity in an Imperfectly Mixed Room. *American Industrial Hygiene Association Journal* **1996**, *57* (6), 542–550. https://doi.org/10.1080/15428119691014756.
(358) Boelter, F. W.; Simmons, C. E.; Berman, L.; Scheff, P. Two-Zone Model Application to Breathing Zone and Area Welding Fume Concentration Data. *Journal of Occupational and Environmental Hygiene* **2009**, *6* (5), 298–306. https://doi.org/10.1080/15459620902809895.
(359) Earnest, C. M.; Corsi, R. L. Inhalation Exposure to Cleaning Products: Application of a Two-Zone Model. *Journal of Occupational and Environmental Hygiene* **2013**, *10* (6), 328–335. https://doi.org/10.1080/15459624.2013.782198.
(360) Rotach, M. W. On the Influence of the Urban Roughness Sublayer on Turbulence and Dispersion. *Atmospheric Environment* **1999**, 8.
(361) Coleman, B. K.; Destaillats, H.; Hodgson, A. T.; Nazaroff, W. W. Ozone Consumption and Volatile Byproduct Formation from Surface Reactions with Aircraft Cabin Materials and Clothing Fabrics. *Atmospheric Environment* **2008**, *42* (4), 642–654. https://doi.org/10.1016/j.atmosenv.2007.10.001.
(362) Siegel, J. A. Primary and Secondary Consequences of Indoor Air Cleaners. *Indoor Air* **2016**, *26* (1), 88–96. https://doi.org/10.1111/ina.12194.
(363) Shair, F. H.; Heitner, K. L. Theoretical Model for Relating Indoor Pollutant Concentrations to Those Outside. *Environ. Sci. Technol.* **1974**, *8* (5), 444–451. https://doi.org/10.1021/es60090a006.
(364) Nazaroff, W. W.; Weschler, C. J. Indoor Ozone: Concentrations and Influencing Factors. *Indoor Air* **2022**, *32* (1). https://doi.org/10.1111/ina.12942.
(365) Gold, D. R.; Allen, G.; Damokosh, A.; Serrano, P.; Castiilejos, M. Comparison of Outdoor and Classroom Ozone Exposures for School Children in Mexico City. **1996**, *46*, 9.
(366) Bennett, D. H.; McKone, T. E.; Evans, J. S.; Nazaroff, W. W.; Margni, M. D.; Jolliet, O.; Smith, K. R. Peer Reviewed: Defining Intake Fraction. *Environmental science & technology* **2002**, *36* (9), 206A-211A.
(367) Smith, K. R. Fuel Combustion, Air Pollution Exposure, and Health: The Situation In Developing Countries. 38. **1993**
(368) Harrison, K.; Hattis, D.; Abbat, K. *Implications of Chemical Use for Exposure Assessment: Development of an Exposure Estimation Methodology for Application in a Use-Clustered Priority Setting System*; Center for Technology, Policy, and Industrial Development, Massachusetts …, **1986**.
(369) Marshall, J.; Teoh, S.; Wnazaroff, W. Intake Fraction of Nonreactive Vehicle Emissions in US Urban Areas. *Atmospheric Environment* **2005**, *39* (7), 1363–1371. https://doi.org/10.1016/j.atmosenv.2004.11.008.
(370) Bare, J. C. Traci. *Journal of Industrial Ecology* **2002**, *6* (3–4), 49–78. https://doi.org/10.1162/108819802766269539.

(371) Hofstetter, P. *Perspectives in Life Cycle Impact Assessment*; Springer US: Boston, MA, **1998**. https://doi.org/10.1007/978-1-4615-5127-0.
(372) Jolliet, O.; Margni, M.; Charles, R.; Humbert, S.; Payet, J.; Rebitzer, G.; Rosenbaum, R. IMPACT 2002+: A New Life Cycle Impact Assessment Methodology. *Int J LCA* **2003**, *8* (6), 324. https://doi.org/10.1007/BF02978505.
(373) van Zelm, R.; Huijbregts, M. A. J.; den Hollander, H. A.; van Jaarsveld, H. A.; Sauter, F. J.; Struijs, J.; van Wijnen, H. J.; van de Meent, D. European Characterization Factors for Human Health Damage of PM10 and Ozone in Life Cycle Impact Assessment. *Atmospheric Environment* **2008**, *42* (3), 441–453. https://doi.org/10.1016/j.atmosenv.2007.09.072.
(374) Humbert, S.; Marshall, J. D.; Shaked, S.; Spadaro, J. V.; Nishioka, Y.; Preiss, P.; McKone, T. E.; Horvath, A.; Jolliet, O. Intake Fraction for Particulate Matter: Recommendations for Life Cycle Impact Assessment. *Environ. Sci. Technol.* **2011**, *45* (11), 4808–4816. https://doi.org/10.1021/es103563z.
(375) Wenger, Y.; Li, D.; Jolliet, O. Indoor Intake Fraction Considering Surface Sorption of Air Organic Compounds for Life Cycle Assessment. *Int J Life Cycle Assess* **2012**, *17* (7), 919–931. https://doi.org/10.1007/s11367-012-0420-0.
(376) United States. Occupational Safety and Health Administration. *OSHA Technical Manual*; [Washington, D.C.] : U.S. Dept. of Labor, Occupational Safety and Health Administration : [For sale by the Supt. of Docs., U.S. G.P.O.], 1990-, 1990.
(377) Brohus, H.; Nielsen, P. V. Personal Exposure in Displacement Ventilated Rooms. *Indoor Air* **1996**, *6* (3), 157–167.
(378) Mullen, N. A. Impact of Natural Gas Appliances on Pollutant Levels in California Homes. **2013**.
(379) Mullen, N. A.; Li, J.; Russell, M. L.; Spears, M.; Less, B. D.; Singer, B. C. Results of the California Healthy Homes Indoor Air Quality Study of 2011–2013: Impact of Natural Gas Appliances on Air Pollutant Concentrations. *Indoor Air* **2016**, *26* (2), 231–245. https://doi.org/10.1111/ina.12190.
(380) Logue, J. M.; Klepeis, N. E.; Lobscheid, A. B.; Singer, B. C. Pollutant Exposures from Natural Gas Cooking Burners: A Simulation-Based Assessment for Southern California. *Environmental Health Perspectives* **2014**, *122* (1), 43–50. https://doi.org/10.1289/ehp.1306673.
(381) Pantelic, J.; Liu, S.; Pistore, L.; Licina, D.; Vannucci, M.; Sadrizadeh, S.; Ghahramani, A.; Gilligan, B.; Sternberg, E.; Kampschroer, K.; Schiavon, S. Personal CO2 Cloud: Laboratory Measurements of Metabolic CO2 Inhalation Zone Concentration and Dispersion in a Typical Office Desk Setting. *J Expo Sci Environ Epidemiol* **2020**, *30* (2), 328–337. https://doi.org/10.1038/s41370-019-0179-5.
(382) Laverge, J.; Spilak, M.; Novoselac, A. Experimental Assessment of the Inhalation Zone of Standing, Sitting and Sleeping Persons. *Building and Environment* **2014**, *82*, 258–266. https://doi.org/10.1016/j.buildenv.2014.08.014.

(383) Murakami, S.; Zeng, J.; Hayashi, T. CFD Analysis of Wind Environment around a Human Body. *Journal of Wind Engineering and Industrial Aerodynamics* **1999**, *83* (1–3), 393–408. https://doi.org/10.1016/S0167-6105(99)00088-4.
(384) Gowadia, H. A.; Settles, G. S. The Natural Sampling of Airborne Trace Signals from Explosives Concealed upon the Human Body. *Journal of Forensic Science* **2001**, *46* (6), 1324–1331.
(385) Clark, R.; Edholm, O. G. *Man and His Thermal Environment*; Edward Arnold London, **1985**.
(386) Craven, B. A.; Settles, G. S. A Computational and Experimental Investigation of the Human Thermal Plume. *Journal of Fluids Engineering* **2006**, *128* (6), 1251–1258. https://doi.org/10.1115/1.2353274.
(387) Rim, D.; Novoselac, A. Transport of Particulate and Gaseous Pollutants in the Vicinity of a Human Body. *Building and Environment* **2009**, *44* (9), 1840–1849. https://doi.org/10.1016/j.buildenv.2008.12.009.
(388) Rim, D.; Novoselec, A.; Morrison, G. The Influence of Chemical Interactions at the Human Surface on Breathing Zone Levels of Reactants and Products. *Indoor Air* **2009**, *19* (4), 324–334. https://doi.org/10.1111/j.1600-0668.2009.00595.x.
(389) Salmanzadeh, M.; Zahedi, Gh.; Ahmadi, G.; Marr, D. R.; Glauser, M. Computational Modeling of Effects of Thermal Plume Adjacent to the Body on the Indoor Airflow and Particle Transport. *Journal of Aerosol Science* **2012**, *53*, 29–39. https://doi.org/10.1016/j.jaerosci.2012.05.005.
(390) Lee, K.; Vallarino, J.; Dumyahn, T.; Ozkaynak, H.; Spengler, J. D. Ozone Decay Rates in Residences. *Journal of the Air & Waste Management Association* **1999**, *49* (10), 1238–1244. https://doi.org/10.1080/10473289.1999.10463913.
(391) Yao, M.; Zhao, B. Surface Removal Rate of Ozone in Residences in China. *Building and Environment* **2018**, *142*, 101–106. https://doi.org/10.1016/j.buildenv.2018.06.010.
(392) RIOPA Team. RIOPA Dataset. Harvard Dataverse, V. 1. **2020**.
(393) Price, D. J.; Day, D. A.; Pagonis, D.; Stark, H.; Algrim, L. B.; Handschy, A. V.; Liu, S.; Krechmer, J. E.; Miller, S. L.; Hunter, J. F.; de Gouw, J. A.; Ziemann, P. J.; Jimenez, J. L. Budgets of Organic Carbon Composition and Oxidation in Indoor Air. *Environ. Sci. Technol.* **2019**, *53* (22), 13053–13063. https://doi.org/10.1021/acs.est.9b04689.
(394) Singer, B. C.; Pass, R. Z.; Delp, W. W.; Lorenzetti, D. M.; Maddalena, R. L. Pollutant Concentrations and Emission Rates from Natural Gas Cooking Burners without and with Range Hood Exhaust in Nine California Homes. *Building and Environment* **2017**, *122*, 215–229. https://doi.org/10.1016/j.buildenv.2017.06.021.
(395) Fischer, A.; Ljungström, E.; Langer, S. Ozone Removal by Occupants in a Classroom. *Atmospheric Environment* **2013**, *81*, 11–17. https://doi.org/10.1016/j.atmosenv.2013.08.054.
(396) Tamas, G.; Weschler, C.; Bakobiro, Z.; Wyon, D.; Stromtejsen, P. Factors Affecting Ozone Removal Rates in a Simulated Aircraft Cabin Environment.

Atmospheric Environment **2006**, *40* (32), 6122–6133. https://doi.org/10.1016/j.atmosenv.2006.05.034.
(397) Ng, L. C.; Musser, A.; Persily, A. K.; Emmerich, S. J. Multizone Airflow Models for Calculating Infiltration Rates in Commercial Reference Buildings. *Energy and Buildings* **2013**, *58*, 11–18. https://doi.org/10.1016/j.enbuild.2012.11.035.
(398) Lai, D.; Karava, P.; Chen, Q. Study of Outdoor Ozone Penetration into Buildings through Ventilation and Infiltration. *Building and Environment* **2015**, *93*, 112–118. https://doi.org/10.1016/j.buildenv.2015.06.015.
(399) Zhao, H.; Stephens, B. A Method to Measure the Ozone Penetration Factor in Residences under Infiltration Conditions: Application in a Multifamily Apartment Unit. *Indoor Air* **2016**, *26* (4), 571–581. https://doi.org/10.1111/ina.12228.
(400) Zuraimi, M. S.; Weschler, C. J.; Tham, K. W.; Fadeyi, M. O. The Impact of Building Recirculation Rates on Secondary Organic Aerosols Generated by Indoor Chemistry. *Atmospheric Environment* **2007**, *41* (25), 5213–5223. https://doi.org/10.1016/j.atmosenv.2006.05.087.
(401) Wang, L.; Chen, Q. Analysis on the Well-Mixing Assumptions Used in Multizone Airflow Network Models; **2007**.
(402) Foken, T.; Nappo, C. J. *Micrometeorology*; Springer: Berlin, **2008**.